Phenomenology of the spin-3 mesons

Shahriyar Jafarzade

Jan Kochanowski University of Kielce, Poland

joint work with Francesco Giacosa and Adrian Koenigstein

Frontiers in Nuclear and Hadronic Physics, 24 Feb-06 Mar 2020

Galileo Galilei Institute for Theoretical Physics

Introduction

- Mesons can be described as quark and anti-quark bound states $(q_i \bar{q}_j)$
- Parity of the states: $P = (-1)^{L+1}$ for the angular momentum L
- Charge conjugation for mesons: $C = (-1)^{L+S}$ for parallel quark states $S = 1$ and $S = 0$ for anti-parallel quarks
- Total spin $J = L + S$ get the values $|L - S| \leq J \leq |L + S|$
- Mesons can be grouped to the nonets which transform under the adjoint transformation of the flavour symmetry $U_V(N_f = 3)$
- This symmetry leaves QCD lagrangian invariant under the exchange of light quarks $q_i = (u, d, s)$ for $m_i = 0$
- We study the mesons with the quantum numbers $J^{PC} = 3^{--}$ for $L = 2$ and $S = 1$
- These mesons are $\rho_3(1690)$, $K_3^*(1780)$, $\phi_3(1850)$ and $\omega_3(1670)$
- One of the theoretical ways to investigate these mesons is the low energy effective model of QCD
- Within this model we consider mesons as effective fields and $SU(N_f = 3)_V$ approximate symmetry as a guide symmetry
- Chiral symmetry of QCD is considered main symmetry for this model

Symmetries of QCD

- QCD Lagrangian

$$\mathcal{L}_{QCD} = \mathrm{tr}\left(\bar{q}_i(i\gamma_\mu D^\mu - m_i)q_i - \frac{1}{2}G_{\mu\nu}G^{\mu\nu}\right),\ G_{\mu\nu:} = D_\mu A_\nu - D_\nu A_\mu - ig[A_\mu, A_\nu]$$

$$D_\mu := \partial_\mu - igA_\mu,\ A_\mu := A^a_\mu t^a,\ [t^a, t^b] = if^{abc}t^c$$

- Color symmetry: $SU(3)_c \rightarrow$ Confinement
- Chiral symmetry:
  $U(N_f)_R \times U(N_f)_L \equiv U(1)_{V=R+L} \times SU(N_f)_V \times SU(N_f)_A \times U(1)_{A=R-L}$:
  works in chiral limit ($m_i \rightarrow 0$)
- Can be broken: 1) explicitly by $m_i \neq 0$ and 2) spontaneously breaking to $SU(N_f = 3)_V \times U(1)_V$
- Spontaneous breaking is the essential property of hadronic world
- Dilitation invariance: $x^\mu \rightarrow \lambda^{-1}x^\mu$ is satisfied in chiral limit and classically
- Quantum level $\rightarrow$ Trace anomaly
- $U(1)_A$: Classical symmetry, broken by quantum effects $\rightarrow$ Axial anomaly

Quark description of mesons

- Considering the representation of $SU(3)$: $3 \otimes \bar{3} = 8 \oplus 1$
- Mesons in terms of light quarks $q_i, q_j \in \{u, d, s\}$ can be grouped to octets and singlets
- Scalars: $J^{PC} = 0^{++}$; $S_{ij} = \bar{q}_j q_i$
- Pseudoscalars: $J^{PC} = 0^{-+}$; $P_{ij} = \bar{q}_j i\gamma^5 q_i$
- Vectors: $J^{PC} = 1^{--}$; $V^{\mu}_{ij} = \sqrt{2}\bar{q}_j \gamma^{\mu} q_i$
- Axial-vectors: $J^{PC} = 1^{++}$; $A^{\mu}_{ij} = \sqrt{2}\bar{q}_j \gamma^{\mu}\gamma^5 q_i$
- Isoscalar states with the same quantum number J^{PC} mix
- Physical resonances are the mixtures of $SU(3)$ wave functions $\Phi_1 \equiv \sqrt{\frac{1}{6}}(u\bar{u} + d\bar{d} + s\bar{s})$ and $\Phi_8 \equiv \sqrt{\frac{1}{6}}(u\bar{u} + d\bar{d} - 2s\bar{s})$

$$\begin{pmatrix} f \\ f' \end{pmatrix} = \begin{pmatrix} \cos\theta & \sin\theta \\ -\sin\theta & \cos\theta \end{pmatrix} \begin{pmatrix} \Phi_1 \\ \Phi_8 \end{pmatrix}$$

Forms of mesons within nonets

- Experimental values for mixing angles $\theta_P = -43.4^\circ$, $\theta_V = -3.9^\circ$, $\theta_X = 5.7^\circ$ and $\theta_W = 3.5^\circ$

$$P = \frac{1}{\sqrt{2}} \begin{pmatrix} \frac{\eta_N + \pi^0}{\sqrt{2}} & \pi^+ & K^+ \\ \pi^- & \frac{\eta_N - \pi^0}{\sqrt{2}} & K^0 \\ K^- & \bar{K}^0 & \eta_S \end{pmatrix}, V^\mu = \frac{1}{\sqrt{2}} \begin{pmatrix} \frac{\omega^\mu_{1,N} + \rho^{0\mu}_1}{\sqrt{2}} & \rho^{+\mu}_1 & K^{*+\mu}_1 \\ \rho^{-\mu} & \frac{\omega^\mu_N - \rho^{0\mu}}{\sqrt{2}} & K^{*0\mu} \\ K^{*-\mu} & \bar{K}^{*0\mu} & \omega^\mu_S \end{pmatrix},$$

$$X^{\mu\nu} = \frac{1}{\sqrt{2}} \begin{pmatrix} \frac{f^{\mu\nu}_{2,N} + a^{0\mu\nu}_2}{\sqrt{2}} & a^{+\mu\nu}_2 & K^{*+\mu\nu}_2 \\ a^{-\mu\nu}_2 & \frac{f^{\mu\nu}_{2,N} - a^{0\mu\nu}_2}{\sqrt{2}} & K^{*0\mu\nu}_2 \\ K^{*-\mu\nu}_2 & \bar{K}^{*0\mu\nu}_2 & f^{\mu\nu}_{2,S} \end{pmatrix}, S^\mu = \frac{1}{\sqrt{2}} \begin{pmatrix} \frac{h^\mu_{1,N} + b^{0\mu}_1}{\sqrt{2}} & b^{+\mu}_1 & K^{+\mu}_{1B} \\ b^{-\mu}_1 & \frac{h^\mu_{1N} - b^{0\mu}_1}{\sqrt{2}} & K^{0\mu}_{1B} \\ K^{-\mu}_{1B} & \bar{K}^{0\mu}_{1B} & h^\mu_{1S} \end{pmatrix}$$

$$W^{\mu\nu\rho} = \frac{1}{\sqrt{2}} \begin{pmatrix} \frac{\omega^{\mu\nu\rho}_{3,N} + \rho^{0\mu\nu\rho}_3}{\sqrt{2}} & \rho^{+\mu\nu\rho}_3 & K^{+\mu\nu\rho}_3 \\ \rho^{-\mu\nu\rho}_3 & \frac{\omega^{\mu\nu\rho}_{3,N} - \rho^{0\mu\nu\rho}_3}{\sqrt{2}} & K^{0\mu\nu\rho}_3 \\ K^{-\mu\nu\rho}_3 & \bar{K}^{0\mu\nu\rho}_3 & \omega^{\mu\nu\rho}_{3,S} \end{pmatrix},$$

Transformations of nonets under the symmetries

- Parity transformation: $P = \gamma^0$
- Charge conjugation: $C = i\gamma^2\gamma^0$
- Flavour symmetry: 3×3 matrix $U^\dagger U = 1$

Nonet	Parity (P)	Charge conjugation (C)	Flavour ($U_V(3)$)
$0^{++} = S$	$S(t, -\vec{x})$	S^t	$USU^\dagger$
$0^{-+} = P$	$-P(t, -\vec{x})$	P^t	$UPU^\dagger$
$1^{--} = V^\mu$	$V_\mu(t, -\vec{x})$	$-(V^\mu)^t$	$UV^\mu U^\dagger$
$1^{++} = A^\mu$	$-A_\mu(t, -\vec{x})$	$(A^\mu)^t$	$UA^\mu U^\dagger$
$1^{+-} = S^\mu$	$-S_\mu(t, -\vec{x})$	$-(S^\mu)^t$	$US^\mu U^\dagger$
$2^{++} = X^{\mu\nu}$	$X_{\mu\nu}(t, -\vec{x})$	$(X^{\mu\nu})^t$	$UX^{\mu\nu} U^\dagger$
$3^{--} = W^{\mu\nu\rho}$	$W_{\mu\nu\rho}(t, -\vec{x})$	$-(W^{\mu\nu\rho})^t$	$UW^{\mu\nu\rho} U^\dagger$

Effective Lagrangians

- Considering the mass relation $M_W > M_A + M_B$
- Interactions minimal number of the derivative terms
- CPT-invariance
- $U(3)_V$ symmetry

Decay Modes	Interaction Lagrangians
$3^{--} \to 0^{-+} + 0^{-+}$	$g_1 \mathrm{tr}\big(W^{\mu\nu\rho}\big[P, (\partial_\mu\partial_\nu\partial_\rho P)\big]_-\big)$
$3^{--} \to 0^{-+} + 0^{++}$	$g_2 \varepsilon_{\mu\nu\rho\sigma} \mathrm{tr}\big(\partial^\nu W^{\mu\alpha\beta}\big[(\partial^\rho S), (\partial^\sigma\partial_\alpha\partial_\beta P)\big]_-\big) = 0$
$3^{--} \to 0^{-+} + 1^{--}$	$g_3 \varepsilon^{\mu\nu\rho\sigma}\, \mathrm{tr}\big[W_{\mu\alpha\beta}\big\{(\partial_\nu V_\rho), (\partial^\alpha\partial^\beta\partial_\sigma P)\big\}_+\big]$
$3^{--} \to 0^{-+} + 1^{+-}$	$g_4 \mathrm{tr}\big[W^{\mu\nu\rho}\big\{S_\mu, (\partial_\nu\partial_\rho P)\big\}_+\big]$
$3^{--} \to 0^{-+} + 1^{++}$	$g_5 \mathrm{tr}\big(W^{\mu\nu\rho}\big[A_\mu, (\partial_\nu\partial_\rho P)\big]_-\big)$
$3^{--} \to 0^{-+} + 2^{++}$	$g_6 \varepsilon_{\mu\nu\rho\sigma} \mathrm{tr}\big(W^{\mu}_{\alpha\beta}\big[(\partial^\nu X^{\rho\alpha}), (\partial^\sigma\partial^\beta P)\big]_-\big)$
$3^{--} \to 1^{--} + 1^{--}$	$g_7 \mathrm{tr}\big(W^{\mu\nu\rho}\big[(\partial_\mu V_\nu), V_\rho\big]_-\big)$

Feynmann rules

- For coupling constant which is the free parameter of the model

$$g \to -i\, g$$

- For each derivatives

$$\partial_\mu \to i k_\mu$$

- Polarization vector for the massive vector field

$$V^\mu \to \epsilon^\mu(\lambda_v,\, \vec{k}_v)$$

- For the tensor-2 field

$$X^{\mu\nu} \to \epsilon^{\mu\nu}(\lambda_t,\, \vec{k}_t)$$

- For the tensor-3 field

$$W^{\mu\nu\rho} \to \epsilon^{\mu\nu\rho}(\lambda_w,\, \vec{k}_w)$$

Polarization sums for vector and tensor-2 fields

- For massive vector fields $V_\mu \propto \int_{dk} \sum_{\lambda=1}^{3} \epsilon_\mu(\lambda,\, \vec{k})(a e^{-ikx} + a^\dagger e^{ikx})$
- $k_\mu \epsilon^\mu = 0$ and $\epsilon_\mu(\lambda)\epsilon^\mu(\lambda') = \delta_{\lambda,\lambda'}$

$$\sum_{\lambda=1}^{3} \epsilon_\mu(\lambda,\, \vec{k})\, \epsilon_\nu(\lambda,\, \vec{k}) = -G_{\mu\nu}$$

- For massive spin-2 tensors $X_{\mu\nu} \propto \int_{dk} \sum_{\lambda=1}^{5} \epsilon_{\mu\nu}(\lambda,\, \vec{k})(a e^{-ikx} + a^\dagger e^{ikx})$
- Fierz-Pauli constraints: $X^{\mu\nu} - X^{\nu\mu} = 0, \quad g_{\mu\nu} X^{\mu\nu} = 0$ and $\partial_\mu X^{\mu\nu} = 0$
- Orthonormality condition $\epsilon^{\mu\nu}(\lambda)\epsilon_{\mu\nu}(\lambda') = -\delta_{\lambda\lambda'}$

$$\sum_{\lambda=1}^{5} \epsilon_{\mu\nu}(\lambda,\, \vec{k})\, \epsilon_{\alpha\beta}(\lambda,\, \vec{k}) = -\frac{G_{\mu\nu} G_{\alpha\beta}}{3} + \frac{G_{\mu\alpha} G_{\nu\beta} + G_{\mu\beta} G_{\nu\alpha}}{2}$$

where

$$G_{\mu\nu} \equiv \eta_{\mu\nu} - \frac{k_\mu k_\nu}{m^2}\,, \quad \eta_{\mu\nu} \equiv \begin{pmatrix} 1 & 0 & 0 & 0 \\ 0 & -1 & 0 & 0 \\ 0 & 0 & -1 & 0 \\ 0 & 0 & 0 & -1 \end{pmatrix}$$

Polarization sum for spin-3 fields

- Fierz-Pauli conditions for spin-3 fields lead:

$$\epsilon^{(\mu\nu\rho)} = 0, \quad \epsilon^{\mu\nu}_{\mu} = 0, \quad k_\mu \epsilon^{\mu\nu\rho} = 0$$

- Orthonormality condition

$$\epsilon^{\mu\nu\rho}(\lambda)\epsilon_{\mu\nu\rho}(\lambda') = -\delta_{\lambda\lambda'}$$

$$\sum_{\lambda=1}^{7} \epsilon_{\mu\nu\rho}(\lambda)\,\epsilon_{\alpha\beta\gamma}(\lambda) = \frac{1}{15}\Big\{ G_{\mu\nu}\Big(G_{\rho\alpha}G_{\beta\gamma} + G_{\rho\beta}G_{\alpha\gamma} + G_{\rho\gamma}G_{\alpha\beta}\Big)$$

$$G_{\mu\rho}\Big(G_{\nu\alpha}G_{\beta\gamma} + G_{\nu\beta}G_{\alpha\gamma} + G_{\nu\gamma}G_{\alpha\beta}\Big) + G_{\nu\rho}\Big(G_{\mu\alpha}G_{\beta\gamma} + G_{\mu\beta}G_{\alpha\gamma} + G_{\mu\gamma}G_{\alpha\beta}\Big)$$

$$-\frac{5}{2}\Big[G_{\mu\alpha}\Big(G_{\nu\beta}G_{\rho\gamma} + G_{\nu\gamma}G_{\rho\beta}\Big) + G_{\mu\beta}\Big(G_{\nu\alpha}G_{\rho\gamma} + G_{\nu\gamma}G_{\rho\alpha}\Big)$$

$$+G_{\mu\gamma}\Big(G_{\nu\alpha}G_{\rho\beta} + G_{\nu\beta}G_{\rho\alpha}\Big)\Big]\Big\}$$

Decay width and Amplitudes

- Formula for the decay rate

$$\Gamma(W \to 1+2) = \frac{|k_z|}{8\pi M_W^2} \times |-i\mathcal{M}|^2 \times \text{channel} \times \theta(M_W - m_1 - m_2)$$

- Using the the conservation of four momenta $(M_W, 0) = (E_1, k_{1z}) + (E_2, k_{2z})$ leads $|k_z| = \frac{1}{2M_W}\sqrt{(M_W^2 - m_1^2 - m_2^2)^2 - 4m_1^2 m_2^2}$

Decay Mode	Amplitude $\lvert -i\mathcal{M}\rvert^2$
$3^{--} \to 0^{-+} + 0^{-+}$	$g^2_{WPP} \times \frac{2k_z^6}{35}$
$3^{--} \to 0^{-+} + 1^{--}$	$g^2_{WPV} \times \frac{8k_z^6 M_W^2}{105}$
$3^{--} \to 0^{-+} + 1^{+-}$	$g^2_{WSP} \times \frac{2k_z^4}{105}(7 + \frac{3k_z^2}{m_S^2})$
$3^{--} \to 0^{-+} + 1^{++}$	$g^2_{WAP} \times \frac{2k_z^4}{105}(7 + \frac{3k_z^2}{m_A^2})$
$3^{--} \to 0^{-+} + 2^{++}$	$g^2_{WXP} \times \frac{2k_z^4 M_W^2}{m_X^2 105}(2k_z^2 + 7m_X^2)$
$3^{--} \to 1^{--} + 1^{--}$	$g^2_{WVV} \times \frac{2k_z^2}{105 m_{v1}^2 m_{v2}^2}(3k_z^2 + 7m_{v1}^2)(k_z^2 + m_{v2}^2)$

Theoretical and experimental results for $W \to P + P$

- For the coupling constant $\tilde{g} \equiv g^2$, experimental results $\tilde{g}_i$ and errors on them Δg, $\Delta \tilde{g}_i$ we define $\chi^2 \equiv \sum_{i=1}^{N} \frac{(\tilde{g}-\tilde{g}_i)^2}{\Delta \tilde{g}_i^2}$
- Minimizing χ^2 with respect to coupling $\frac{d\chi^2}{d\tilde{g}} = 0$ leads to

$$\tilde{g} = \frac{\sum_{i=1}^{N} \frac{\tilde{g}_i}{\Delta \tilde{g}_i^2}}{\sum_{j=1}^{N} \frac{1}{\Delta \tilde{g}_j^2}}, \quad \Delta \tilde{g} = \sqrt{\frac{1}{\sum_{j=1}^{N} \frac{1}{\Delta g_j^2}}}, \quad \to g^2_{WPP} = (1.5 \pm 0.1) \cdot 10^{-10} (\mathrm{MeV})^{-4}$$

Decay process (in model)	Theory (MeV)	Experiment (MeV)
$\rho_3(1690) \longrightarrow \pi\,\pi$	32.7 ± 2.3	$38.0 \pm 3.2 \leftrightarrow (23.6 \pm 1.3)\%$
$\rho_3(1690) \longrightarrow \bar{K}\,K$	4.0 ± 0.3	$2.54 \pm 0.45 \leftrightarrow (1.58 \pm 0.26)\%$
$K_3^*(1780) \longrightarrow \pi\,\bar{K}$	18.5 ± 1.3	$29.9 \pm 4.3 \leftrightarrow (18.8 \pm 1.0)\%$
$K_3^*(1780) \longrightarrow \bar{K}\,\eta$	7.4 ± 0.6	$47.7 \pm 21.6 \leftrightarrow (30 \pm 13)\%$
$K_3^*(1780) \longrightarrow \bar{K}\,\eta'(958)$	0.02 ± 0.01	
$\omega_3(1670) \longrightarrow \bar{K}\,K$	3.0 ± 0.2	
$\phi_3(1850) \longrightarrow \bar{K}\,K$	18.8 ± 1.4	seen

Theoretical and experimental results for $W \to V + P$

- Repeating the same calculations in the previous section

$$g^2_{WVP} = (9.2 \pm 1.9) \cdot 10^{-16} (\mathrm{MeV})^{-6}$$

Decay process (in model)	Theory (MeV)	Experiment (MeV)
$\rho_3(1690) \longrightarrow \rho(770)\,\eta$	3.8 ± 0.8	seen
$\rho_3(1690) \longrightarrow \rho(770)\,\eta'(958)$	0	
$\rho_3(1690) \longrightarrow \bar{K}^*(892)\,K + \mathrm{c.c.}$	3.4 ± 0.7	
$\rho_3(1690) \longrightarrow \omega(782)\,\pi$	35.8 ± 7.4	$25.8 \pm 9.8 \leftrightarrow (16 \pm 6)\%$
$\rho_3(1690) \longrightarrow \phi(1020)\,\pi$	0.17 ± 0.04	
$K_3^*(1780) \longrightarrow \rho(770)\,K$	16.8 ± 3.4	$49.3 \pm 15.7 \leftrightarrow (31 \pm 9)\%$
$K_3^*(1780) \longrightarrow \bar{K}^*(892)\,\pi$	27.2 ± 5.6	$31.8 \pm 9.0 \leftrightarrow (20 \pm 5)\%$
$K_3^*(1780) \longrightarrow \bar{K}^*(892)\,\eta$	0.09 ± 0.02	
$K_3^*(1780) \longrightarrow \bar{K}^*(892)\,\eta'(958)$	0	
$K_3^*(1780) \longrightarrow \omega(782)\,\bar{K}$	4.3 ± 0.9	
$K_3^*(1780) \longrightarrow \phi(1020)\,\bar{K}$	1.2 ± 0.3	

Decay process (in model)	Theory (MeV)	Experiment (MeV)
$\omega_3(1670) \longrightarrow \rho(770)\,\pi$	96.9 ± 19.9	seen
$\omega_3(1670) \longrightarrow \bar{K}^*(892)\,K + \text{c.c.}$	2.9 ± 0.6	
$\omega_3(1670) \longrightarrow \omega(782)\,\eta$	2.8 ± 0.6	
$\omega_3(1670) \longrightarrow \omega(782)\,\eta'(958)$	0	
$\omega_3(1670) \longrightarrow \phi(1020)\,\eta$	≈ 0	
$\omega_3(1670) \longrightarrow \phi(1020)\,\eta'(958)$	0	
$\phi_3(1850) \longrightarrow \rho(770)\,\pi$	1.1 ± 0.3	
$\phi_3(1850) \longrightarrow \bar{K}^*(892)\,K + \text{c.c.}$	35.5 ± 7.3	seen
$\phi_3(1850) \longrightarrow \omega(782)\,\eta$	0.01 ± 0.01	
$\phi_3(1850) \longrightarrow \omega(782)\,\eta'(958)$	≈ 0	
$\phi_3(1850) \longrightarrow \phi(1020)\,\eta$	3.8 ± 0.8	
$\phi_3(1850) \longrightarrow \phi(1020)\,\eta'(958)$	0	

Table: The total decay widths are $\Gamma^{\text{tot}}_{\rho_3(1690)} = (161 \pm 10)$ MeV, $\Gamma^{\text{tot}}_{K_3^*(1780)} = (159 \pm 21)$ MeV, $\Gamma^{\text{tot}}_{\omega_3(1670)} = (168 \pm 10)$ MeV and $\Gamma^{\text{tot}}_{\phi_3(1850)} = (87^{+28}_{-23})$ MeV

Results for $W \to X + P$

- We used the following PDG data for defining the coupling constant $\frac{\Gamma(\rho_3 \to a_2 \pi)}{\Gamma(\rho_3 \to \rho \eta)} = 5.5 \pm 2.0$ MeV
  - $g^2_{WXP} = (2.83 \pm 1.18) \cdot 10^{-9} (\text{MeV})^{-4}$

Decay process (in model)	Theory (MeV)	Experiment (MeV)
$\rho_3(1690) \longrightarrow a_2(1320)\,\pi$	20.9 ± 8.8	seen
$\rho_3(1690) \longrightarrow \bar{K}_2^*(1430)\,K + \text{c.c.}$	0	
$K_3^*(1780) \longrightarrow a_2(1320)\,K$	0	
$K_3^*(1780) \longrightarrow \bar{K}_2^*(1430)\,\pi$	5.9 ± 2.5	$< 25.4 \leftrightarrow < 16\%$
$K_3^*(1780) \longrightarrow \bar{K}_2^*(1430)\,\eta$	0	
$K_3^*(1780) \longrightarrow \bar{K}_2^*(1430)\,\eta'(958)$	0	
$K_3^*(1780) \longrightarrow f_2(1270)\,\bar{K}$	≈ 0	
$K_3^*(1780) \longrightarrow f_2'(1525)\,\bar{K}$	0	
$\omega_3(1670) \longrightarrow \bar{K}_2^*(1430)\,K + \text{c.c.}$	0	
$\phi_3(1850) \longrightarrow \bar{K}_2^*(1430)\,K + \text{c.c.}$	0	

Theoretical limits for $W \to V + V$

- For this channel there is no enough information in PDG for defining the coupling constant
- We could only find the boundary for it $g^2_{WVV} \leq (1036 \pm 41)$

Decay process (in model)	Theory (MeV)	Experiment (MeV)
$\rho_3(1690) \longrightarrow \rho(770)\,\rho(770)$	$\leq 107.9 \pm 36.0$	seen
$\rho_3(1690) \longrightarrow \bar{K}^*(892)\,K^*(892)$	0	
$K_3^*(1780) \longrightarrow \rho(770)\,\bar{K}^*(892)$	$\leq 44.5 \pm 1.8$	
$K_3^*(1780) \longrightarrow \bar{K}^*(892)\,\omega(782)$	$\leq 13.3 \pm 0.5$	
$K_3^*(1780) \longrightarrow \bar{K}^*(892)\,\phi(1020)$	0	
$\omega_3(1670) \longrightarrow \bar{K}^*(892)\,K^*(892)$	0	
$\phi_3(1850) \longrightarrow \bar{K}^*(892)\,K^*(892)$	$\leq 31.1 \pm 1.2$	

Table: The total decay widths are $\Gamma^{\text{tot}}_{\rho_3(1690)} = (161 \pm 10)$ MeV, $\Gamma^{\text{tot}}_{K_3^*(1780)} = (159 \pm 21)$ MeV, $\Gamma^{\text{tot}}_{\omega_3(1670)} = (168 \pm 10)$ MeV and $\Gamma^{\text{tot}}_{\phi_3(1850)} = (87^{+28}_{-23})$ MeV

Theoretical predictions for Glueballs

- Glueballs are not experimentally observed yet
- Lattice results for the mass of $J^{PC} = 3^{--}$ glueballs are about $m_{G_3} = 4.2 GeV$
- Decay of the tensor-glueball to the vector and pseudo-scalar mesons
- Interaction lagrangian

$$\mathcal{L}_I = c_{GVP} G_{\mu\alpha\beta} \varepsilon^{\mu\nu\rho\sigma} \left\{ (\partial_\nu V_\rho), (\partial^\alpha \partial^\beta \partial_\sigma P) \right\}$$

- We can only calculate the decay ratios

BR for $G_3(4200)$	Theory
$\frac{\Gamma(G_3 \to \rho_1 \pi)}{\Gamma(G_3 \to \omega_1 \eta)}$	5.74
$\frac{\Gamma(G_3 \to K_1 K)}{\Gamma(G_3 \to \omega_1 \eta)}$	6.36
$\frac{\Gamma(G_3 \to K_1 K)}{\Gamma(G_3 \to \phi_1 \eta')}$	10.44
$\frac{\Gamma(G_3 \to K_1 K)}{\Gamma(G_3 \to \phi_1 \eta)}$	11.28
$\frac{\Gamma(G_3 \to K_1 K)}{\Gamma(G_3 \to \omega_1 \eta')}$	12.43

Table: Decay ratios for tensor Glueballs $J^{PC} = 3^{--}$

Conclusion

- Phenomenology of the spin-3 mesons is studied
- PDG data is explained using the effective lagrangian description for tree level
- $SU(N_f = 3)_V$ approximate symmetry is considered main symmetry for effective model
- Other symmetries of QCD such as $SU(N_c = 3)$ and $U(1)_V$ are still exist within this model since mesons are colorless and $B = 0$ objects
- $U(1)_A$ symmetry does not exist because of the quantum effects
- $SU(N_f = 3)_A$ is also broken since the model is not in chiral regime ($m_i = 0$)
- We predict some values for decay rates which can be tested in future
- We do not have enough experimental information for theoretical calculations of $3^{--} \to [0^{-+} + 1^{++}]$ & $[0^{-+} + 1^{+-}]$ decay products
- Some theoretical predictions for decay ratios for 3^{--} glueballs are presented
- Only allowed decay channels for 3^{--} glueball are $S + P$ and $V + P$

Thank you for your attention!

On the phase structure and equation of state of strongly-interacting matter

Mario Motta
in collaboration with W.Alberico, A.Beraudo and R. Stiele

University of Turin
Frontiers in Nuclear and Hadronic Physics 2020

March 4 2020,Florence

Contents

Exploration of the QCD phase diagram

- Phase Diagram
- Observables
- PNJL
- Thermodynamic and Fluctuations
- Results
- Conclusion a outlook

Phase Diagram

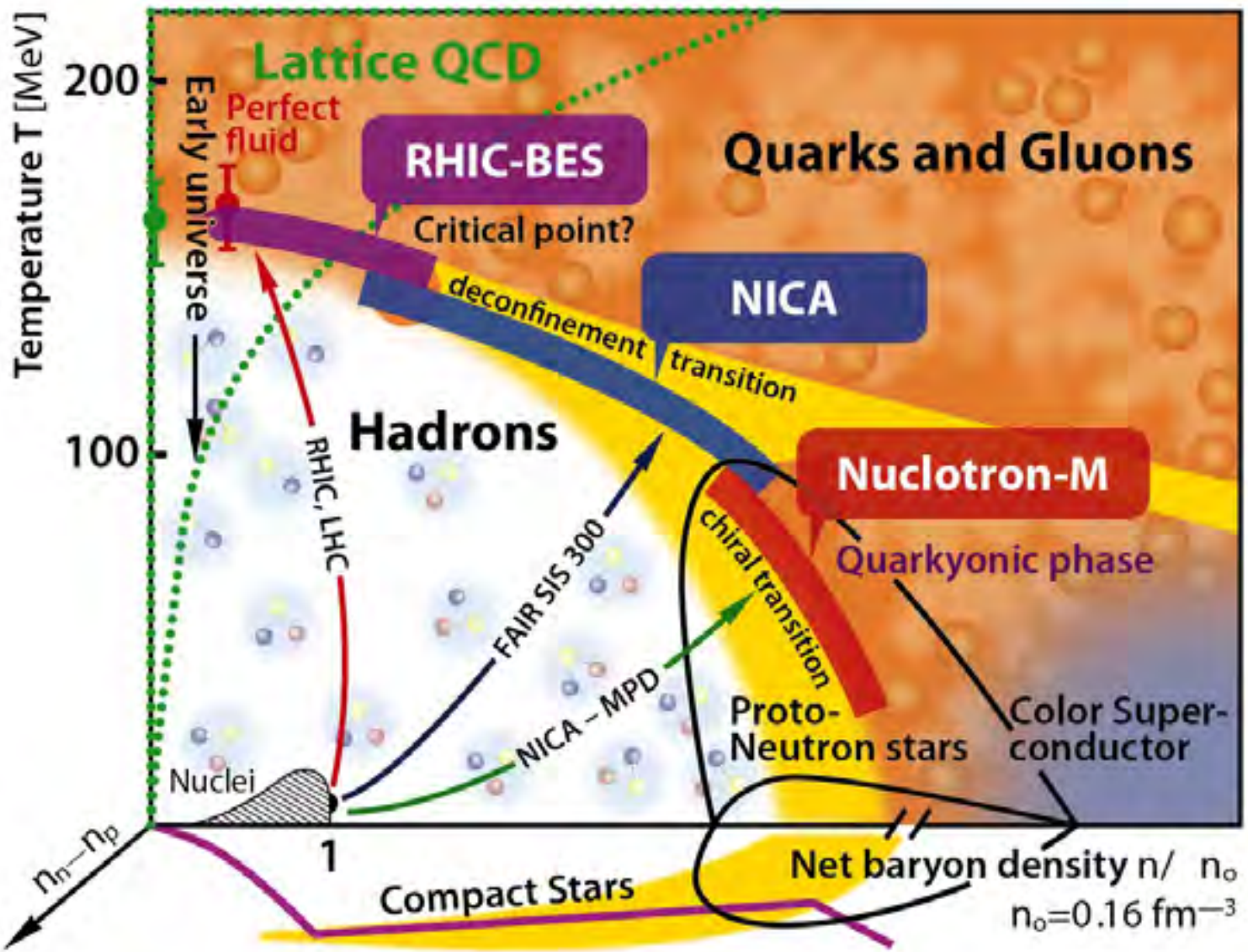

Why we explore the QCD Phase Diagram?

The description of nuclear matter and the interaction between nucleons in the nuclei should ultimately be provided by QCD. This theory contains two important features:

- confinement
- spontaneous chiral symmetry breaking

The knowledge of these two QCD features is not complete. the explorations of the phase diagram (in particular the region where chiral symmetry is restored and confinement does not occur) may provide a full understanding of these two phenomena

Observables

Which Observables are important for the explorations of the Phase Diagram?

- isentropic trajectories

Observables

Which Observables are important for the explorations of the Phase Diagram?

- isentropic trajectories
- speed of sound

Observables

Which Observables are important for the explorations of the Phase Diagram?

- isentropic trajectories
- speed of sound
- order parameters

Observables

Which Observables are important for the explorations of the Phase Diagram?

- isentropic trajectories
- speed of sound
- order parameters
- fluctuations of conserved charge of QCD

Isentropic trajectories

Along isentropic trajectories, the system evolves in time keeping constant entropy. The QGP expands, during this expansion baryon number density and entropy density change (pure dilution), but $s/n = cost$. Then the isentropic trajectories is replaced by "Iso-s/n" trajectories

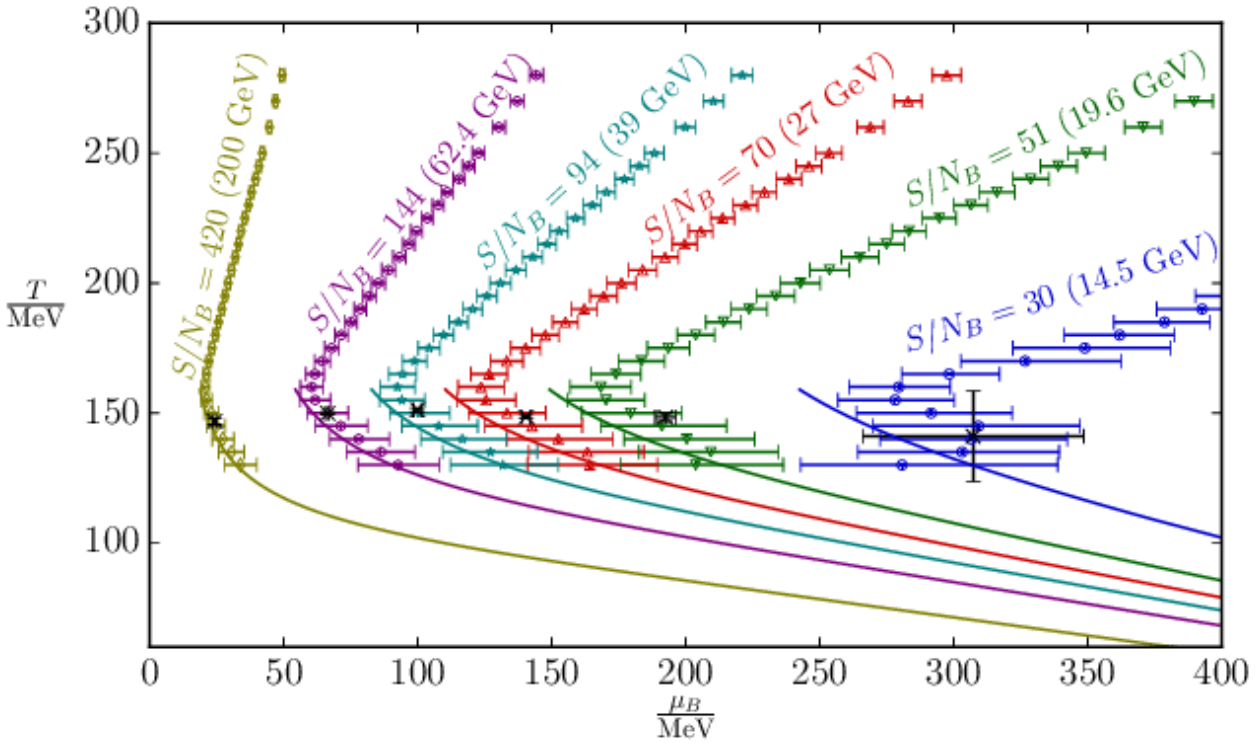

Figure: isentropic trajectories from N.Guenther et al Nucl.Phys. A967 (2017) 720-723

Speed of sound

The speed of sound is one of the most important characteristics in hydrodynamics: it is responsible for the collective acceleration of the fireball and it governs the evolution of the fireball produced in the heavy-ion collision as well as one of the most important observables for describing of QGP formation: the elliptic flow.

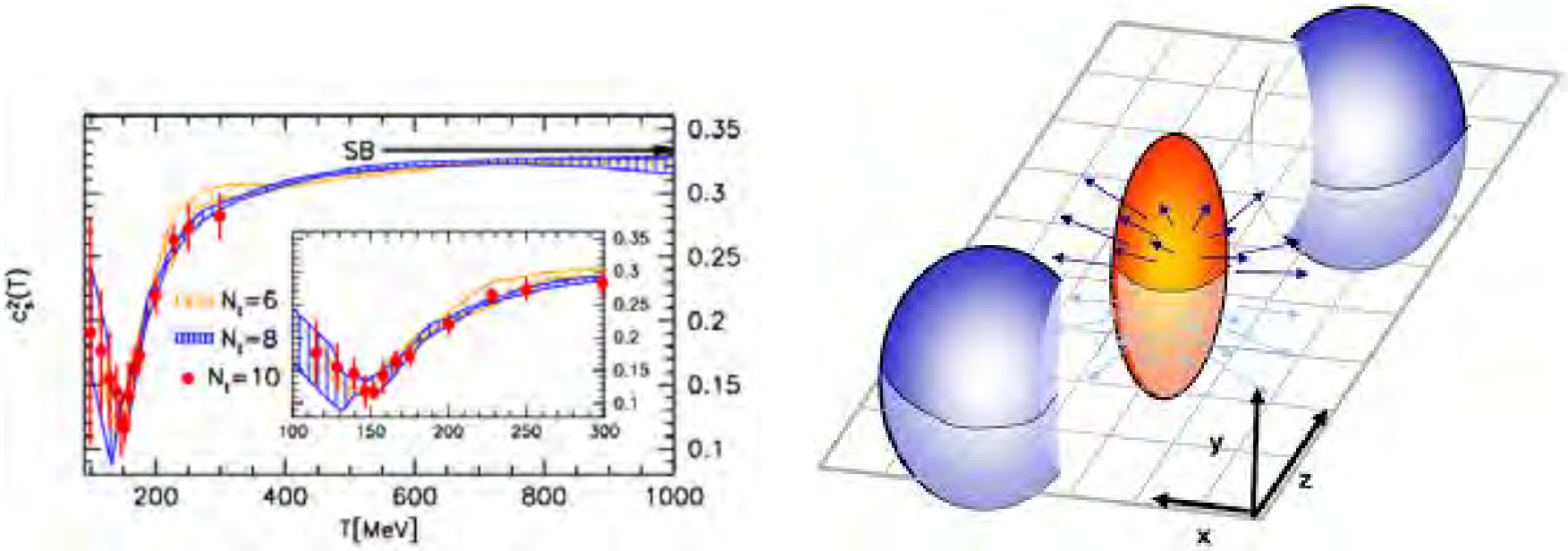

Figure: the square of speed of sound (Szabolcs Borsanyi et all JHEP 1011 (2010) 077) and a picture of HIC

Speed of sound

The speed of sound is one of the most important characteristics in hydrodynamics: it is responsible for the collective acceleration of the fireball and it governs the evolution of the fireball produced in the heavy-ion collision as well as one of the most important observables for describing of QGP formation: the elliptic flow.

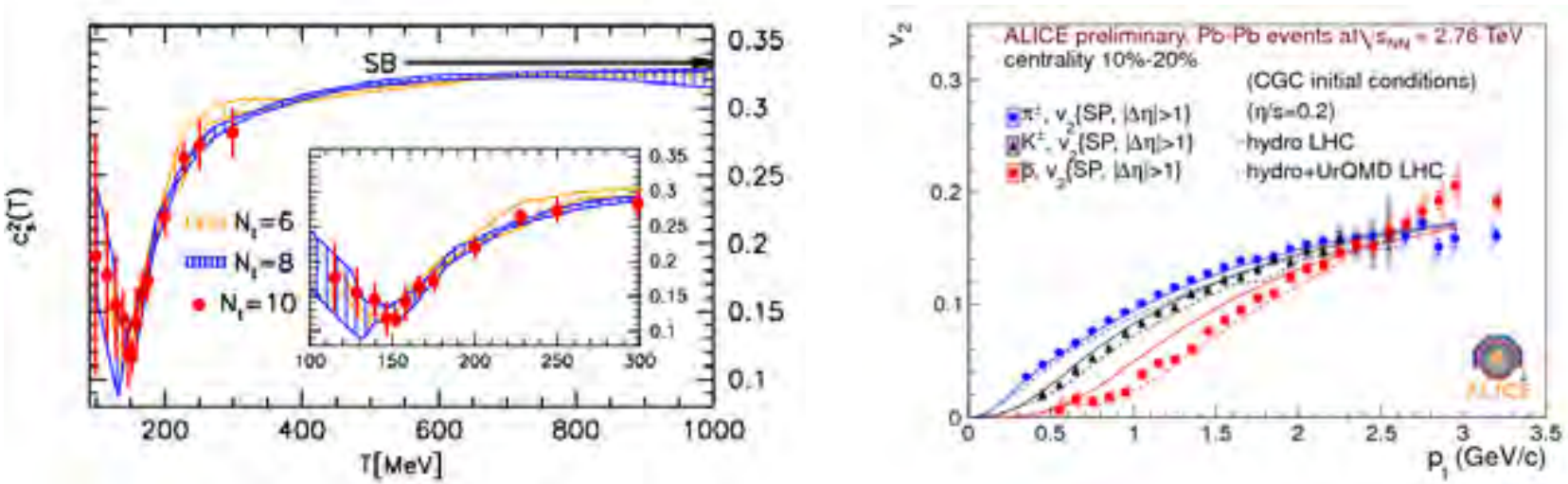

Figure: the square of speed of sound and the Elliptic Flow

Speed of sound

The speed of sound is one of the most important characteristics in hydrodynamics: it is responsible for the collective acceleration of the fireball and it governs the evolution of the fireball produced in the heavy-ion collision as well as one of the most important observables for describing of QGP formation: the elliptic flow.

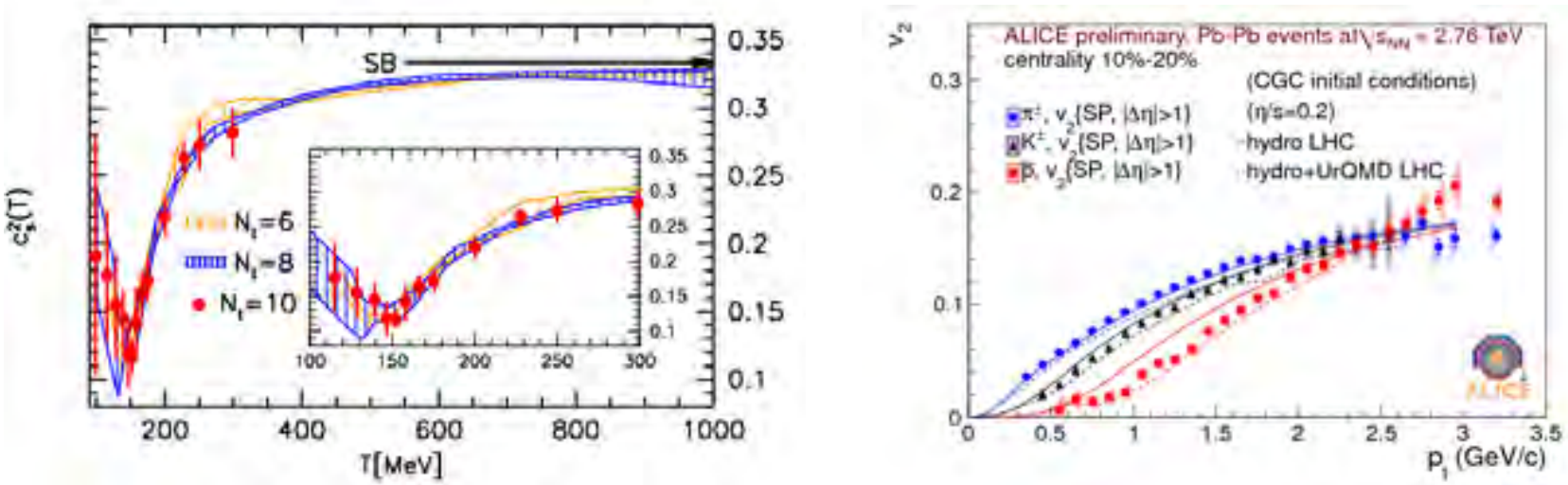

Figure: the square of speed of sound and the Elliptic Flow

$$(\epsilon + P)\frac{dv^i}{dt} = -c_s^2\frac{d\epsilon}{dx^i} \tag{1}$$

Order Parameters

The order parameters signal the transition lines and their behaviour near the transition fixes the order of transition (cross-over, 1^{st}-order, 2^{st}-order,ect.)

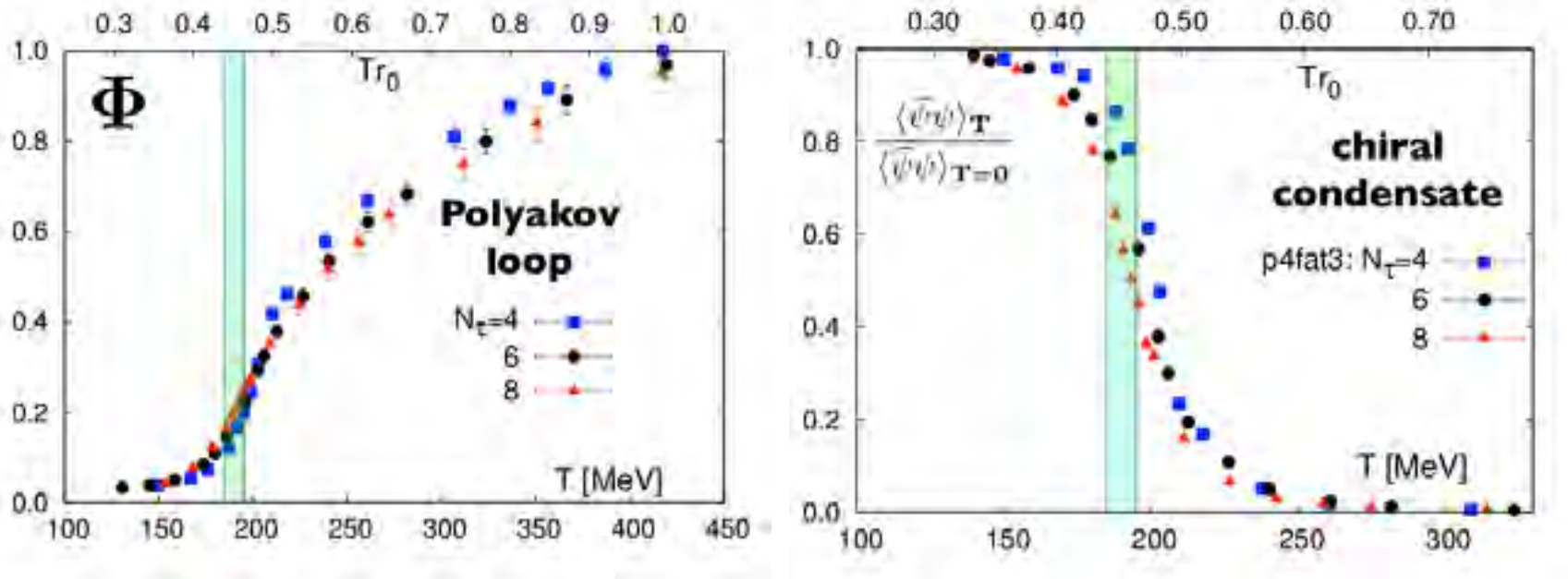

Figure: the order parameters for deconfinament and chiral symmetry restoration transition W.Weise,174,JPS,10.1143/PTPS.174.1

Fluctuations of QCD conserved charges

In many different fields, the study of fluctuations can provide physical insights into the underlying microscopic physics. The fluctuations can become invaluable physical observable in spite of their difficult character. Fluctuations are powerful tools to diagnose microscopic physics, to trace back the history of the system and the nature of its elementary degrees of freedom (see M. Asakawa and M. Kitazawa, Prog. Part. Nucl.Phys. 90, 299 (2016) doi:10.1016/j.ppnp.2016.04.002).

Fluctuations of QCD conserved charges

In many different fields, the study of fluctuations can provide physical insights into the underlying microscopic physics. The fluctuations can become invaluable physical observable in spite of their difficult character. Fluctuations are powerful tools to diagnose microscopic physics, to trace back the history of the system and the nature of its elementary degrees of freedom (see M. Asakawa and M. Kitazawa, Prog. Part. Nucl.Phys. 90, 299 (2016) doi:10.1016/j.ppnp.2016.04.002).

My work is focused on fluctuations of conserved charges in the QCD Phase Diagram (B, Q, S) explored through their cumulants.

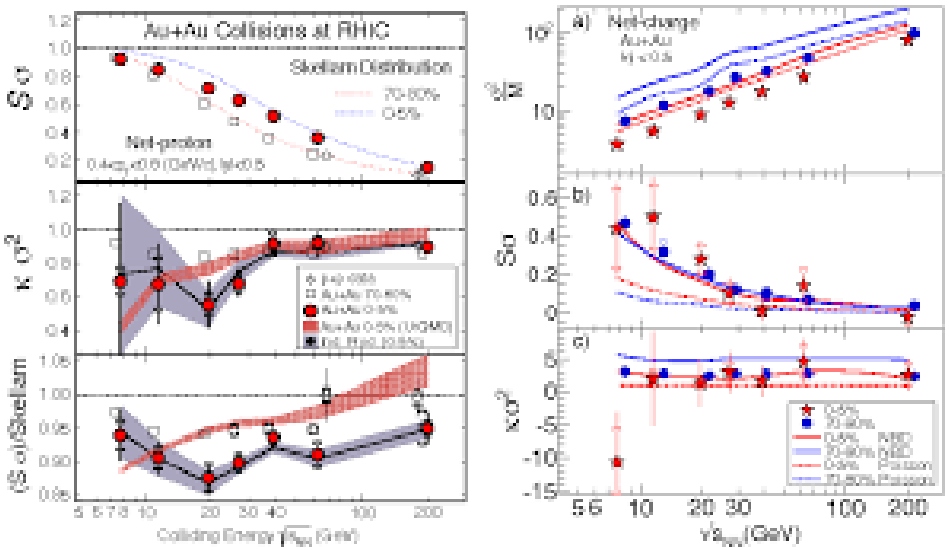

Figure: Combinations of Cumulants in HIC N.R.Sahoo and the Star Collaboration 2014 J.Phys.:Conf. Ser. 535 012007

How can we explore the Phase Diagram?

Effective Field Theories

The basic idea of an Effective Field Theories (EFT) is that, if one is interested in describing phenomena occurring at a certain (low) energy scale, one does not need to solve the exact microscopic theory in order to provide useful predictions.

How can we explore the Phase Diagram?

Effective Field Theories

The basic idea of an Effective Field Theories (EFT) is that, if one is interested in describing phenomena occurring at a certain (low) energy scale, one does not need to solve the exact microscopic theory in order to provide useful predictions.

In general, Effective Field Theories are low-energy approximations of more fundamental theories. Instead of solving the underlying theory,low-energy physics is described with a set of variables that are suited to the particular energy region one is interested in.

PNJL

$$\mathcal{L}_{PNJL} = \bar{q}(i\gamma^\mu D_\mu - \hat{m})q + \frac{1}{2}G[(\bar{q}\vec{\tau}q)^2 + (\bar{q}i\gamma^5\vec{\tau}q)^2] + \\ + K\{det[\bar{q}(1+\gamma^5)q] + det[\bar{q}(1-\gamma^5)q]\} - \mathcal{U}(\Phi[A], \bar{\Phi}[A], T) \tag{2}$$

Here $D^\mu = \partial^\mu - iA^\mu$, $A^\mu = \delta^\mu_0 A^0$, the fields Φ and $\bar{\Phi}$ are Polyakov fields defined as:

$$\Phi \equiv \frac{1}{N_c} Tr\langle\langle L\rangle\rangle \qquad \bar{\Phi} \equiv \frac{1}{N_c} Tr\langle\langle L^\dagger\rangle\rangle \tag{3}$$

Where L is the Polyakov loop defined in terms of the gauge field A_4,after Wick rotation:

$$L(\vec{x}) \equiv \mathcal{P}\Big\{ i \int_0^\beta d\tau A_4(\tau, \vec{x}) \Big\} \tag{4}$$

Due to the second term in (2) the PNJL isn't renormalizable and I introduce a cut-off (Λ) for regularizing the integrals.
Below I indicate the quark chiral condensate as:

$$\langle \bar{q}_i q_i \rangle \equiv \varphi_i \quad i = u, d, s \tag{5}$$

Polyakov Potential

The Polyakov Potential replaces the gluonic interaction of QCD in this EFT. I'm using these two parametrizations:

- Polynomial:

$$\frac{\mathcal{U}}{T^4} = -\frac{b_2(T)}{2}\bar{\Phi}\Phi - \frac{b_3}{6}(\bar{\Phi}^3 + \Phi^3) + \frac{b_4}{4}(\bar{\Phi}\Phi)^2 \tag{6}$$

$$b_2(T) = a_0 + a_1\frac{T_0}{T} + a_2\left(\frac{T_0}{T}\right)^2 + a_3\left(\frac{T_0}{T}\right)^3$$

- Logarithmic:

$$\frac{\mathcal{U}}{T^4} = a(T)\bar{\Phi}\Phi + b(T)\ln\left[1 - 6\bar{\Phi}\Phi + 4(\bar{\Phi}^3 + \Phi^3) - 3(\bar{\Phi}\Phi)^2\right] \tag{7}$$

$$a(T) = a_0 + a_1\frac{T_0}{T} + a_2\left(\frac{T_0}{T}\right)^2, \quad b(T) = b_3\left(\frac{T_0}{T}\right)^3$$

The Parameters are fixed for reproducing the lattice data for pure YM-Theory (C.Ratti,et al in Phys.Rev. D 73,014019 (2006) and Nuc.Phys A Vol 814, 1-4 (2008))

Thermodynamics

From PNJL Lagrangian one obtains the Thermodynamic Grand Potential per unit volume($\omega = \Omega/V$) in Mean Fields Approximation:

$$\omega(\Phi, \bar{\Phi}, T, M_j, \mu_j) = \mathcal{U}(\Phi, \bar{\Phi}, T) + G \sum_{i=u,d,s} \varphi_i^2 + 4K\varphi_u\varphi_d\varphi_s +$$

$$-2 \sum_{i=u,d,s} \left(N_c \int^{\Lambda} \frac{d^3p}{(2\pi)^3} E_i + T \int^{\Lambda} \frac{d^3p}{(2\pi)^3} \left\{ z_{\Phi}^{i+}(E_i, \mu_i) + z_{\Phi}^{i-}(E_i, \mu_i) \right\} \right)$$

Thermodynamics

From PNJL Lagrangian one obtains the Thermodynamic Grand Potential per unit volume($\omega = \Omega/V$) in Mean Fields Approximation:

$$\omega(\Phi, \bar{\Phi}, T, M_j, \mu_j) = \mathcal{U}(\Phi, \bar{\Phi}, T) + G \sum_{i=u,d,s} \varphi_i^2 + 4K\varphi_u\varphi_d\varphi_s +$$

$$-2 \sum_{i=u,d,s} \left(N_c \int^{\Lambda} \frac{d^3p}{(2\pi)^3} E_i + T \int^{\Lambda} \frac{d^3p}{(2\pi)^3} \{ z_{\Phi}^{i+}(E_i, \mu_i) + z_{\Phi}^{i-}(E_i, \mu_i) \} \right)$$

From ω it is possible to obtain all thermodynamics quantities of interest:

$$P = -\omega, \quad s = -\frac{\partial \omega}{\partial T}, \quad n_i = -\frac{\partial \omega}{\partial \mu_i}, \quad \chi_n^i = -\frac{\partial^n \omega}{\partial \mu_i^n} \tag{8}$$

$$\epsilon = -P + sT + \sum_i \mu_i n_i \tag{9}$$

Cumulants

To describe the fluctuations of conserved charge we can use the cumulants. The relations between the first four moments and first cumulants read:

Cumulants

To describe the fluctuations of conserved charge we can use the cumulants. The relations between the first four moments and first cumulants read:

$$\begin{aligned}
\langle x \rangle_c &= \langle x \rangle \equiv M \\
\langle x^2 \rangle_c &= \langle x^2 \rangle - \langle x \rangle^2 \equiv \sigma^2 \\
\langle x^3 \rangle_c &= \langle (x - \langle x \rangle)^3 \rangle \equiv \gamma \sigma^3 \\
\langle x^4 \rangle_c &= \langle (x - \langle x \rangle)^4 \rangle - 3\sigma^4 \equiv \kappa \sigma^4
\end{aligned} \tag{10}$$

Cumulants

To describe the fluctuations of conserved charge we can use the cumulants. The relations between the first four moments and first cumulants read:

$$\begin{aligned}
\langle x \rangle_c &= \langle x \rangle \equiv M \\
\langle x^2 \rangle_c &= \langle x^2 \rangle - \langle x \rangle^2 \equiv \sigma^2 \\
\langle x^3 \rangle_c &= \langle (x - \langle x \rangle)^3 \rangle \equiv \gamma \sigma^3 \\
\langle x^4 \rangle_c &= \langle (x - \langle x \rangle)^4 \rangle - 3\sigma^4 \equiv \kappa \sigma^4
\end{aligned} \tag{10}$$

κ is called kurtosis and γ is called skewness. This two quantities represent respectively the "sharpness" and asymmetry of the distribution.

Cumulants

To describe the fluctuations of conserved charge we can use the cumulants. The relations between the first four moments and first cumulants read:

$$\begin{aligned}
\langle x \rangle_c &= \langle x \rangle \equiv M \\
\langle x^2 \rangle_c &= \langle x^2 \rangle - \langle x \rangle^2 \equiv \sigma^2 \\
\langle x^3 \rangle_c &= \langle (x - \langle x \rangle)^3 \rangle \equiv \gamma \sigma^3 \\
\langle x^4 \rangle_c &= \langle (x - \langle x \rangle)^4 \rangle - 3\sigma^4 \equiv \kappa \sigma^4
\end{aligned} \tag{10}$$

κ is called kurtosis and γ is called skewness. This two quantities represent respectively the "sharpness" and asymmetry of the distribution.
The cumulants are more convenient than moments, e.g, when one consider the products of distributions, the cumulant of the product distribution is the product of cumulants.

Cumulants

To describe the fluctuations of conserved charge we can use the cumulants. The relations between the first four moments and first cumulants read:

$$\begin{aligned}
\langle x \rangle_c &= \langle x \rangle \equiv M \\
\langle x^2 \rangle_c &= \langle x^2 \rangle - \langle x \rangle^2 \equiv \sigma^2 \\
\langle x^3 \rangle_c &= \langle (x - \langle x \rangle)^3 \rangle \equiv \gamma \sigma^3 \\
\langle x^4 \rangle_c &= \langle (x - \langle x \rangle)^4 \rangle - 3\sigma^4 \equiv \kappa \sigma^4
\end{aligned} \tag{10}$$

κ is called kurtosis and γ is called skewness. This two quantities represent respectively the "sharpness" and asymmetry of the distribution.
The cumulants are more convenient than moments, e.g, when one consider the products of distributions, the cumulant of the product distribution is the product of cumulants.
In my work I consider the following combinations of cumulants:

$$\kappa\sigma^2 = \frac{\langle x^4 \rangle_c}{\langle x^2 \rangle_c} \qquad \frac{\gamma\sigma^3}{M} = \frac{\langle x^3 \rangle_c}{\langle x \rangle_c} \tag{11}$$

Results

In the last part of my presentation I show the numerical results obtained with PNJL for the following observables:

- isentropic trajectories
- speed of sound
- fluctuations of net Baryon number

Results

In the last part of my presentation I show the numerical results obtained with PNJL for the following observables:

- isentropic trajectories
- speed of sound
- fluctuations of net Baryon number

From a general point of view the phase diagram of QCD is a 4-dimension space: 3 dimensions for the quark chemical potentials and 1 for temperature.I perform my calculations in the following scenarios:

Results

In the last part of my presentation I show the numerical results obtained with PNJL for the following observables:

- isentropic trajectories
- speed of sound
- fluctuations of net Baryon number

From a general point of view the phase diagram of QCD is a 4-dimension space: 3 dimensions for the quark chemical potentials and 1 for temperature.I perform my calculations in the following scenarios:

- Symmetric chemical potential: $\mu_u = \mu_d = \mu_s = \frac{1}{3}\mu_B$
- (Quasi-)Neutral Strangeness: $\mu_u = \mu_d = \frac{1}{3}\mu_B$, $\mu_s = 0$
- HIC: $\frac{n_Q}{n_B} = 0.4$, $n_s = 0$

Results:isentropic trajectories

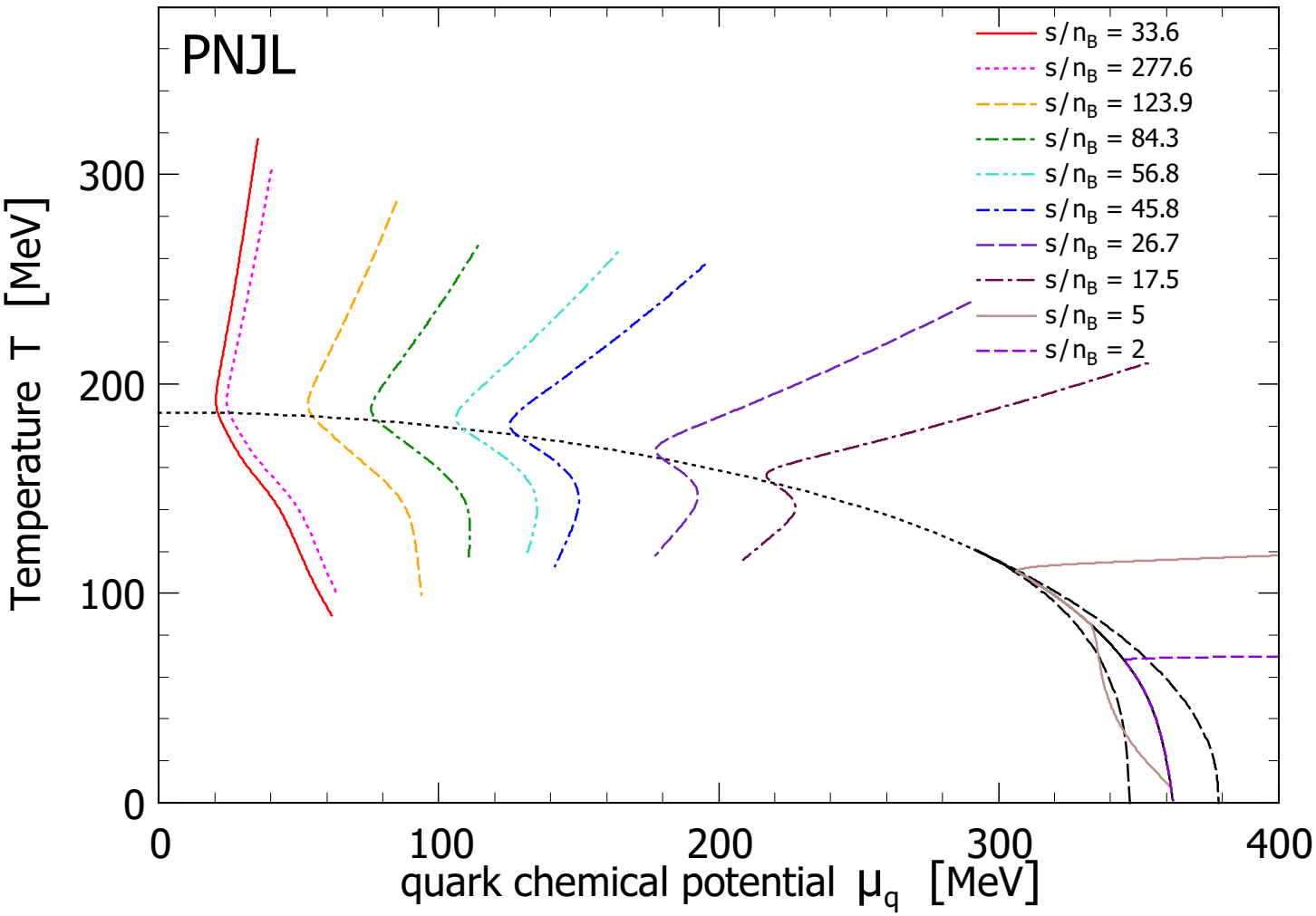

Figure: Isentropic Trajectories in the (Quasi)-neutral strangeness (M.Motta et al in prep.(March 2020)

Results:EoS

$$\epsilon_{SB} = 3P_{SB} \tag{12}$$

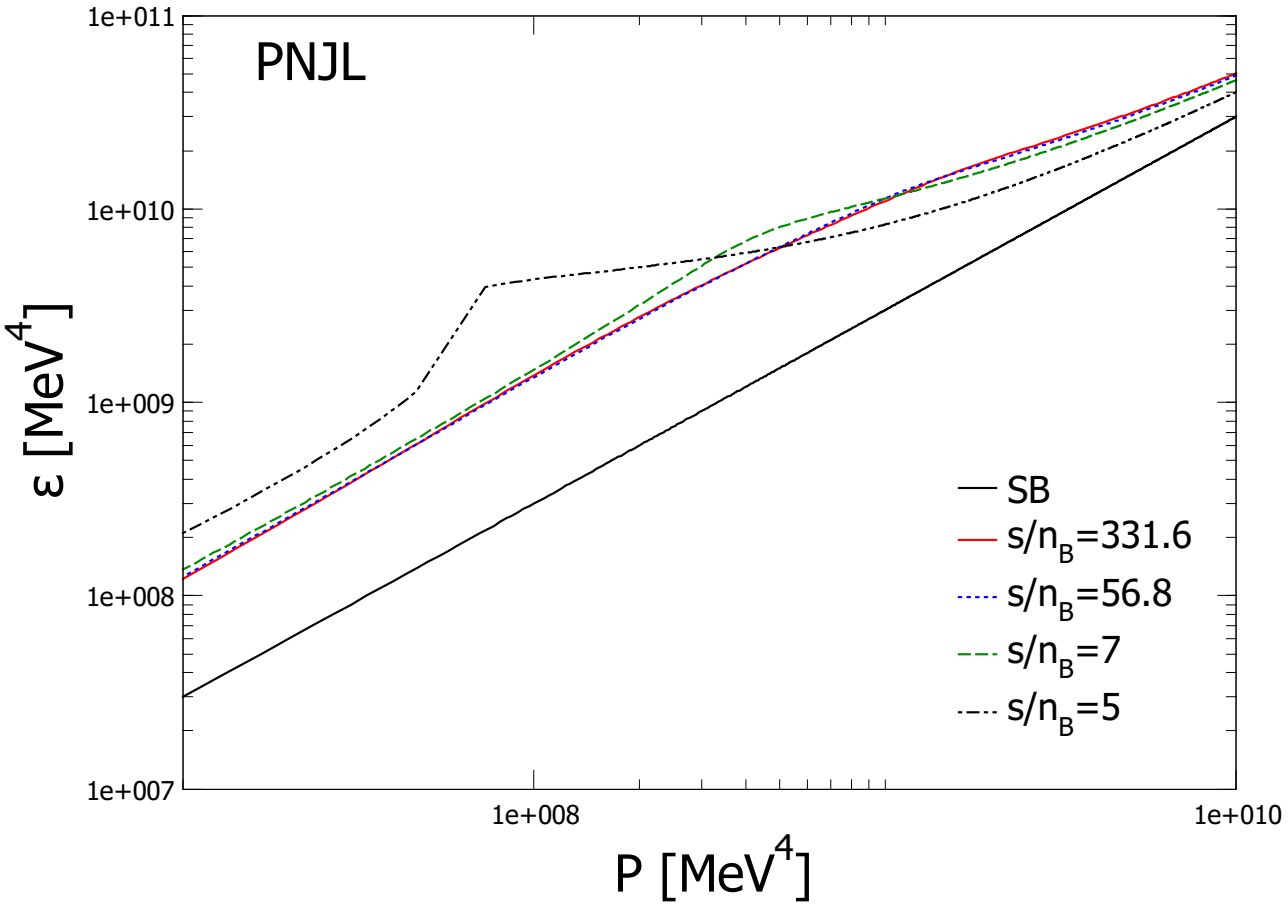

Figure: Equation of State in the QNS scenaio on the isentropic trajectories

Results:speed of sound

$$c_s^2 = \frac{\partial P}{\partial \epsilon} \tag{13}$$

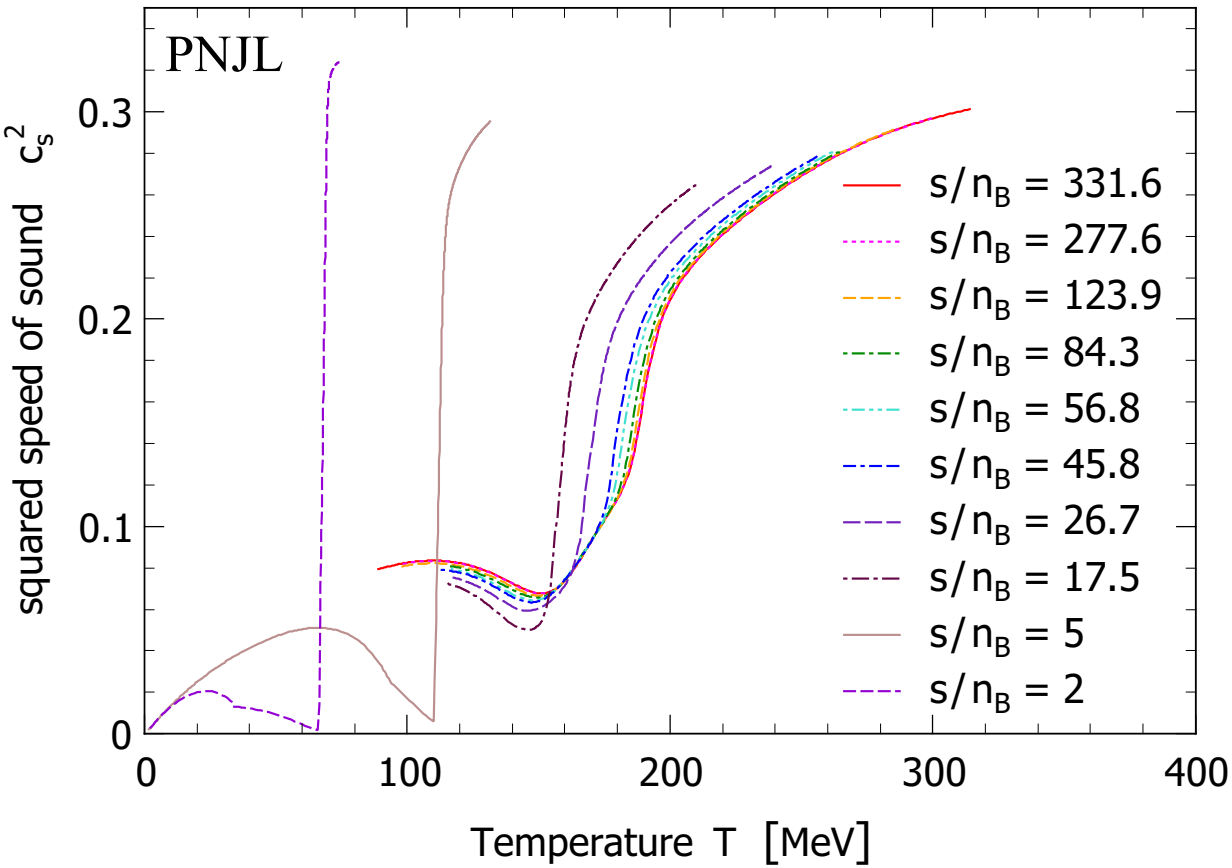

Figure: Speed of sound in the (Quasi)-neutral strangeness on the isentropic

Results:fluctuations in Symmetric scenario

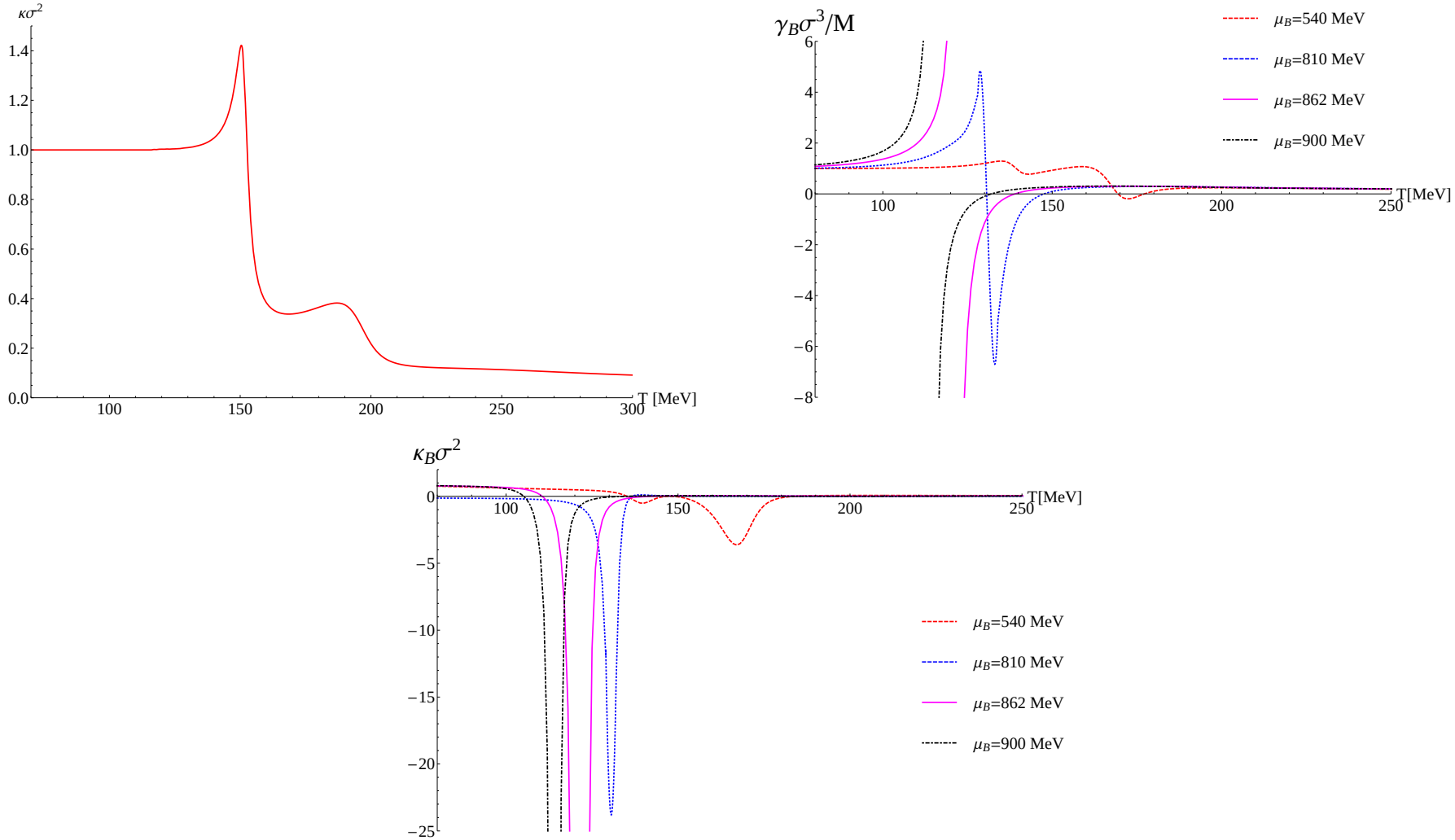

Figure: M.Motta et al [1909.05037]

Results:fluctuations in (Quasi-)Neutral strangness scenario

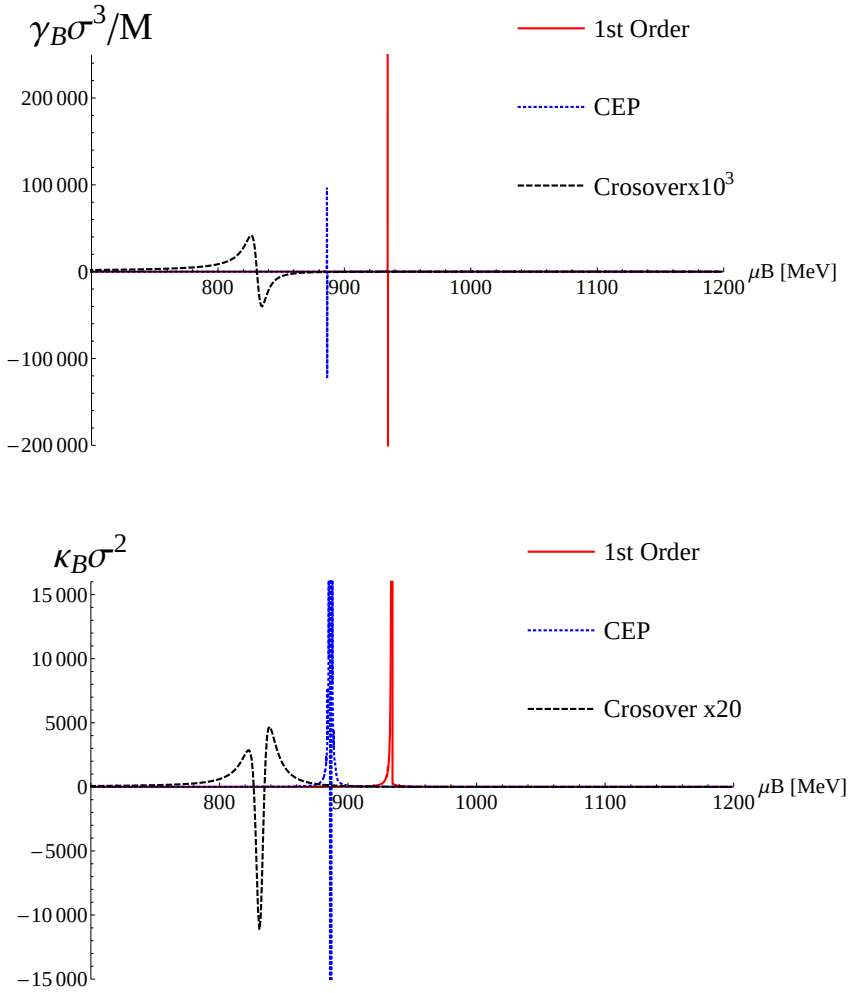

Figure: ($T_1 = 122.9$, $T_2 = 132.9$, $T_3 = 142.9$) MeV,M.Motta et al [1909.05037]

Conclusions and outlook

Conclusions:

- PNJL model provides a good qualitative and semi-quantitative guidance to describe the chiral and deconfinement QCD transition
- Nature of the active degrees of freedom is displayed by high order cumulants (e.g. kurtosis)

outlook:

- Calculation in the HIC scenarios are in progress and other thermodynamic quantities are currently under investigation
- I'm going to perform the calculation of mixed flavours susceptibility for the comparison with Lattice QCD and experimental results.

Thank you for your attention!

Polyakov Fields

The value of Polyakov Fields is connected to the energy for produce a free quark from the vacuum:

$$\Phi \sim \mathrm{e}^{-\beta F_q} \tag{14}$$

In the confined region, where it is not possible to create a sigle quarks from vacuum, $F_q \to +\infty$ then $\Phi \to 0$.
In the deconfined region F_q is finite and $\Phi \neq 0$.
At extremely high temperature $\Phi \to 1$. In any case Φ is smaller than unity

Generators of Fermi Functions

In PNJL lagrangian appears the functions $z_{\Phi}^{i\pm}$

$$z_{\Phi}^{i+}(E_i,\mu_i) \equiv \ln[1+N_c(\Phi+\bar{\Phi}\,\mathrm{e}^{-\beta(E_i-\mu_i)})\,\mathrm{e}^{-\beta(E_i-\mu_i)}+\mathrm{e}^{-3\beta(E_i-\mu_i)}] \quad (15)$$

$$z_{\Phi}^{i-}(E_i,\mu_i) \equiv \ln[1+N_c(\bar{\Phi}+\Phi\,\mathrm{e}^{-\beta(E_i+\mu_i)})\,\mathrm{e}^{-\beta(E_i+\mu_i)}+\mathrm{e}^{-3\beta(E_i+\mu_i)}] \quad (16)$$

The derivative of this function on chemical potential μ_i are the Fermi modified function:

$$\begin{aligned} f_{\Phi}^{i\pm}(E_i,\mu_i) &\equiv \pm\frac{T}{N_c}\frac{\partial z^{i\pm}}{\partial\mu_i} \\ &= \frac{(\Phi+2\bar{\Phi}\,\mathrm{e}^{-\beta(E_i\pm\mu_i)})\,\mathrm{e}^{-\beta(E_i\pm\mu_i)}+\mathrm{e}^{-3\beta(E_i\pm\mu_i)}}{1+N_c(\Phi+\bar{\Phi}\,\mathrm{e}^{-\beta(E_i\pm\mu_i)})\,\mathrm{e}^{-\beta(E_i\pm\mu_i)}+\mathrm{e}^{-3\beta(E_i\pm\mu_i)}} \end{aligned} \quad (17)$$

Mass Gap Equation

The PNJL Lagrangian is chiral symmetric if $m_l = 0$. For non vanishing current mass chiral symmetry is explicitly broken. Moreover, at low temperature and chemical potential, chiral symmetry is also dynamically broken by self-interaction of quarks: the chiral condensate is negative and large.

Mass Gap Equation

The PNJL Lagrangian is chiral symmetric if $m_i = 0$. For non vanishing current mass chiral symmetry is explicitly broken. Moreover, at low temperature and chemical potential, chiral symmetry is also dynamically broken by self-interaction of quarks: the chiral condensate is negative and large. The mass gap equation for the quark of species i reads:

$$M_i = m_i - 2G\varphi_i - 2K\varphi_j\varphi_k, \quad i \neq j \neq k \tag{18}$$

Mass Gap Equation

The PNJL Lagrangian is chiral symmetric if $m_i = 0$. For non vanishing current mass chiral symmetry is explicitly broken. Moreover, at low temperature and chemical potential, chiral symmetry is also dynamically broken by self-interaction of quarks: the chiral condensate is negative and large. The mass gap equation for the quark of species i reads:

$$M_i = m_i - 2G\varphi_i - 2K\varphi_j\varphi_k, \quad i \neq j \neq k \tag{18}$$

The second term of the RHS of the equation is due to the 4-fermion interaction vertex and the third term is due to the 6-fermion interaction vertex. This vertex mixes the chiral condensates one with an others.

QCD Phase Diagram from Holographic Black Holes

Joaquin Grefa

UNIVERSITY of HOUSTON

DEPARTMENT OF PHYSICS

with: Claudia Ratti & Israel Portillo(UH), Romulo Rougemont (UFRN), Jacquelyn Noronha-Hostler & Jorge Norhona (UIUC)

Frontiers in Nuclear and Hadronic Physics 2020,
February 24 - March 6, 2020

Table of Contents

QCD Phase Diagram

QCD is a nonabelian gauge theory: strongly interacting at low energies, and weakly interacting at large energies.

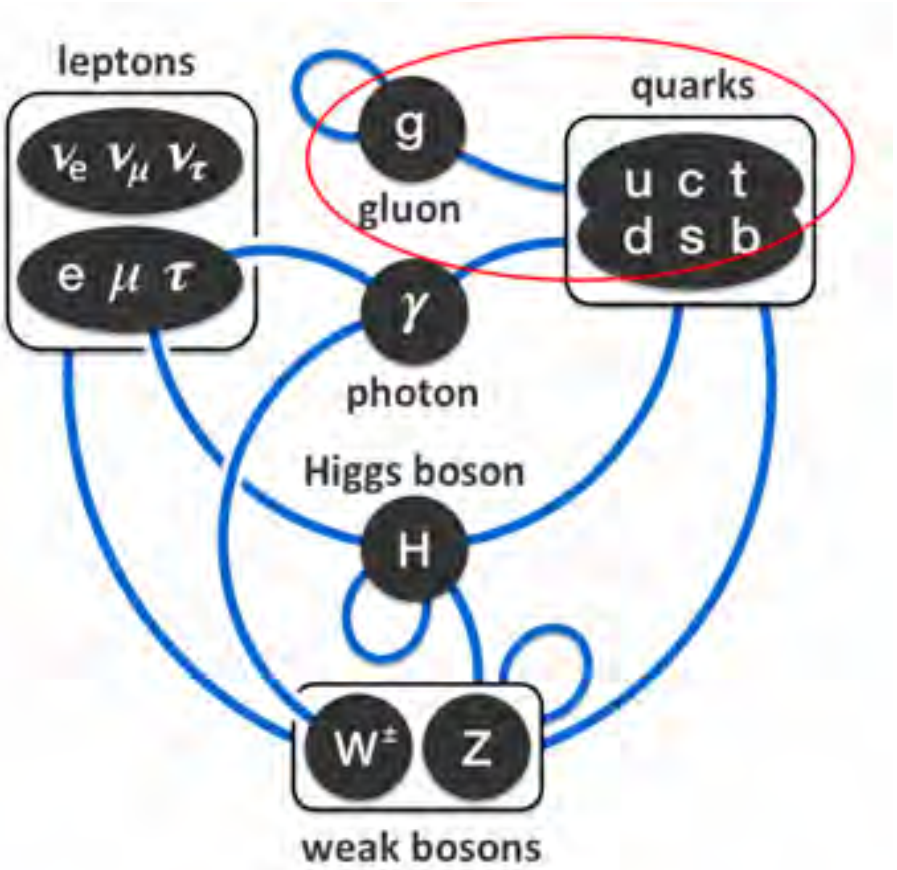

QCD Phase Diagram

QCD is a nonabelian gauge theory: strongly interacting at low energies, and weakly interacting at large energies.

We can explore the QCD phase diagram by changing $\sqrt{s}$ in relativistic heavy ion collisions

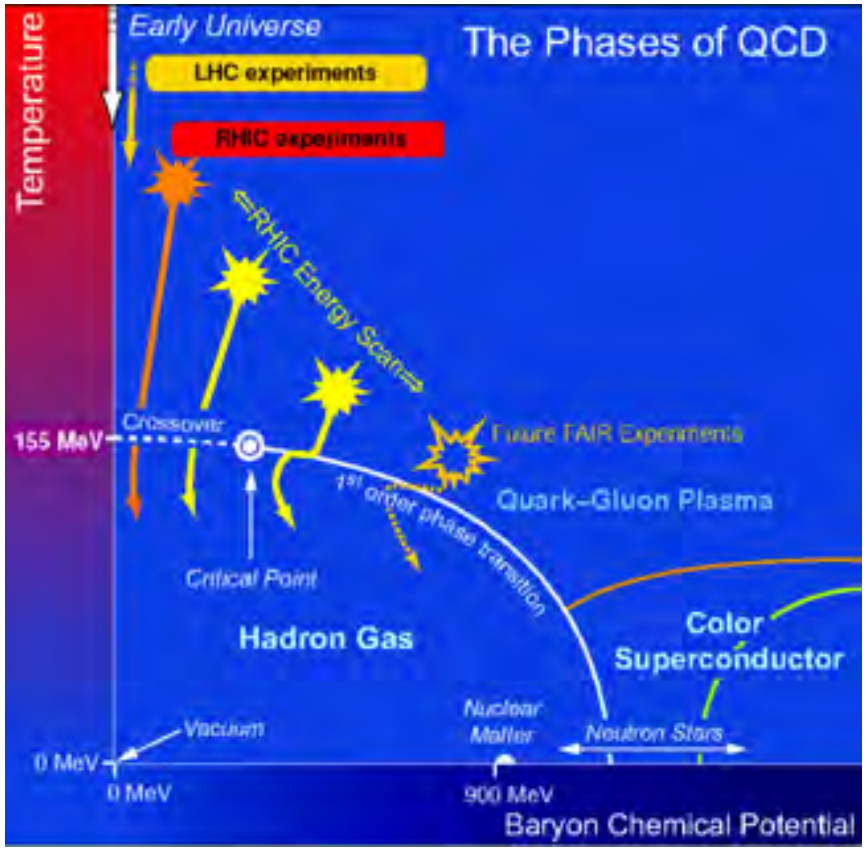

QCD Phase Diagram

QCD is a nonabelian gauge theory: strongly interacting at low energies, and weakly interacting at large energies.

We can explore the QCD phase diagram by changing $\sqrt{s}$ in relativistic heavy ion collisions

We can solve the theory by using Lattice QCD.

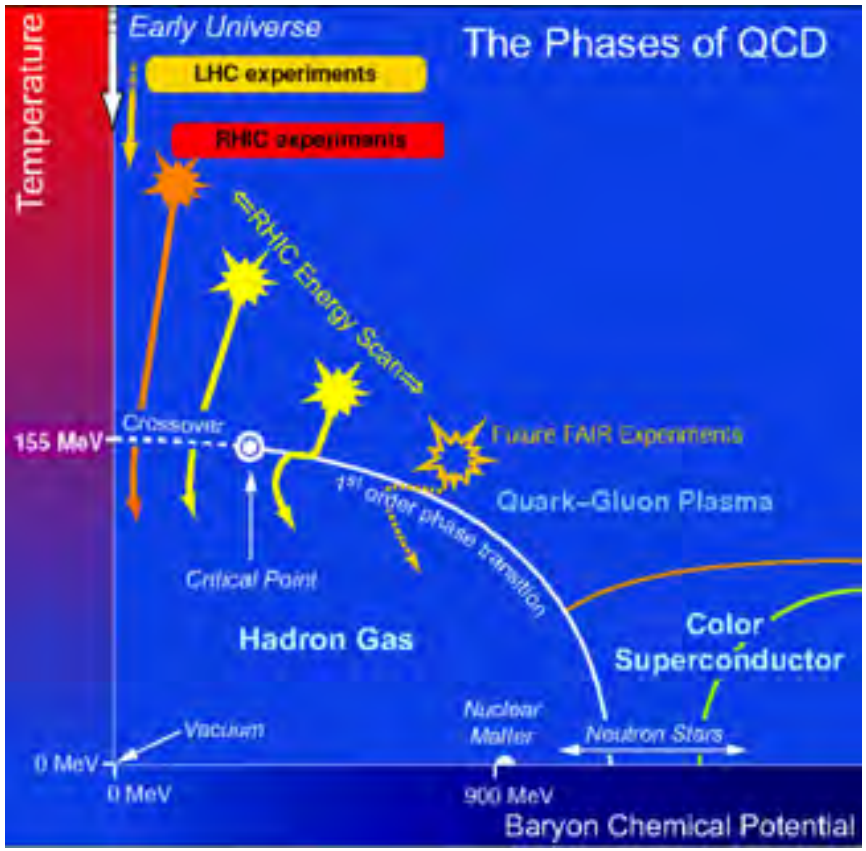

Limitations of Lattice QCD

Fermi sign problem:

It only provides the Equation of State (EoS) at $\mu_B = 0$.

Taylor Expansion for small μ_B

$$\frac{P(T,\mu_B) - P(T,\mu_B = 0)}{T^4} = \Sigma_{n=1}^{\infty} \frac{1}{(2n)!} \chi_{2n}(T) \left(\frac{\mu_B}{T}\right)^{2n}$$

where $\chi_n(T,\mu_B) = \frac{\partial^n (P/T^4)}{\partial(\mu_B/T)^n}$

As a consequence,

a large part of the QCD phase diagram remains unknown.

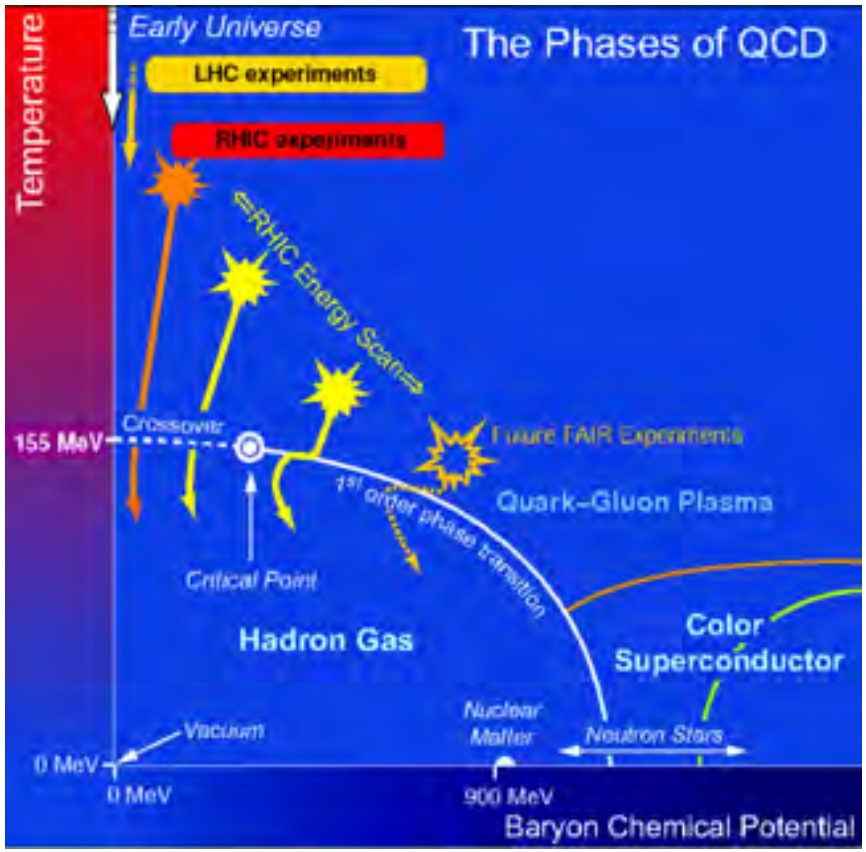

Model Requirements

The model should exhibit:

-Deconfinement
-Nearly perfect fluidity
-Agreement with Lattice EoS at $\mu_B = 0$
-Agreement with baryon susceptibilities at $\mu_B = 0$

- How can we fulfill these conditions?

Model Requirements

The model should exhibit:

-Deconfinement
-Nearly perfect fluidity
-Agreement with Lattice EoS at $\mu_B = 0$
-Agreement with baryon susceptibilities at $\mu_B = 0$

- How can we fulfill these conditions?

  ...BLACK HOLES...!!!

Table of Contents

Holography (Gauge/String duality)

Holographic gauge/gravity correspondance

String Theory/Classical Gravity in 5-dimensions $\Longleftrightarrow$ Quantum Field Theory in 4-dimensions

Maldacena 1997; Witten 1998; Gubser, Polyakov, Klebanov 1998

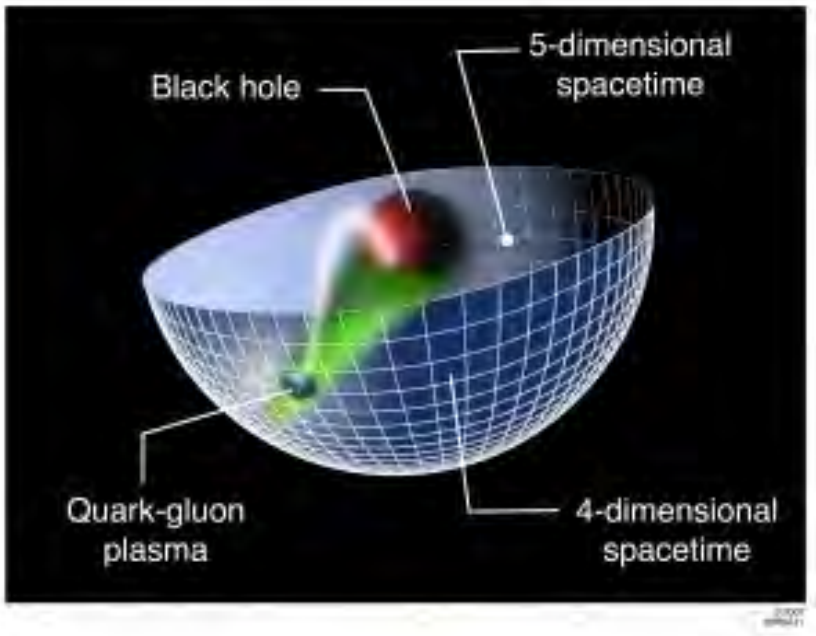

- Near Perfect fluidity
- vanishing coupling in GR $\rightarrow$ strong coupling in QFT
- BH solutions $\rightarrow$ T and μ_B in QFT

Gravitational Action

$$S = \frac{1}{2\kappa_5^2}\int_{M_5} d^5x\sqrt{-g}\left[R - \frac{(\partial_\mu\phi)^2}{2} - \underbrace{V(\phi)}_{\text{nonconformal}} - \underbrace{\frac{f(\phi)F_{\mu\nu}^2}{4}}_{\mu_B\neq 0}\right]$$

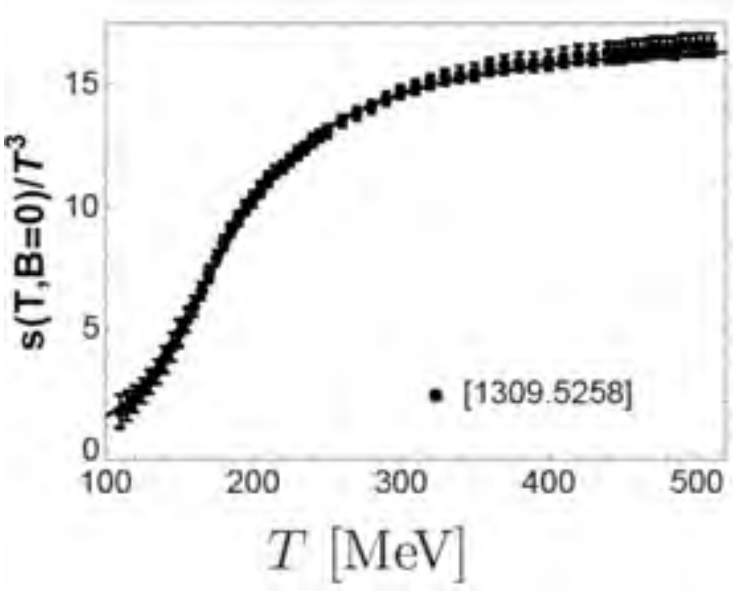

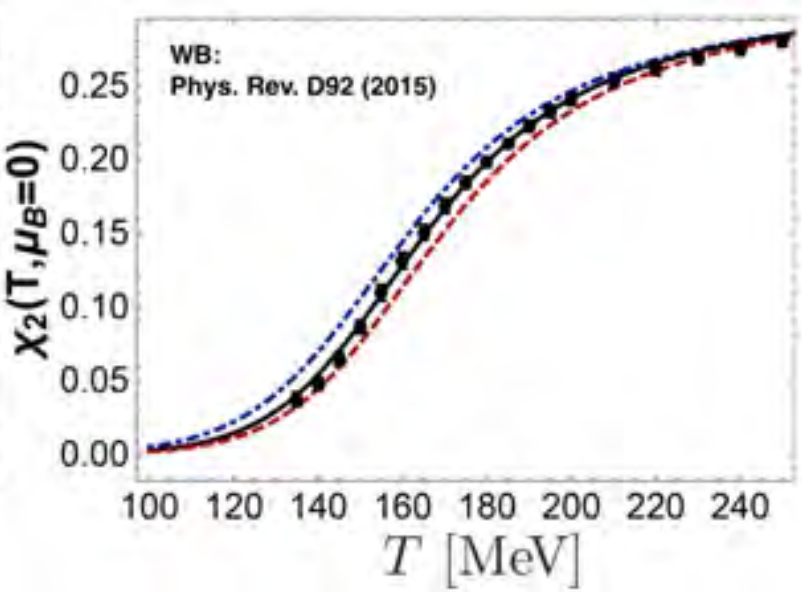

$V(\phi)$ and $f(\phi)$

The free parameters of the EMD holografic model are fixed to match the holografic results for the entropy density (s/T^3) and second order baryon susceptibility (χ_2) to state-of-the-art lattice QCD results for these quantities.

Free Parameters for the Holographic Model

$$\kappa_5^2 = 8\pi G_5 = 8\pi(0.46), \qquad \Lambda = 1053.83 MeV,$$

$$V(\phi) = -12\cosh(0.63\phi) + 0.65\phi^2 - 0.05\phi^4 + 0.003\phi^6,$$

$$f(\phi) = \frac{\text{sech}(c_1\phi + c_2\phi^2)}{1 + c_3} + \frac{c_3}{1 + c_3}\text{sech}(c_4\phi),$$

where

$$c_1 = -0.27, \quad c_2 = 0.4, \quad c_3 = 1.7, \quad c_4 = 100$$

Equations of Motion

$$S = \frac{1}{2\kappa_5^2}\int_{M_5} d^5x\sqrt{-g}\left[R - \frac{(\partial_\mu\phi)^2}{2} - \underbrace{V(\phi)}_{\text{nonconformal}} - \underbrace{\frac{f(\phi)F_{\mu\nu}^2}{4}}_{\mu_B\neq 0}\right]$$

$$\begin{aligned} ds^2 &= e^{2A(r)}[-h(r)dt^2 + d\vec{x}^2] + \frac{e^{2B(r)}dr^2}{h(r)} \\ \phi &= \phi(r) \\ A_\mu dx^\mu &= \Phi(r)dt \end{aligned}$$

Equations of Motion

$$\phi''(r) + \left[\frac{h'(r)}{h(r)} + 4A'(r)\right]\phi'(r) - \frac{1}{h(r)}\left[\frac{\partial V(\phi)}{\partial\phi} - \frac{e^{-2A(r)}\Phi'(r)^2}{2}\frac{\partial f(\phi)}{\partial\phi}\right] = 0$$

$$\Phi''(r) + \left[2A'(r) + \frac{d[\ln f(\phi)]}{d\phi}\phi'(r)\right]\Phi'(r) = 0$$

$$A''(r) + \frac{\phi'(r)^2}{6} = 0$$

$$h''(r) + 4A'(r)h'(r) - e^{-2A(r)}f(\phi)\Phi'(r)^2 = 0$$

$$h(r)[24A'(r)^2 - \phi'(r)^2] + 6A'(r)h'(r) + 2V(\phi) + e^{-2A(r)}f(\phi)\Phi'(r)^2 = 0$$

Solutions

Far-Region asymptotic:

$$A(r) = \alpha(r) + \mathcal{O}\left(e^{-2\nu\alpha(r)}\right), \quad \text{where:} \quad \alpha(r) = A_{-1}^{\text{far}} r + A_0^{\text{far}}$$
$$h(r) = h_0^{\text{far}} + \mathcal{O}\left(e^{-4\alpha(r)}\right),$$
$$\phi(r) = \phi_A e^{-\nu\alpha(r)} + \mathcal{O}\left(e^{-2\nu\alpha(r)}\right),$$
$$\Phi(r) = \Phi_0^{\text{far}} + \Phi_2^{\text{far}} e^{-2\alpha(r)} + \mathcal{O}\left(e^{-(2+\nu)\alpha(r)}\right),$$

Thermodynamics:

$$T = \frac{1}{4\pi\phi_A^{1/\nu}\sqrt{h_0^{\text{far}}}}\Lambda \qquad s = \frac{2\pi}{\kappa_5^2\,\phi_A^{3/\nu}}\Lambda^3$$
$$\mu_B = \frac{\Phi_0^{\text{far}}}{\phi_A^{1/\nu}\sqrt{h_0^{\text{far}}}}\Lambda \qquad \rho_B = -\frac{\Phi_2^{\text{far}}}{\kappa_5^2\,\phi_A^{3/\nu}\sqrt{h_0^{\text{far}}}}\Lambda^3$$

Thermodynamics at $\mu_B = 0$

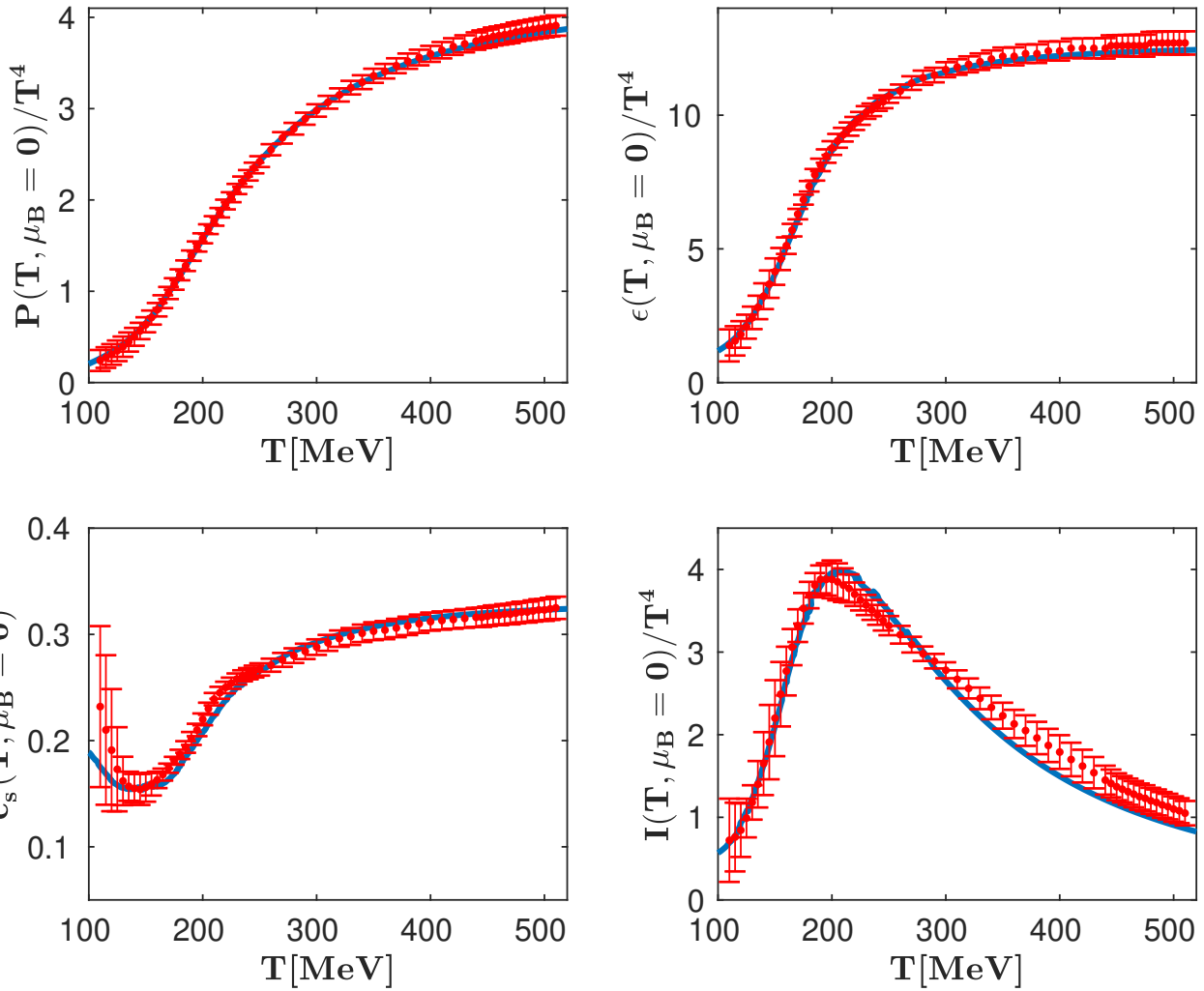

Lattice Results: [WB] S Borsanyi et al.Phys. Lett. B730.99.

Table of Contents

Mapping the QCD phase diagram from Black Hole solutions

The BH solutions are parametrized by (ϕ_0, Φ_1), where

$\phi_0 \rightarrow$ value of the scalar field at the horizon, and

$\Phi_1 \rightarrow$ electric field in the radial direction at the horizon

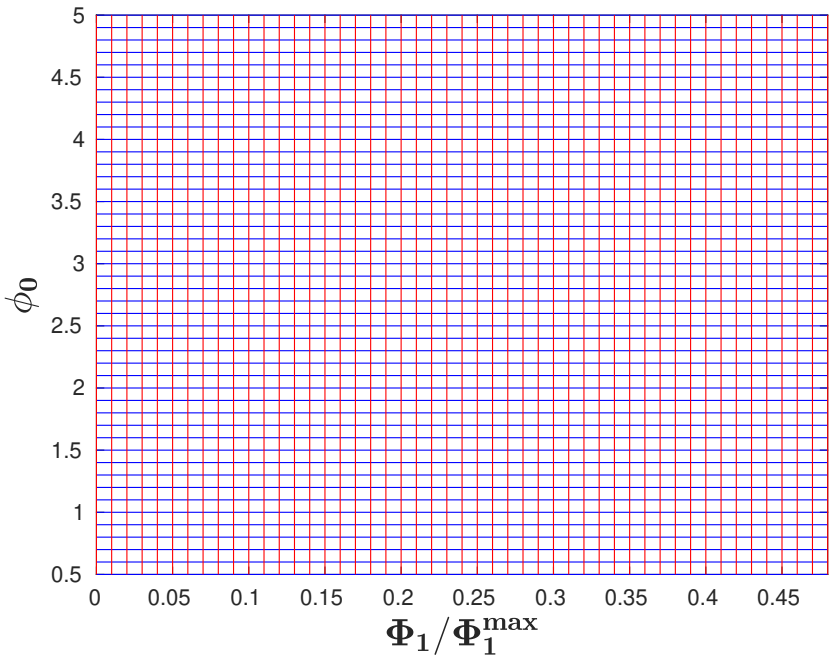

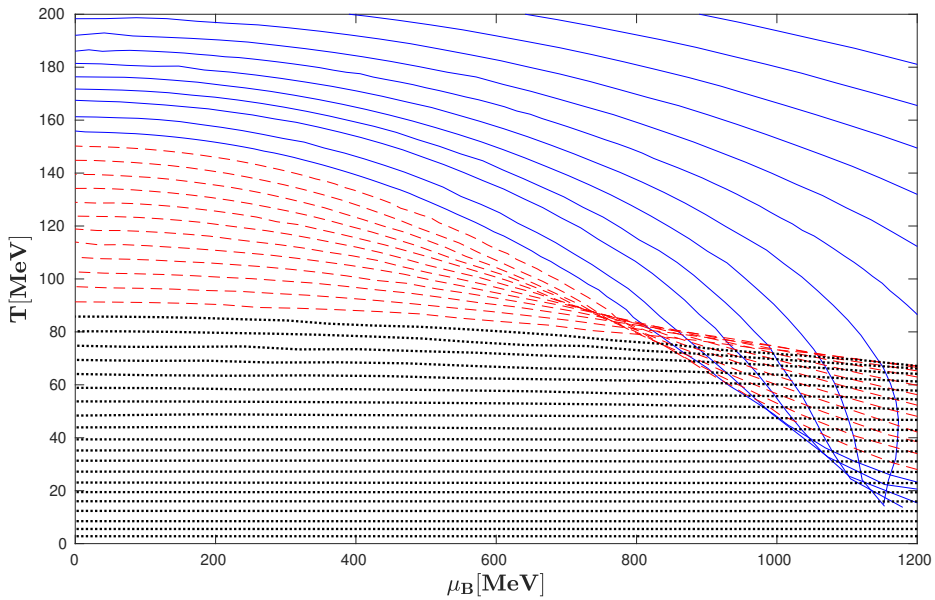

Locating the Critical End Point (CEP)

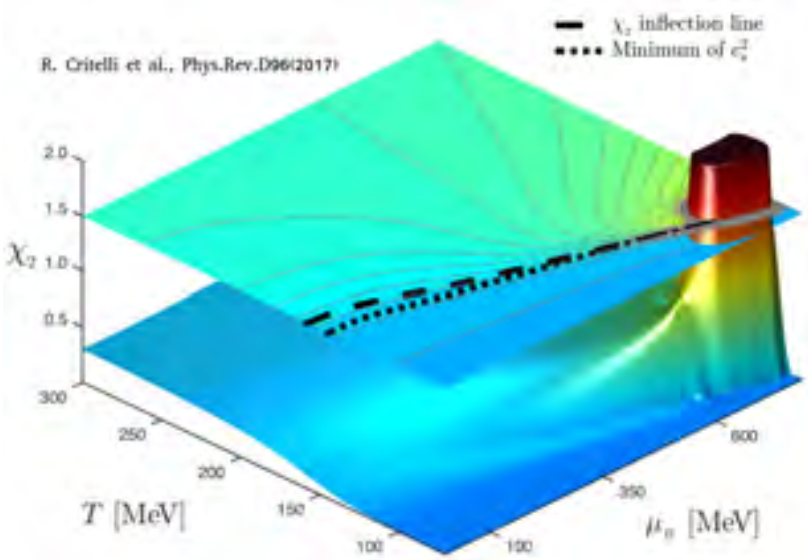

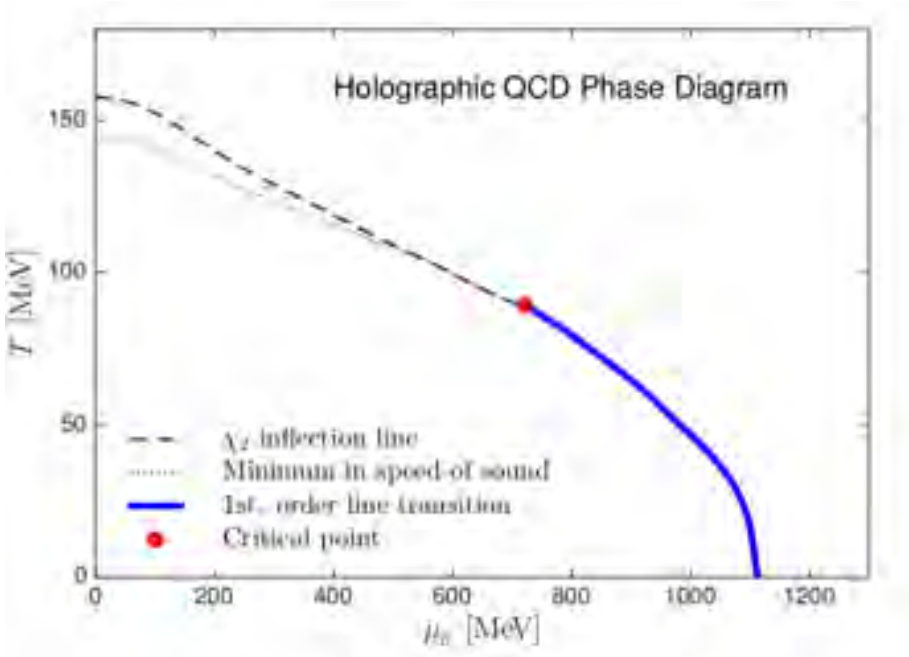

$$T_{CEP} = 89 \text{ MeV and } \mu_B^{CEP} = 724 \text{ MeV}$$

Thermodynamics at finite μ_B

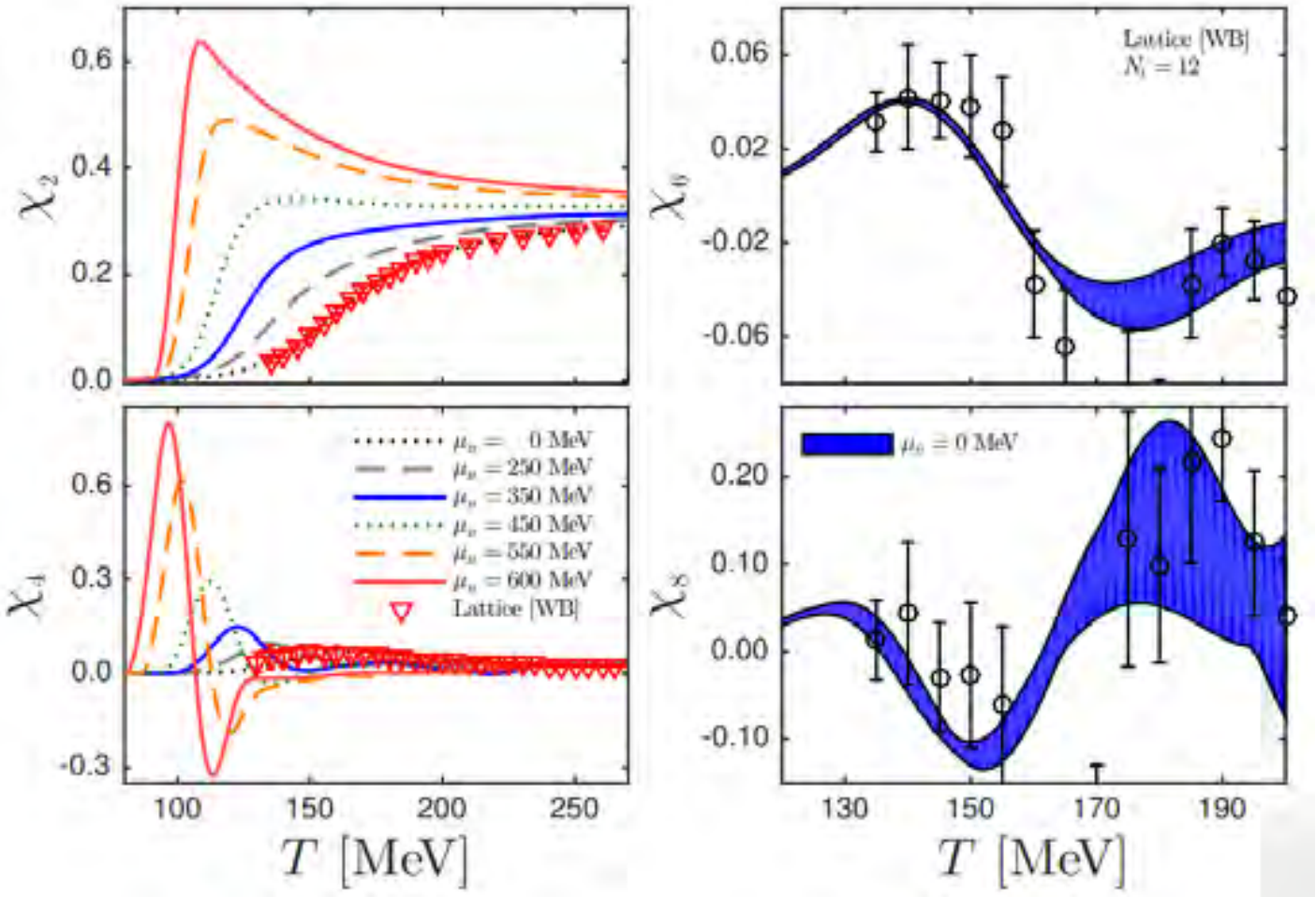

Lattice Results: [WB] S Borsanyi et al. arXiv:1805.04445v1.

BH curves: R. Critelli et al., Phys.Rev.D96(2017).

Equation of State

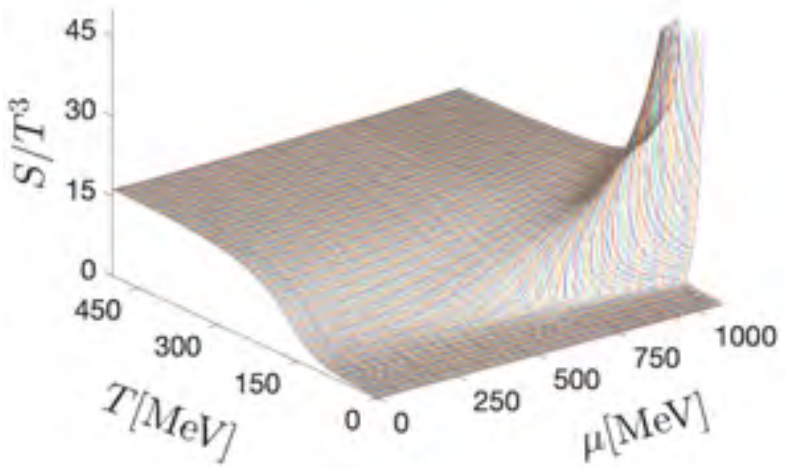

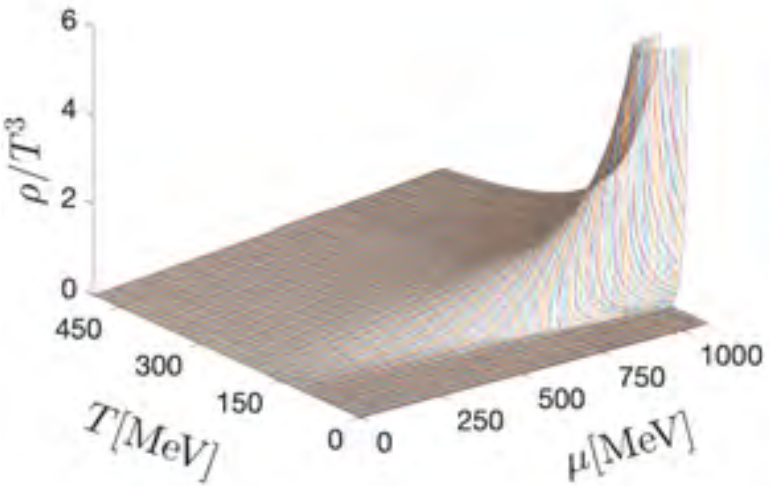

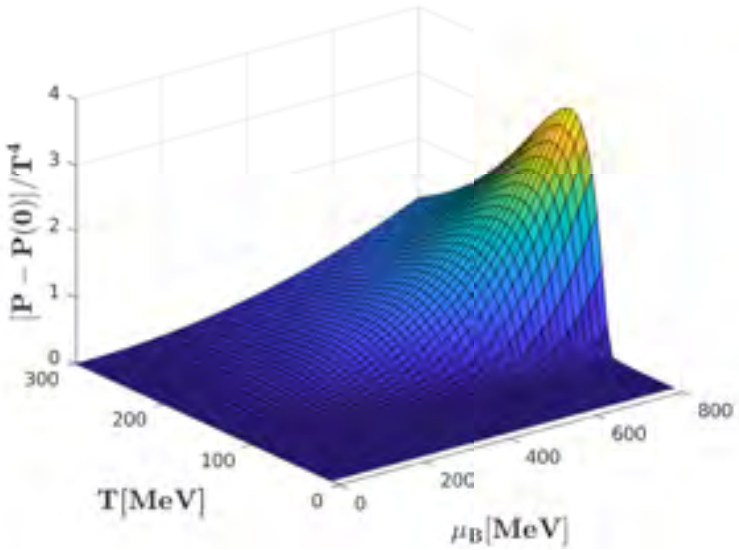

Table of Contents

Conclusions

- The Lattice EoS was reproduced for small μ_B.
- Holographic Black Holes predict a CEP:

$$T_{CEP} = 89 \text{ MeV}, \ \mu_B^{CEP} = 724 \text{ MeV}$$

- The first order transition line was located in the QCD phase diagram.
- We are able to compute higher order susceptibilities.
- We obtained state variables for a larger region in the QCD phase diagram.
- Future work:
  -Calculate critical exponents.
  -Obtain other state variables.
  -Use QCD EoS to better understand structure of compact stellar objects.
  -Extend the model to include other conserved quantities.

Thanks

THANKS..!

Collision Energy Estimates

We estimate a collision energy needed to hit the CEP

- $\sqrt{s} = 2.5 - 4.1$ GeV

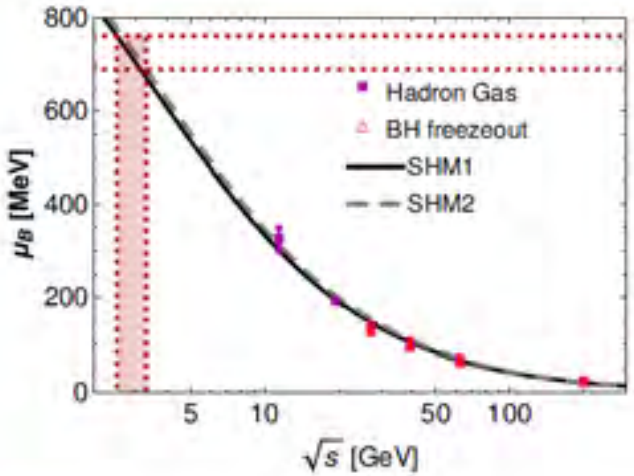

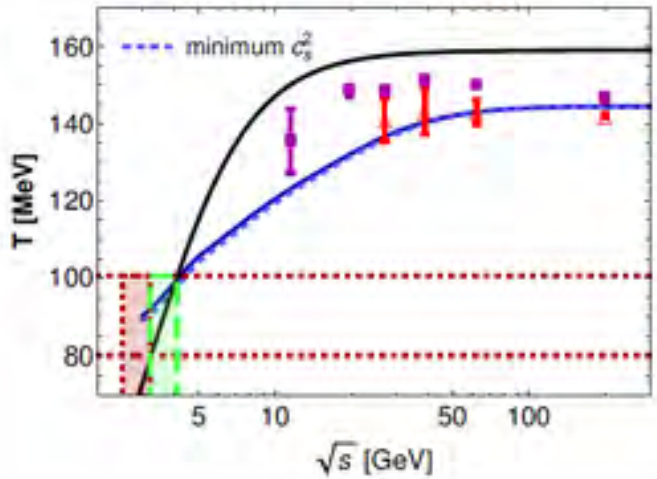

- The collision energy is reachable by the next generation of experiments.

[BH] R.Critelli, I.P. et al., Phys.Rev.D**96**(2017).
[HRG] Paolo Alba et al. Phys.Lett.B**738**(2014),
[SHM1] A. Andronic et al. Phys.Lett.B**673**(2009).
[SHM2] J. Cleymans et al. Phys.Rev.C**73**(2006).

χ measurements

- Baryonic Susceptibilities: $\chi_n^B(T,\mu_B) = \frac{\partial^n}{\partial(\mu_B/T)^n}\left(\frac{P}{T^4}\right)$
- The susceptibilities (χ_n) are related directly to the moments of the distribution.
- The volume-independent ratios are useful quantities to compare to experimental data.

$$\begin{aligned} \text{mean}: \quad & M = \chi_1 \\ \text{variance}: \quad & \sigma^2 = \chi_2 \\ \text{skewness}: \quad & S = \chi_3/\chi_2^{3/2} \\ \text{kurtosis}: \quad & \kappa = \chi_4/\chi_2^2 \end{aligned}$$

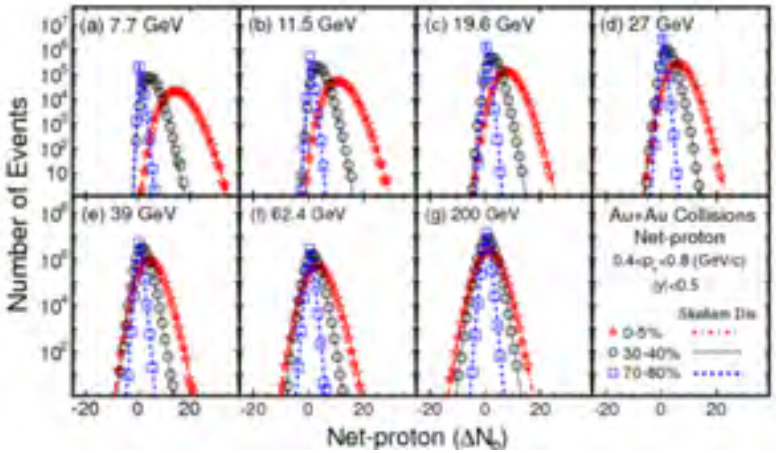

$$\begin{aligned} M/\sigma^2 &= \chi_1/\chi_2 \\ S\sigma &= \chi_3/\chi_2 \\ \kappa\sigma^2 &= \chi_4/\chi_2 \\ S\sigma^3/M &= \chi_3/\chi_1 \end{aligned}$$

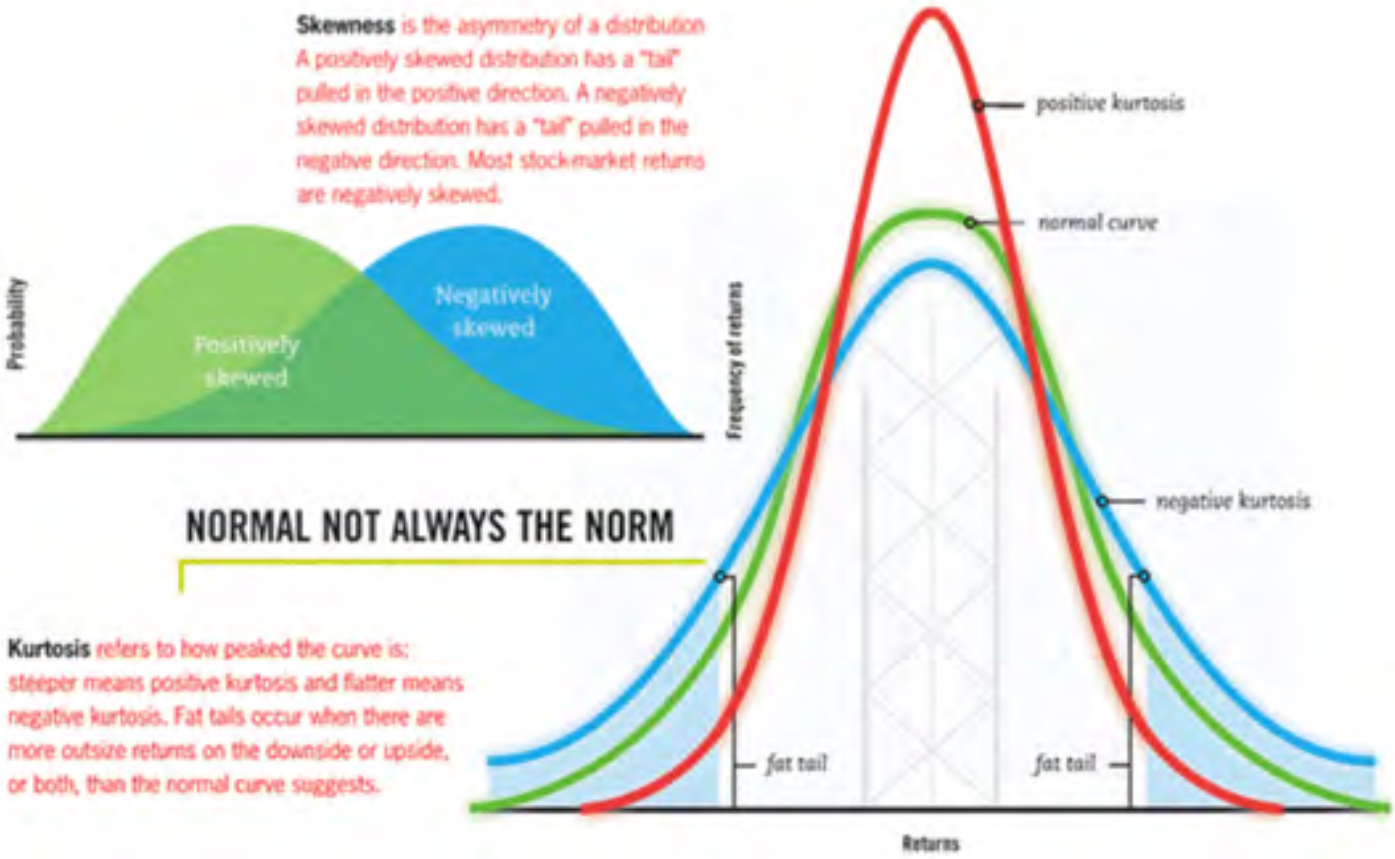
Skewness is the asymmetry of a distribution
A positively skewed distribution has a "tail" pulled in the positive direction. A negatively skewed distribution has a "tail" pulled in the negative direction. Most stock-market returns are negatively skewed.
Probability
Positively skewed
Negatively skewed
NORMAL NOT ALWAYS THE NORM
Kurtosis refers to how peaked the curve is: steeper means positive kurtosis and flatter means negative kurtosis. Fat tails occur when there are more outsize returns on the downside or upside, or both, than the normal curve suggests.
positive kurtosis
normal curve
negative kurtosis
Frequency of returns
fat tail
fat tail
Returns

Critical Exponents

We will calculate four standard thermodynamic critical exponents α, β, γ and δ. In calculating the exponents, it is vital to specify whether one is approaching the critical point along the axis defined by the first order line, or by another direction. The exponent α is defined by the power law behavior of the specific heat at constant ρ as the critical point is approached along the axis defined by the first order line:

$$C_\rho \sim |T - T_c|^{-\alpha}, \qquad \text{along first order axis}.$$

The exponent β comes from the discontinuity of ρ across the first-order line. $\Delta\rho$ is finite at a generic point on the first-order line, and goes to zero as one approaches the critical point along the line:

$$\Delta\rho \sim (T_c - T)^\beta, \qquad \text{along first order line}.$$

The exponent γ is analogous to α, but instead of C_ρ, it is χ_2 that is tracked along the first-order axis:

$$\chi_2 \sim |T - T_c|^{-\gamma}, \qquad \text{along first order axis}.$$

Finally, δ is defined at the critical isotherm $T = T_c$ by the relation between $\rho - \rho_c$ and $\mu - \mu_c$.

$$\rho - \rho_c \sim |\mu - \mu_c|^{1/\delta}, \qquad \text{for } T = T_c.$$

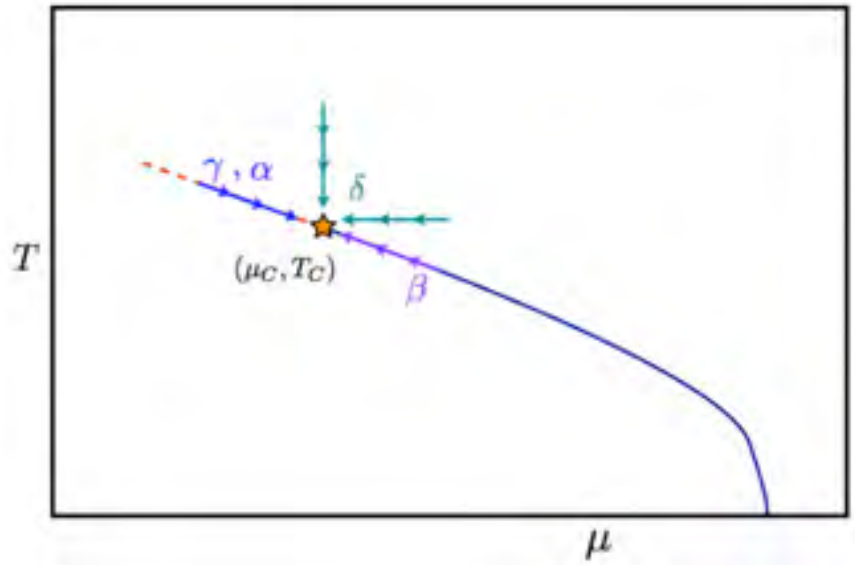

constant value lines

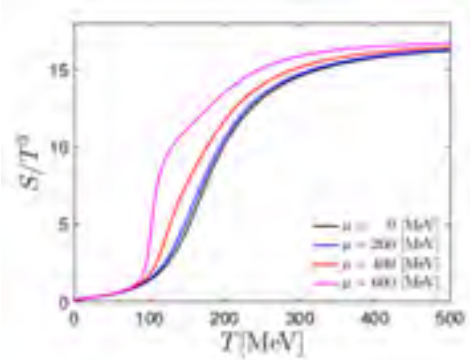

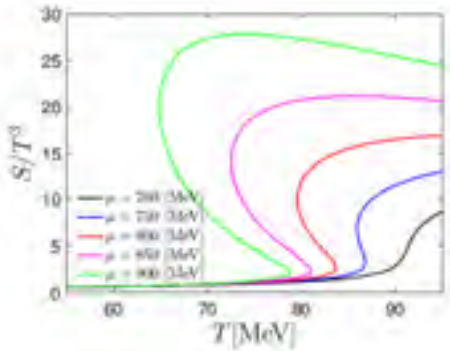

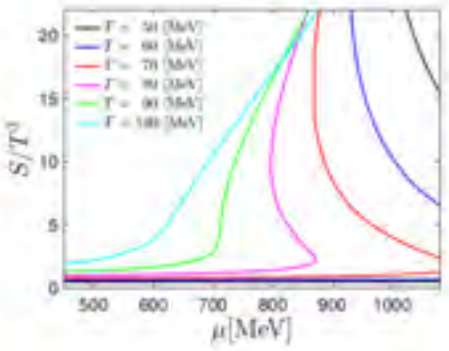

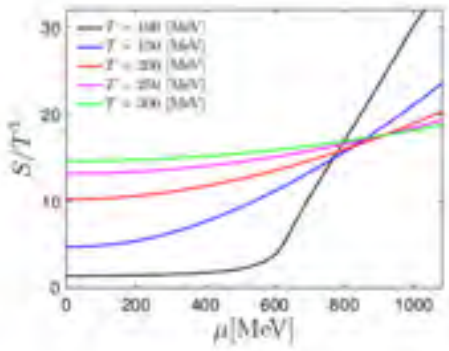

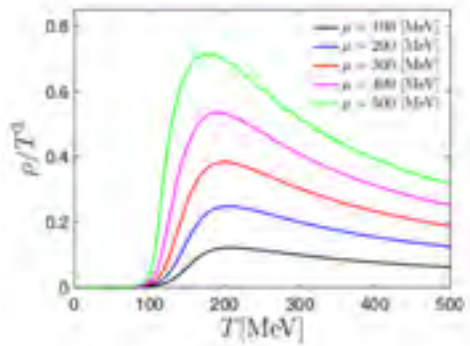

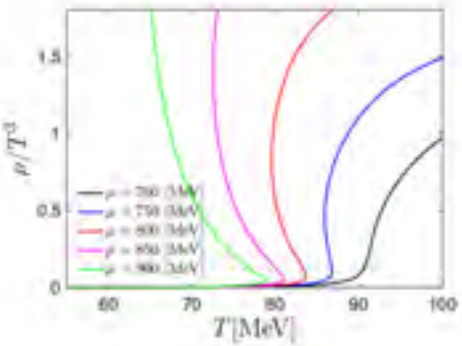

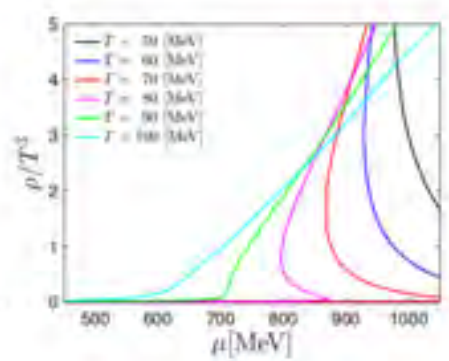

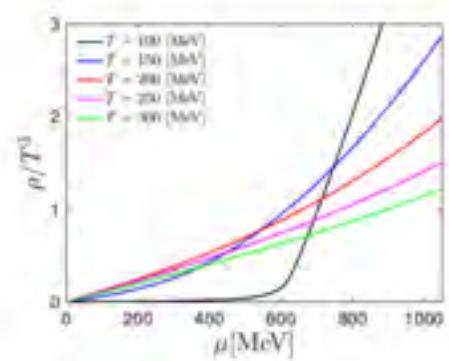

Points on First Order transition Line

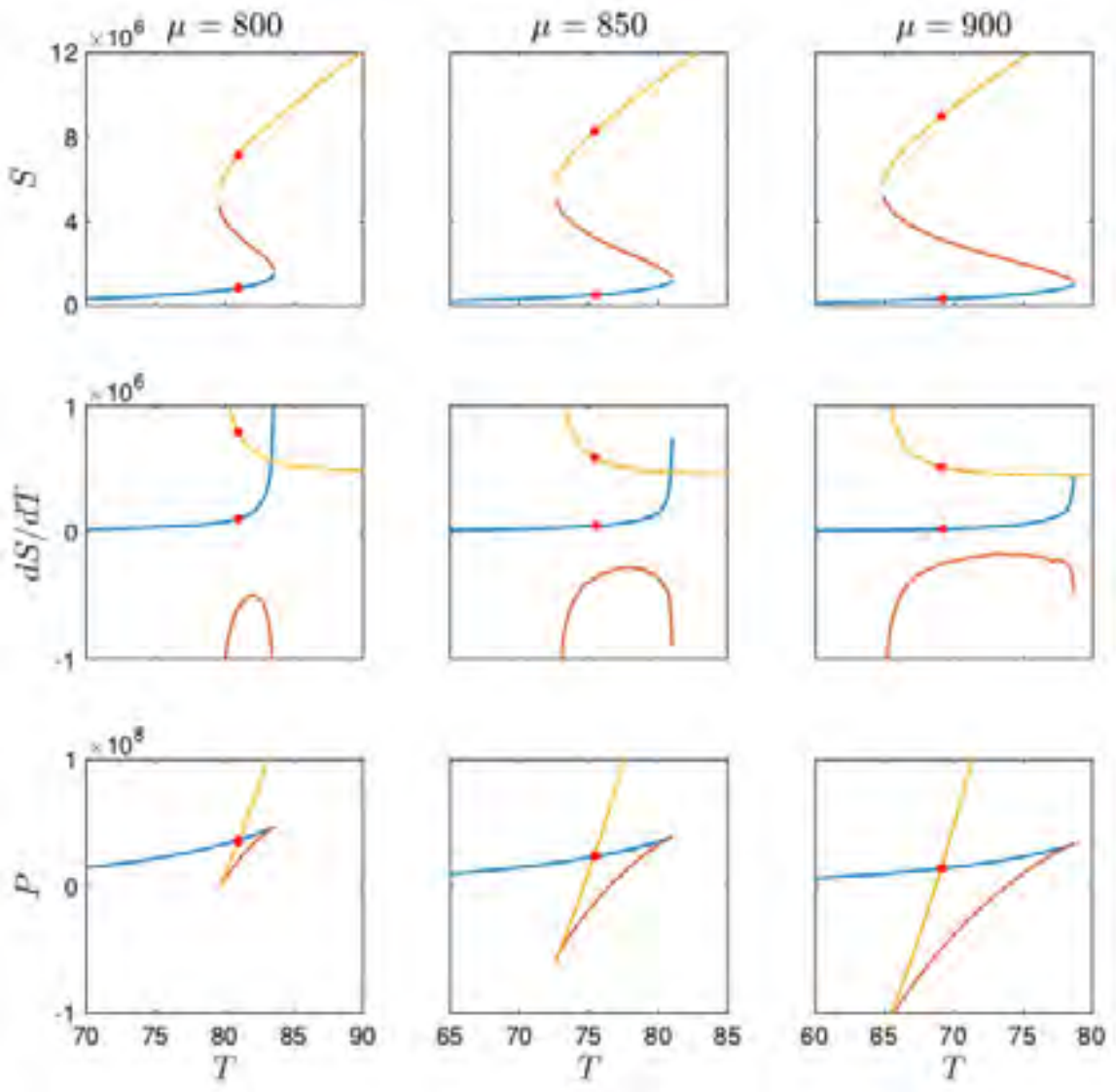

IFT - UNESP
INSTITUTO DE FÍSICA TEÓRICA

SPRACE

Femtoscopy of the D meson and nucleon interaction

Isabela Maietto*, Gastao Krein, Sandra Padula

Institute of Theoretical Physics - IFT - UNESP

Outline

- Motivation
- Femtoscopy and Correlations
- $\bar{D}N$ observables
- Results
- Summary

Motivation

- Femtoscopy: correlation function of two particles as a function of relative momentum q
  - Obtain the source size
  - Sensitive to the effects of the final-state interaction
    - Coulomb interaction
    - Strong Interaction
    - Isospin

Motivation

- Femtoscopy: correlation function of two particles as a function of relative momentum q
  - Obtain the source size
  - Sensitive to the effects of the final-state interaction
    - Coulomb interaction
    - Strong Interaction
    - Isospin

- Here, discuss **DN interaction**, no experimental data available yet
  - Important for the quest of possible existence of D-mesic nuclei (an exotic nuclear state)
  - Through D-mesic nuclei, one can possibly access chiral symmetry restoration effects
    - Properties of light quarks in D mesons are sensitive to temperature and density

Correlation Function

Two-particle correlation function:

$$C(\mathbf{p_1}, \mathbf{p_2}) = \frac{P(\mathbf{p_1}, \mathbf{p_2})}{P(\mathbf{p_1})P(\mathbf{p_2})} \tag{1}$$

Experimentally can be obtained as:

$$C(q) \propto \frac{N_{\text{same}}(q)}{N_{\text{mixed}}(q)} \tag{2}$$

Correlation Function

Two-particle correlation function:

$$C(\mathbf{p_1}, \mathbf{p_2}) = \frac{P(\mathbf{p_1}, \mathbf{p_2})}{P(\mathbf{p_1})P(\mathbf{p_2})} \tag{1}$$

Experimentally can be obtained as:

$$C(q) \propto \frac{N_{\text{same}}(q)}{N_{\text{mixed}}(q)} \tag{2}$$

If $C(\mathbf{p_1}, \mathbf{p_2}) \to 1$ no particle correlation

If $C(\mathbf{p_1}, \mathbf{p_2}) \neq 1$ particles are correlated

Correlation Function

The Correlation Function can be written with an equal-time approximation, e.g., the particles states are emitted simultaneously in the pair rest frame $t_1 = t_2$ and $p_1 + p_2 = 0$:

$$C(\mathbf{p_1}, \mathbf{p_2}) = \frac{P(\mathbf{p_1}, \mathbf{p_2})}{P(\mathbf{p_1})P(\mathbf{p_2})} \approx \int d\mathbf{r} S_{12}(\mathbf{r}) |\Psi(\mathbf{r}, \mathbf{q})|^2 \tag{3}$$

Correlation Function

The Correlation Function can be written with an equal-time approximation, e.g., the particles states are emitted simultaneously in the pair rest frame $t_1 = t_2$ and $p_1 + p_2 = 0$:

$$C(\mathbf{p_1}, \mathbf{p_2}) = \frac{P(\mathbf{p_1}, \mathbf{p_2})}{P(\mathbf{p_1})P(\mathbf{p_2})} \approx \int d\mathbf{r} S_{12}(\mathbf{r}) |\Psi(\mathbf{r}, \mathbf{q})|^2 \tag{3}$$

where,

- $S(\mathbf{r})$ is the source function. Tipically, this can be represented with a spherical Gaussian source:

$$S_{12}(\mathbf{r}) = \frac{1}{(4\pi R^2)^{\frac{3}{2}}} \exp\left[-\frac{r^2}{4R^2}\right] \tag{4}$$

  - R is the width of the source.

- $\Psi(\mathbf{r}, \mathbf{q})$ is the wave function, where $\mathbf{q}$ is the relative momentum: $q = |p_1 - p_2|$

Correlation Function

Partial Wave Decomposition:

$$\Psi(r,q) = \sum_{l=0}^{\infty} (2l+1) i^l \psi_l(r) P_l(cos\theta) \tag{5}$$

Correlation Function

Partial Wave Decomposition:

$$\Psi(r,q) = \sum_{l=0}^{\infty} (2l+1) i^l \psi_l(r) P_l(cos\theta) \tag{5}$$

Supose now, that only the s-wave is affected by the interaction:

$$\Psi(r,q) \quad = \quad \psi_0(r,q) + \sum_{l=1}^{\infty} (2l+1) i^l \psi_l^{free}(r,q) P_l(\cos\theta)$$

Correlation Function

Partial Wave Decomposition:

$$\Psi(r,q) = \sum_{l=0}^{\infty} (2l+1) i^l \psi_l(r) P_l(cos\theta) \tag{5}$$

Supose now, that only the s-wave is affected by the interaction:

$$\begin{aligned} \Psi(r,q) &= \psi_0(r,q) + \sum_{l=1}^{\infty} (2l+1) i^l \psi_l^{free}(r,q) P_l(\cos\theta) \\ &= \psi_0(r,q) + \sum_{l=0}^{\infty} (2l+1) i^l \psi_l^{free}(r,q) P_l(\cos\theta) - \psi_0^{free} \end{aligned} \tag{6}$$

- ψ_0 is the wave function for $l = 0$;
- $\psi_0^{free} = j_0(qr) = \dfrac{\sin(qr)}{qr}$; $\displaystyle\sum_l \psi_l^{free}(r,q) P_l(\cos\theta) = e^{iqr}$

Correlation Function

Then,

$$\Psi(r,q) = \psi_0(r,q) + e^{iqr} - j_0(qr) \tag{7}$$

Replacing this expression in (2):

Correlation Function

Then,

$$\Psi(r,q) = \psi_0(r,q) + e^{iqr} - j_0(qr) \tag{7}$$

Replacing this expression in (2):

$$C(q) = 1 + 4\pi \int dr r^2 S(r) \left[|\psi_0(q,r)|^2 - j_0^2(qr) \right] \tag{8}$$

Correlation Function

Then,

$$\Psi(r,q) = \psi_0(r,q) + e^{iqr} - j_0(qr) \tag{7}$$

Replacing this expression in (2):

$$C(q) = 1 + 4\pi \int dr r^2 S(r) \left[|\psi_0(q,r)|^2 - j_0^2(qr) \right] \tag{8}$$

Expressing ψ_0 in the assymptotic form:

$$\begin{aligned} \psi_0(r,q) &= \frac{1}{qr} \sin\left(qr + \delta_0(q)\right) = \frac{1}{2iqr} \left(e^{ikr + i\delta_0} - e^{-ikr - i\delta_0} \right) \\ &= \frac{e^{-i\delta_0}}{qr} \left(sin(qr) + q e^{iqr} f_0(q) \right) \end{aligned} \tag{9}$$

Correlation Function - Lednicky Model

Finally, one can obtain the Lednicky Model for the Correlation Function [Lednicky, 1982]:

Correlation Function - Lednicky Model

Finally, one can obtain the Lednicky Model for the Correlation Function [Lednicky, 1982]:

$$C(q) = 1 + \frac{|f(q)|^2}{2R^2} + \frac{2\,\mathrm{Re}\,[f(q)]}{\sqrt{\pi}R}F_1(2qR) - \frac{\mathrm{Im}\,[f(q)]}{R}F_2(2qR) \tag{10}$$

- $F_1(z) = \int_0^z \frac{e^{t^2-z^2}}{z}dt$, with $z = 2qR$;
- $F_2(z) = \frac{(1-e^{-z^2})}{z}$

Correlation Function - Lednicky Model

Finally, one can obtain the Lednicky Model for the Correlation Function [Lednicky, 1982]:

$$C(q) = 1 + \frac{|f(q)|^2}{2R^2} + \frac{2\,\mathrm{Re}\,[f(q)]}{\sqrt{\pi}R}F_1(2qR) - \frac{\mathrm{Im}\,[f(q)]}{R}F_2(2qR) \tag{10}$$

- $F_1(z) = \int_0^z \frac{e^{t^2-z^2}}{z}dt$, with $z = 2qR$;
- $F_2(z) = \frac{(1-e^{-z^2})}{z}$

An additional commonly used approximation is to use the effective range expansion for the scattering amplitude:

- $f(q) \approx \left[-\frac{1}{a_l^I} + \frac{1}{2}r_l^I q^2 + iq\right]^{-1}$, for $q \to 0$

  a_l^I is the scattering lenght and r_l^I is the effective range

$\bar{D}N$ s-wave phase shifts for $I = 0$ channel

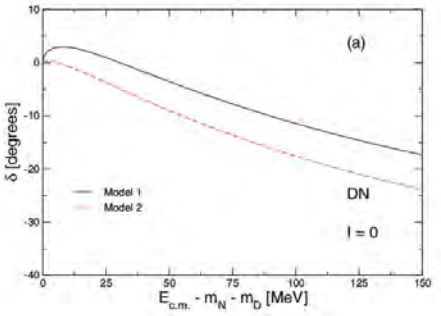

- Models:
  - Short distance: quark-interchange (Model 1 and Model 2)
  - Long distance: meson-exchange
- Model 1 (MELTT):
  - Lattice Simulation of QCD in Coulomb gauge
- Model 2 (MESS2):
  - Szczepaniak and Swanson

C. E. Fontoura, G. Krein, and V. E. Vizcarra, 2013

$\bar{D}N$ s-wave phase shifts for $I = 0$ channel

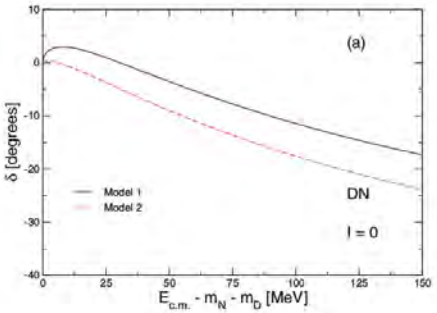

C. E. Fontoura, G. Krein, and V. E. Vizcarra, 2013

- Models:
  - Short distance: quark-interchange (Model 1 and Model 2)
  - Long distance: meson-exchange
- Model 1 (MELTT):
  - Lattice Simulation of QCD in Coulomb gauge
- Model 2 (MESS2):
  - Szczepaniak and Swanson

Extract the observables (for I=0):

$$q \cot \delta_0^I(q) \approx -\frac{1}{a_0^I} + \frac{1}{2} r_0^I q^2$$

Results

MELTT_model1: $a_0^0 = -0.16$ fm and $r_0^0 = 21$ fm

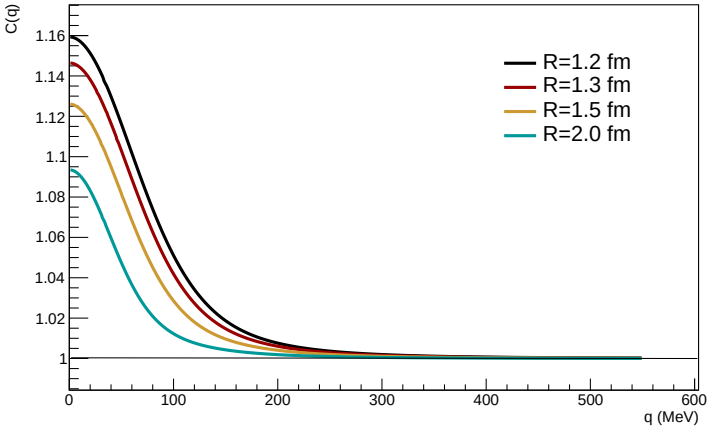

MELTT_model1 and MESS2_model2

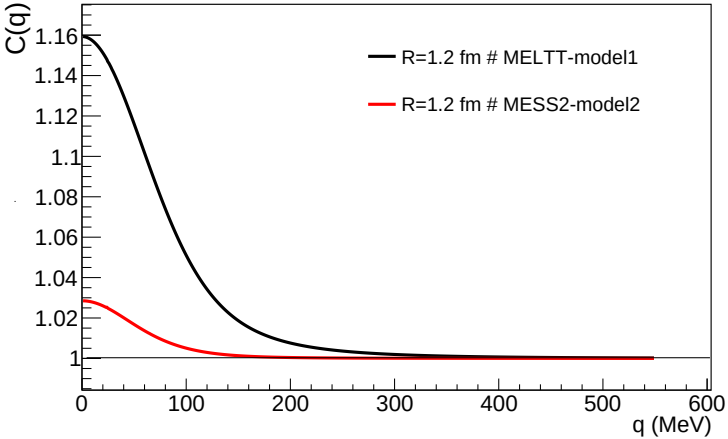

Summary

Summary

- Correlation function of the D meson and Nucleon
  - Contains information on the DN interaction, unknown so far
- Important for quest D-mesic nuclei [1,2]
- D-mesic nuclei, possibly access chiral symmetry restoration in medium
- Explore other models for the DN interaction

[1] K. Tsushima, D. H. Lu, A. W. Thomas, K. Saito, and R. H. Landau, 1999
[2] G. Krein, A. W. Thomas, K. Tsushima, 2018

Thanks!

Grazie mille!

Acknowledgment

The Galileo Galilei Institute
For Theoretical Physics
Centro Nazionale di Studi Avanzati dell'Istituto Nazionale di Fisica Nucleare

Backup

Microscopic Hamiltonian

$$H = H_0 + H_{int} \tag{11}$$

with,

$$\begin{aligned} H_{int} &= -\frac{1}{2}\int dxdy\rho^a(x)V_C(|x-y|)\rho^a(y) \\ &+ \frac{1}{2}\int dxdy J_i^a(x)D^{ij}(|x-y|)J_j^a(y) \end{aligned} \tag{12}$$

Models

- Model 1:

$$V_C(k) = \frac{8\pi}{k^4}\sigma_{Coul} + \frac{4\pi}{k^2}C \tag{13}$$

with $\sigma_{Coul} = (552\ \mathrm{MeV})^2$ and $C = 6.0$

- Model 2:

$$V_C(k) = \frac{8\pi}{k^4}\sigma + \frac{4\pi}{k^2}\alpha(k) \tag{14}$$

with,

$$\alpha(k) = \frac{4\pi Z}{\beta^{\frac{3}{2}} \ln\left(C + \frac{k^2}{\Lambda_{\mathrm{QCD}}}\right)^{\frac{3}{2}}}$$

and $\Lambda_{\mathrm{QCD}} = 250\ \mathrm{MeV}$, $Z = 5.94$, $C = 40.68$, $\beta = \frac{121}{12}$

MELTT_model1: $a_0^1 = 0.25$ fm and $r_0^1 = 2.2$ fm

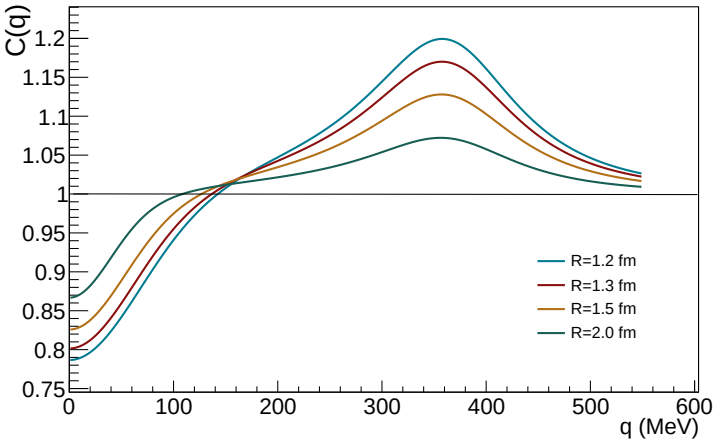

MELTT_model1 and MESS2_model2 for I=1, L=0

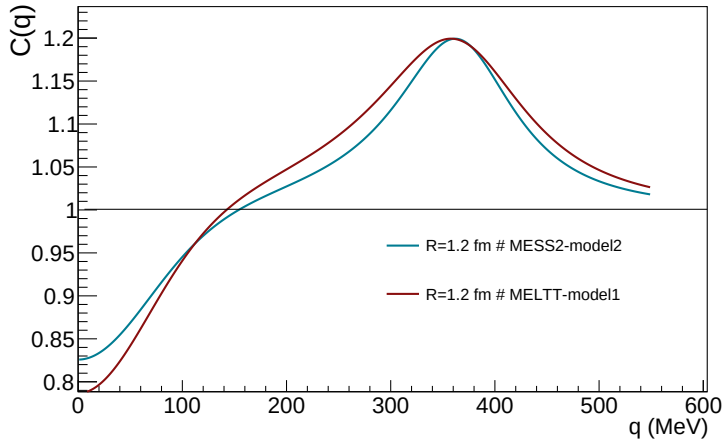

MESS2_I0_Model2 - (Lednicky Model) - $a_0 = 0.03$ fm and $r_0 = 350$ fm

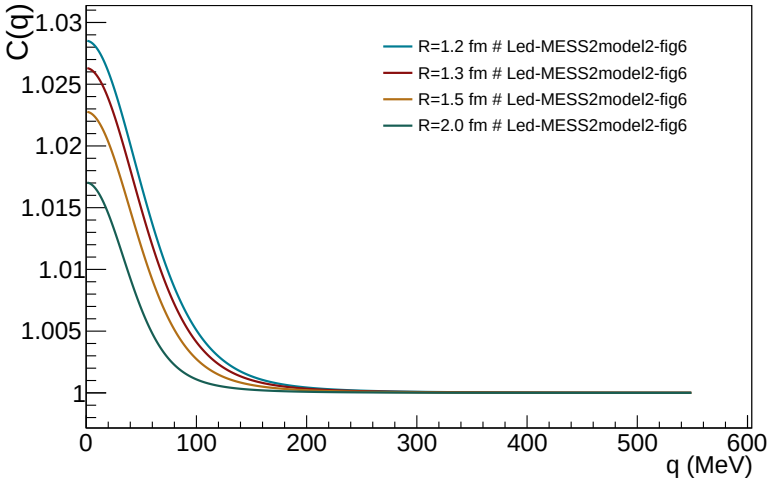

Fluctuating Open Heavy Flavour Energy Loss in a Strongly Coupled Plasma with Observables from RHIC and the LHC

Blessed Arthur Ngwenya
Supervisor: Associate Professor W. A. Horowitz

University of Cape Town

March 4, 2020 (Frontiers in Nuclear and Hadronic Physics 2020)

Outline

Introduction

- What happened shortly after the Big Bang?

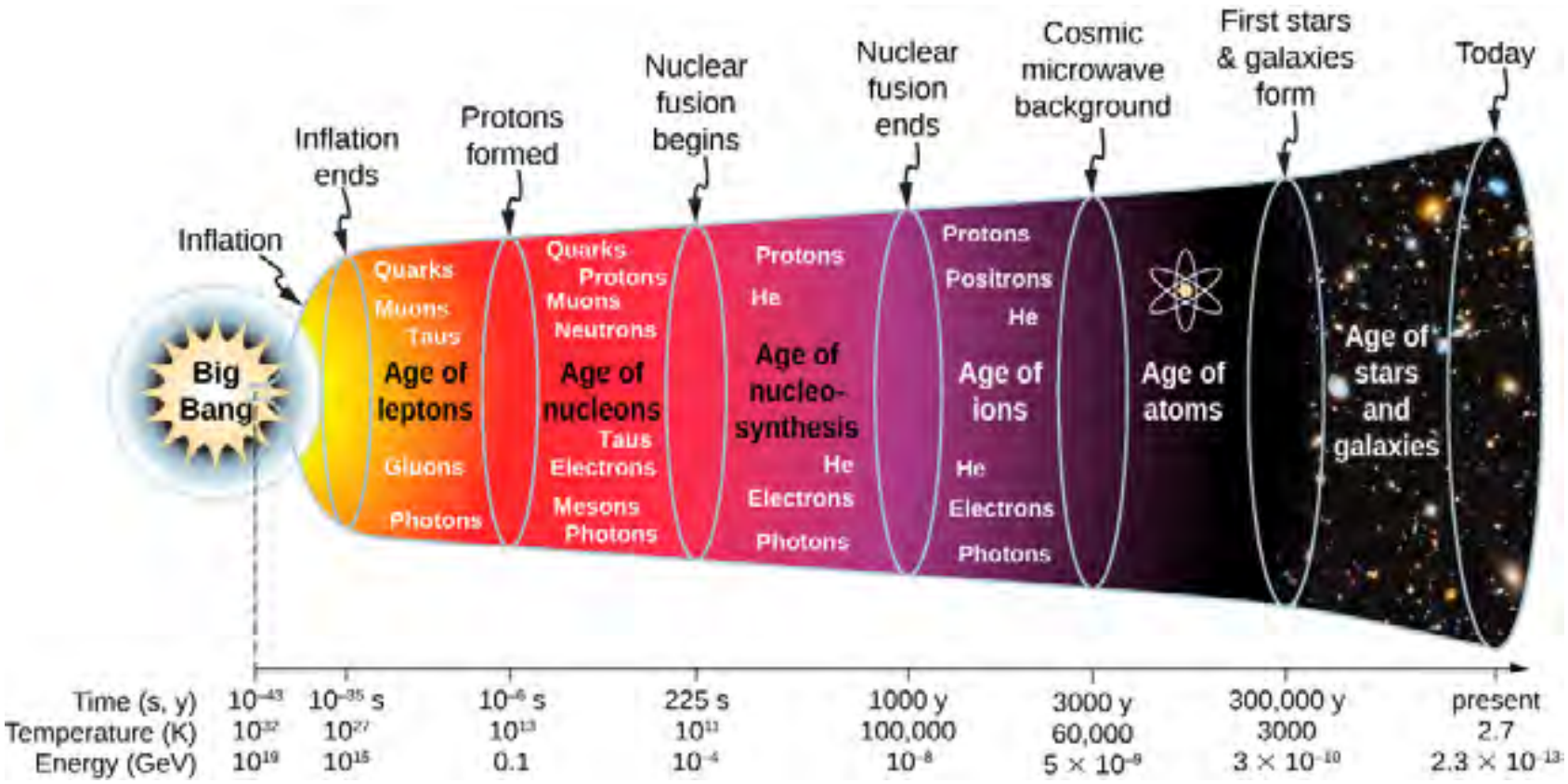

Figure 1: Approximate timeline of the evolution of the universe [1]

Emergent phenomenon

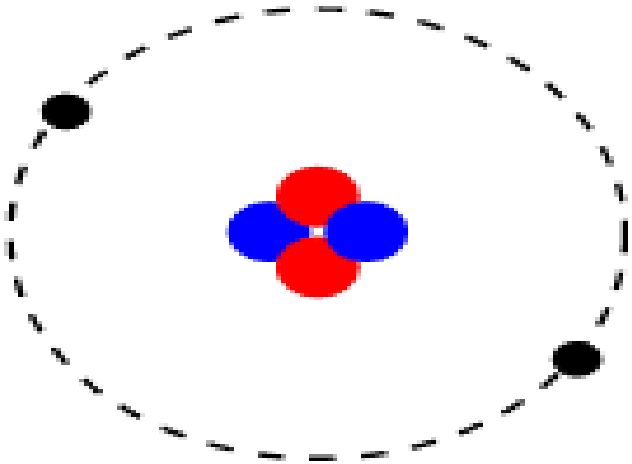

(a) Helium atom [2]

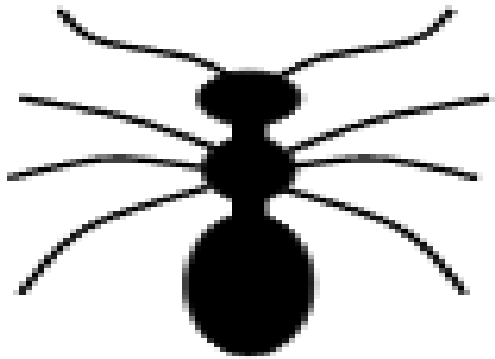

(b) A single ant [2]

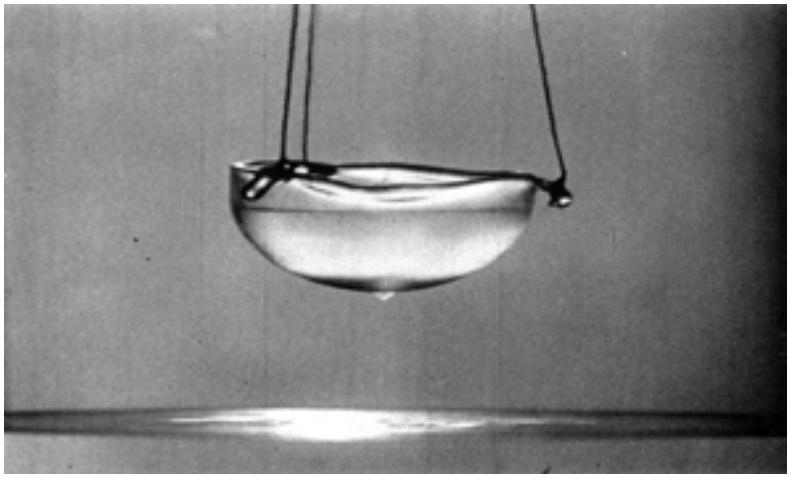

(c) Liquid helium [3]

(d) Colony of ants [4]

- In practice, the phase diagram of water can't be computed by Newton's 2nd law and Maxwell's equations applied to individual H_2O molecules.

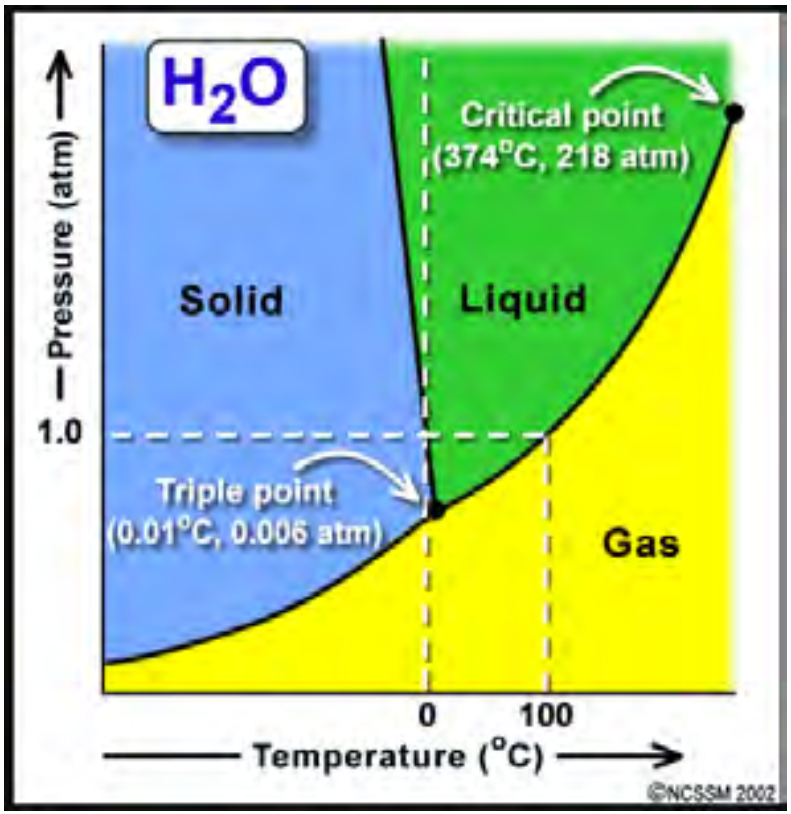

(e) Water [5]

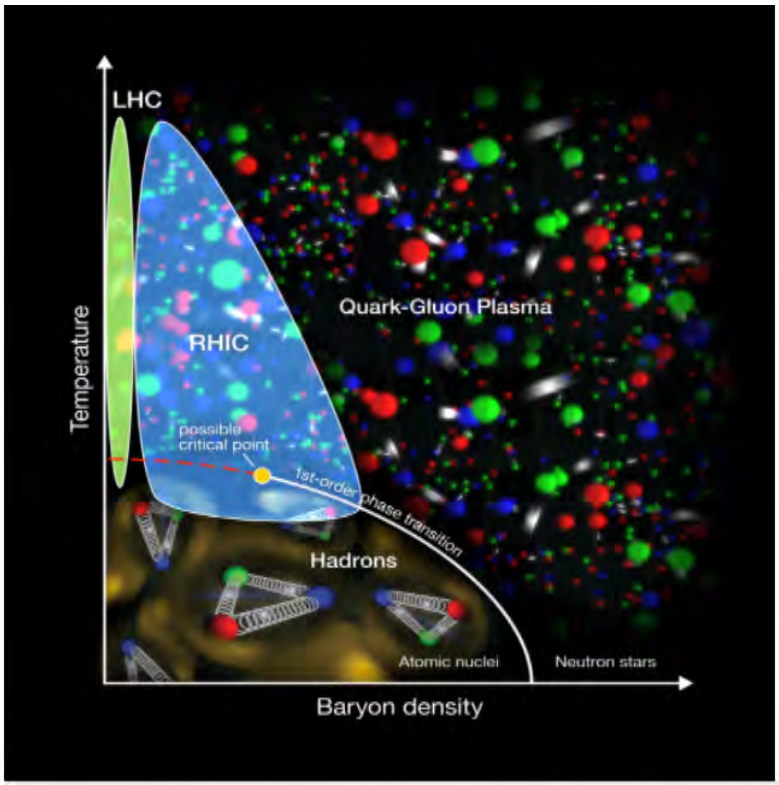

(f) Nuclear matter [6]

Heavy Ion Collisions

- We make use of powerful particle accelerators to recreate conditions of early universe.
- Study heavy-ion collisions
  - RHIC: Gold nuclei (Au^{197}) are collided releasing total $E \approx 40\,TeV$
  - LHC: Collides Pb^{208} which releases a total $E \approx 1000\,TeV$

Figure 2: Heavy objects colliding[7]

- Nuclei melt and form a new phase of matter

Quark Gluon Plasma

- T is 100 000 $>$ than the T at core of the sun
- Very low viscosity
- 10^{-23} seconds later, hadronization occurs

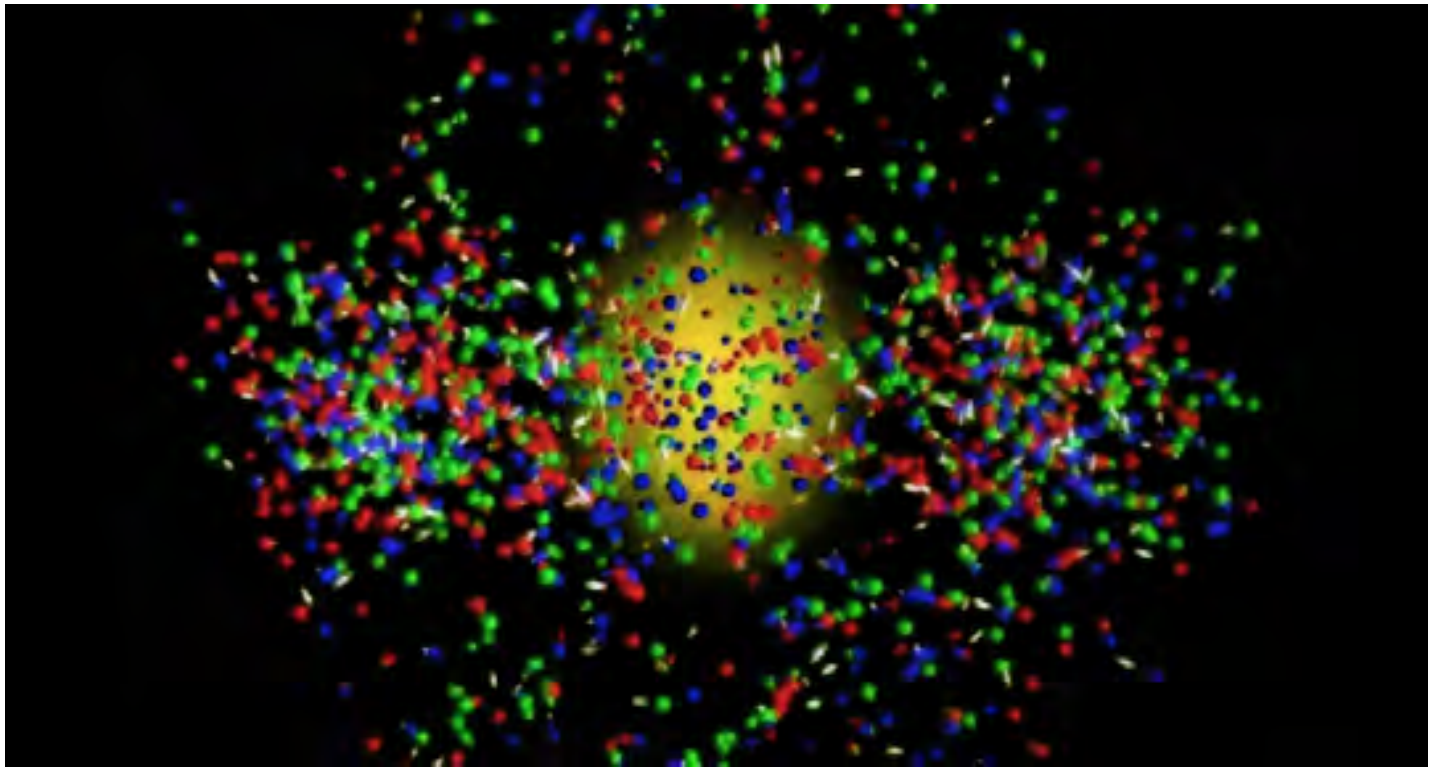

Figure 3: Quark Gluon Plasma [8]

The Mini-Bang

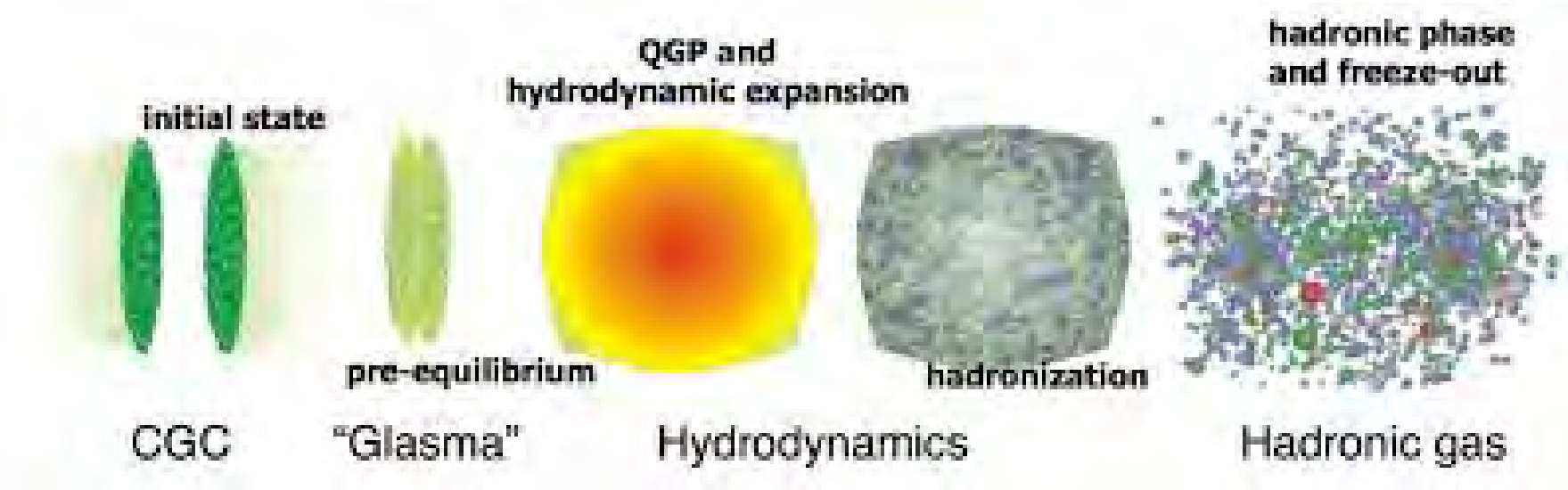

Figure 4: Schematic view of a relativistic heavy-ion collision [9]

Experimental results

- Experimental results simultaneously suggest:
  1. strongly coupled plasma that evolves hydrodynamically with $\alpha \gtrsim 1$ from low p_T observables (low T)
  2. weakly coupled gas of slightly modified quarks and gluons with $\alpha < 1$ (high T)

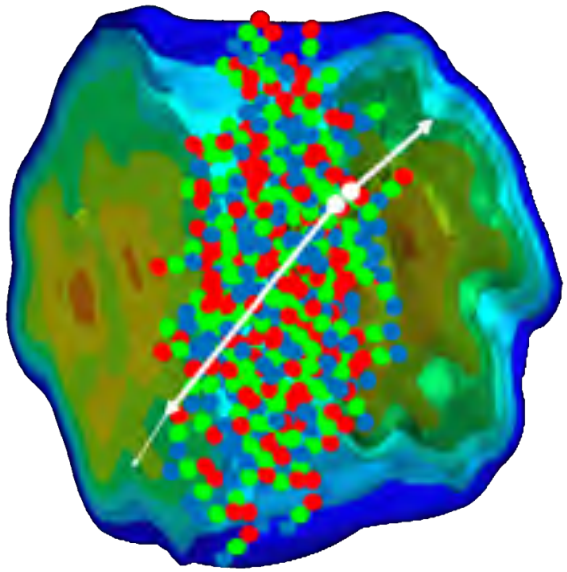

Figure 5: Quark Gluon Plasma [10]

What are we interested in?

- Probes of QGP

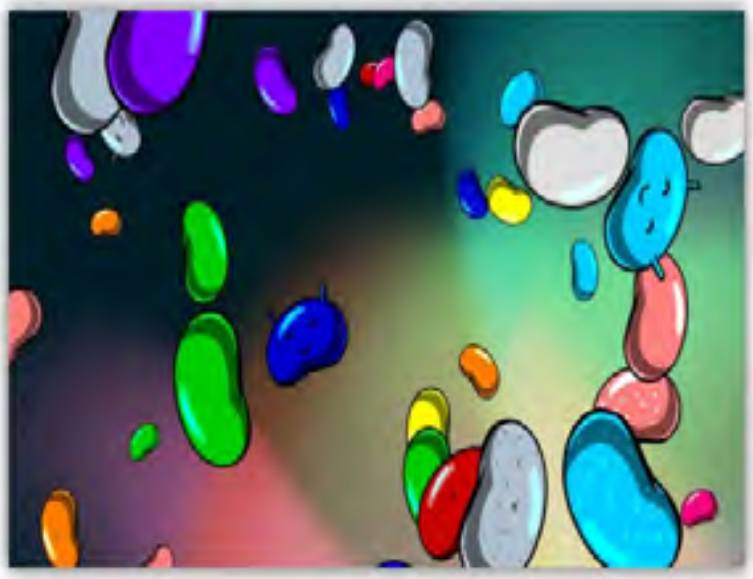

(a) "Heavy quarks" [11]

(b) "Heavy quarks in QGP" [12]

- Want to model energy loss of a heavy quark propagating through QGP
- If we assume strong coupling for QGP, the dynamics of heavy quarks interacting with QGP is described by a stochastic DE (Langevin equation)

Langevin Energy Loss

- Need to solve a stochastic differential equation

$$\frac{dp_i}{dt} = -\mu p_i + F_i^L + F_i^T \tag{1}$$

- The above is a stochastic equation of motion for a heavy quark in the fluid's rest frame.
- $\mu = \frac{\pi\sqrt{\lambda}T^2}{2M_Q}$ is the drag loss coefficient, where M_Q is the mass of a heavy quark in a plasma of temperature T.
- λ is the Hooft coupling constant.
- F_i^L and F_i^T are longitudinal and transverse momentum kicks with respect to the quark's direction of propagation

Nuclear modification factor

$$R_{AA}(p_T) = \frac{dN^{AA}/dp_T}{< N_{coll} > dN^{pp}/dp_T} = \frac{dN^{AA}/dp_T}{T_{AA} d\sigma^{pp}/dp_T} \quad (2)$$

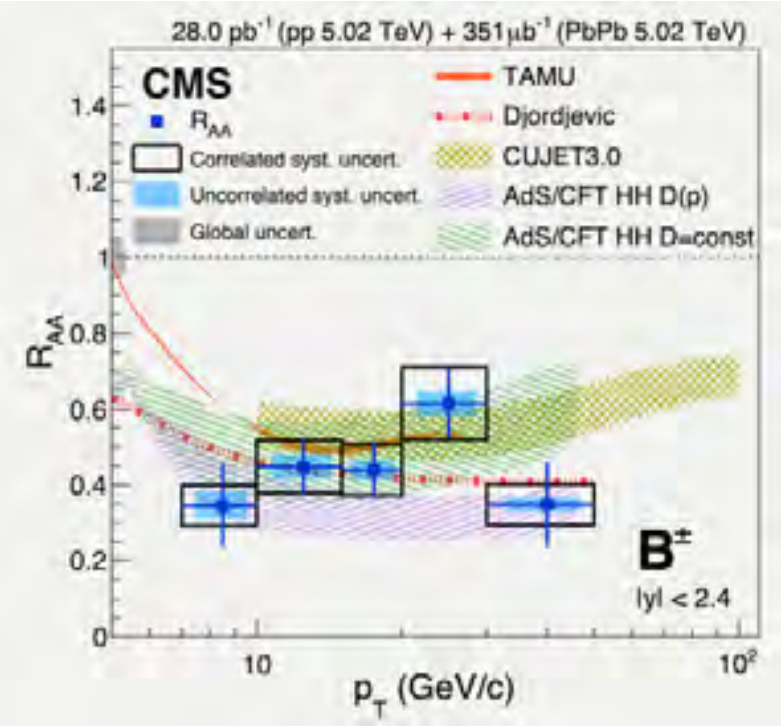

Figure 6: R^B_{AA} vs p_T, The CMS Collaboration, arXiv:1705.04727. Phys.Rev.Lett. 119 (2017) no.15, 152301

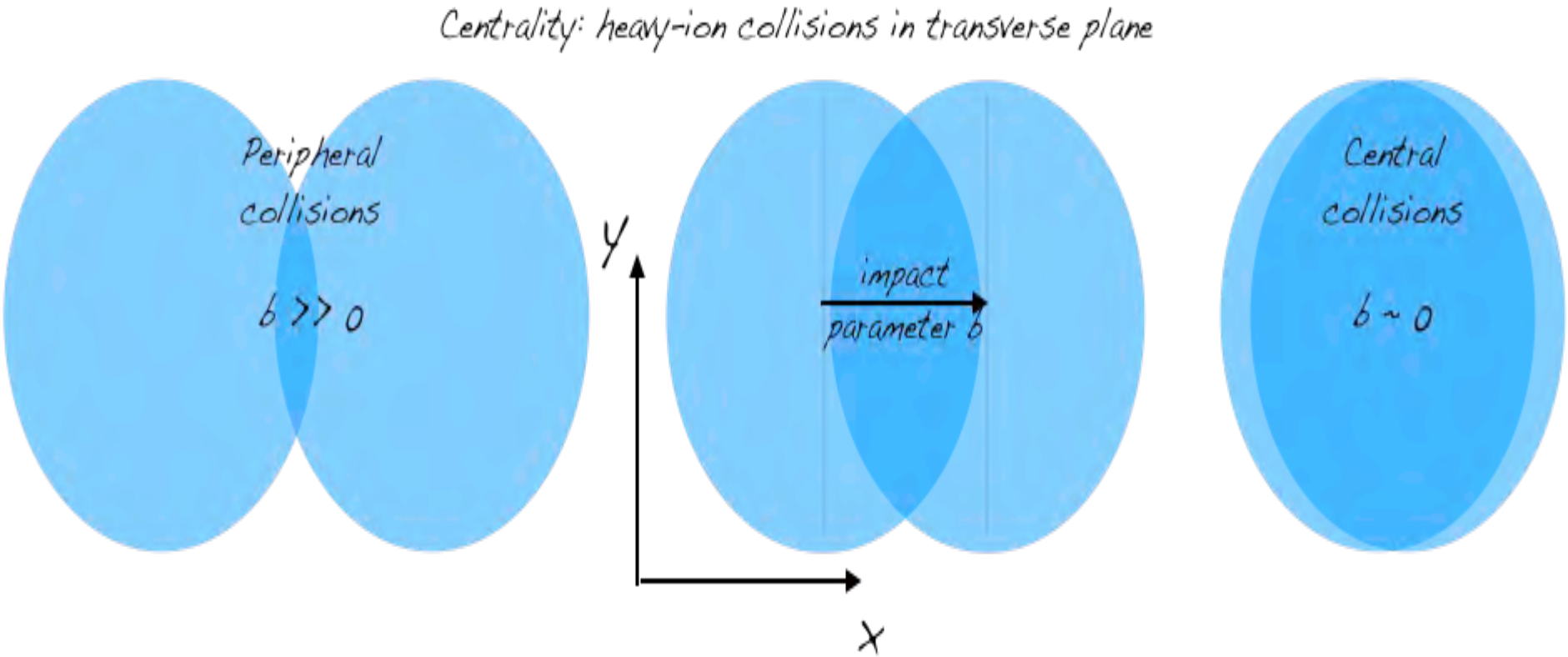

Figure 7: Centrality of heavy-ion collisions in the transverse plane, M. Ploskon, arXiv:1808.01411v1 [hep-ex]

Centrality on heavy quark production

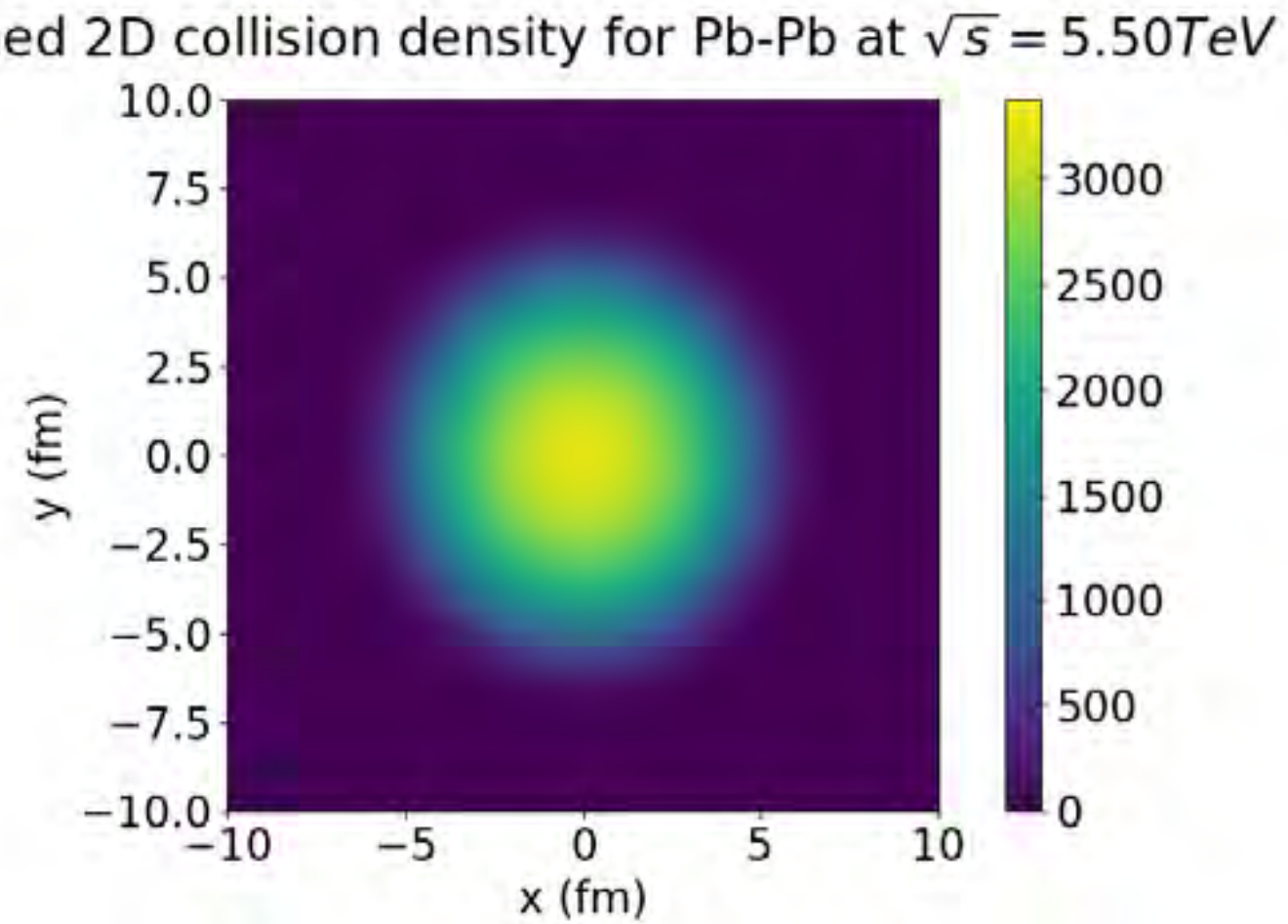

Figure 8: Full 2D collision density binned at b=2.37fm (0-5% centrality class)

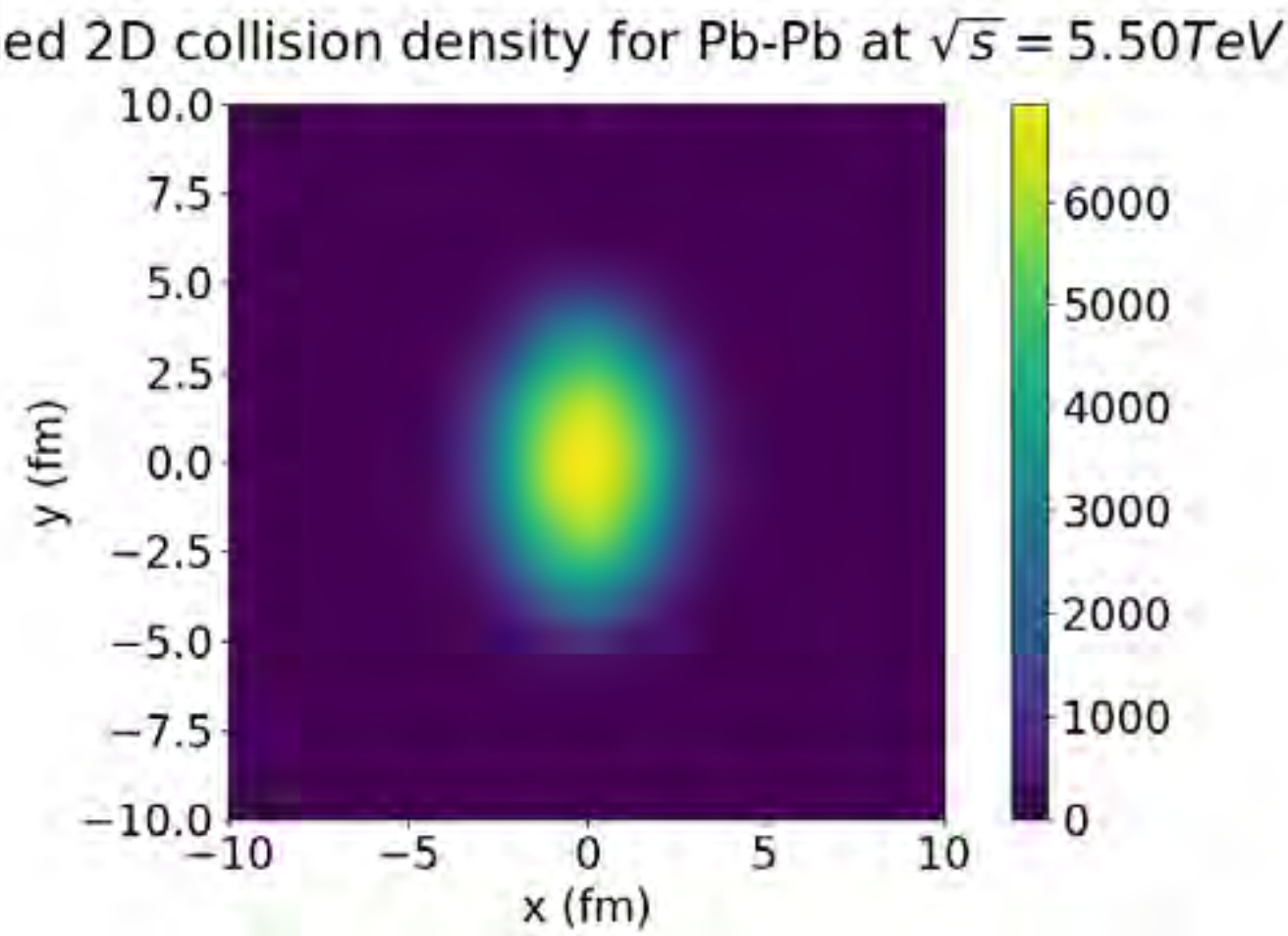

Figure 9: Full 2D collision density binned at b=7.92fm (20-30% centrality class)

Horowitz, 2012 Gubser and Reasonable

- Showed the R_{AA} at 2.75TeV for 0-10%

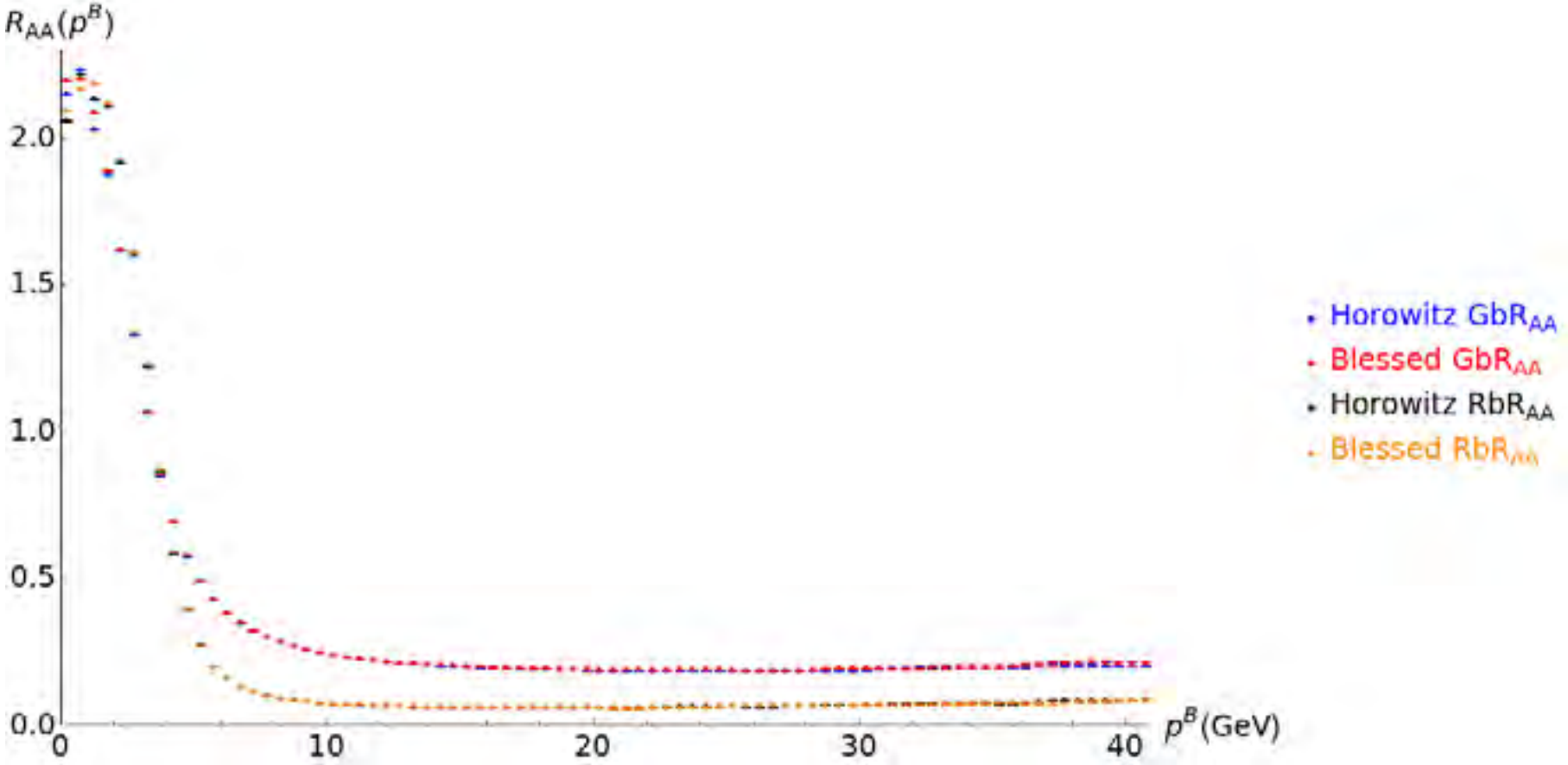

Figure 10: R^B_{AA} vs p^B, for Gubser and 'Reasonable' parameters, W.A Horowitz, arXiv:1210.8330v1 [nucl-th], S. Gubser arXiv:1210.8330v1 [nucl-th]

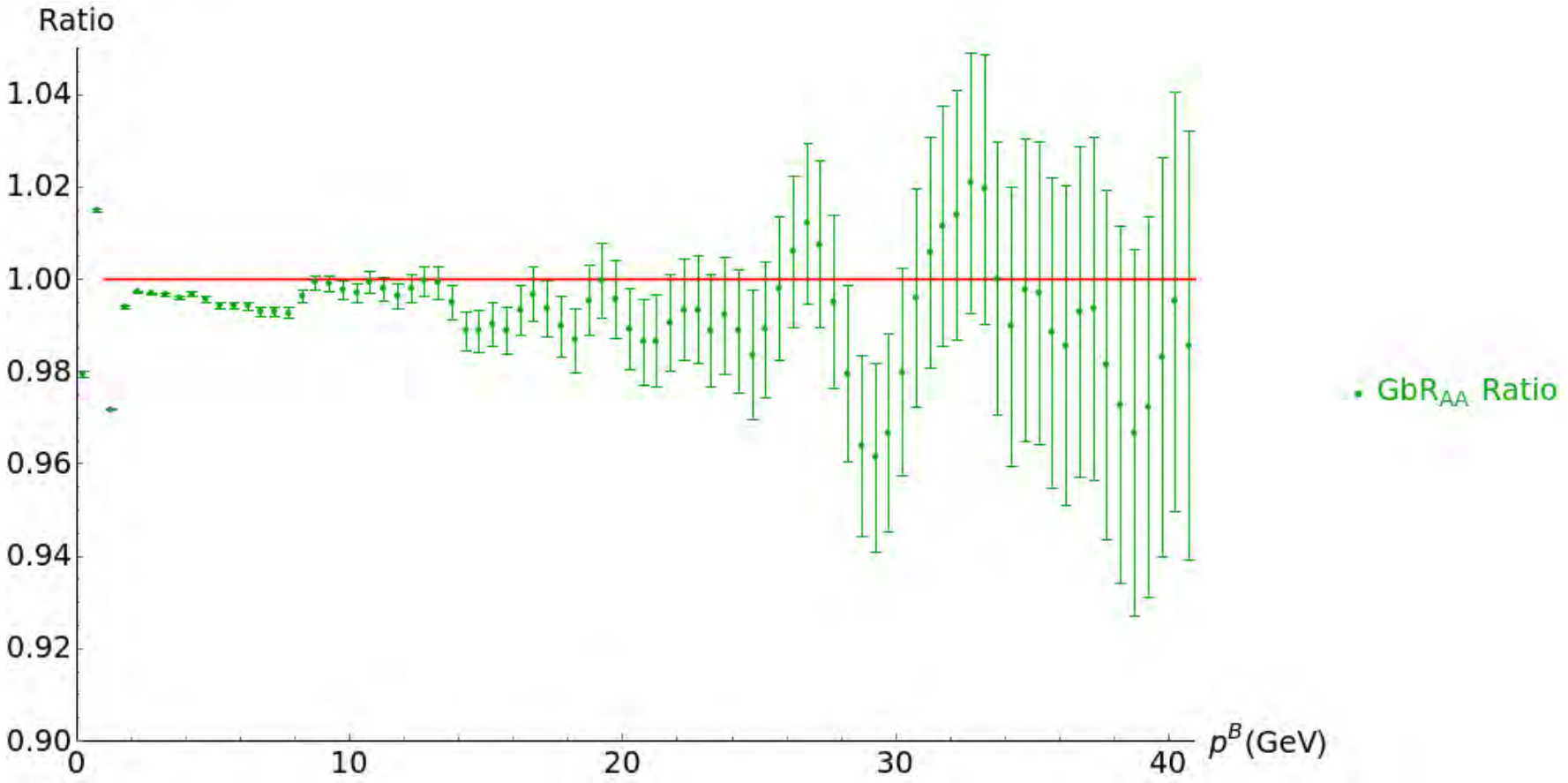

Figure 11: Ratio of RAA vs p^B (Gubser parameters) with corresponding uncertainties at 2.75TeV

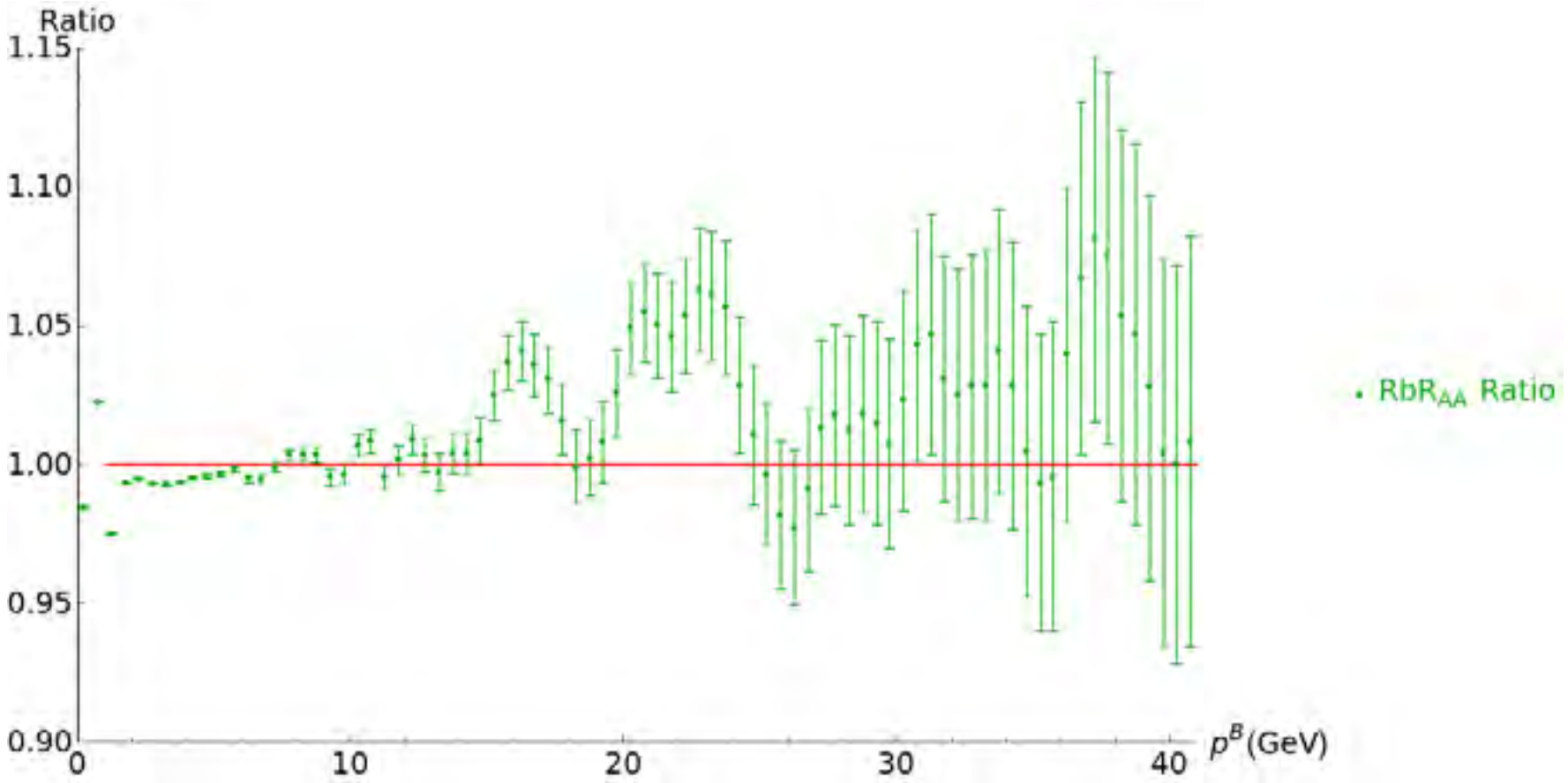

Figure 12: Ratio of RAA vs p^B ('Reasonable' parameters) with corresponding uncertainties at 2.75TeV

Gubser double quarks and half dt

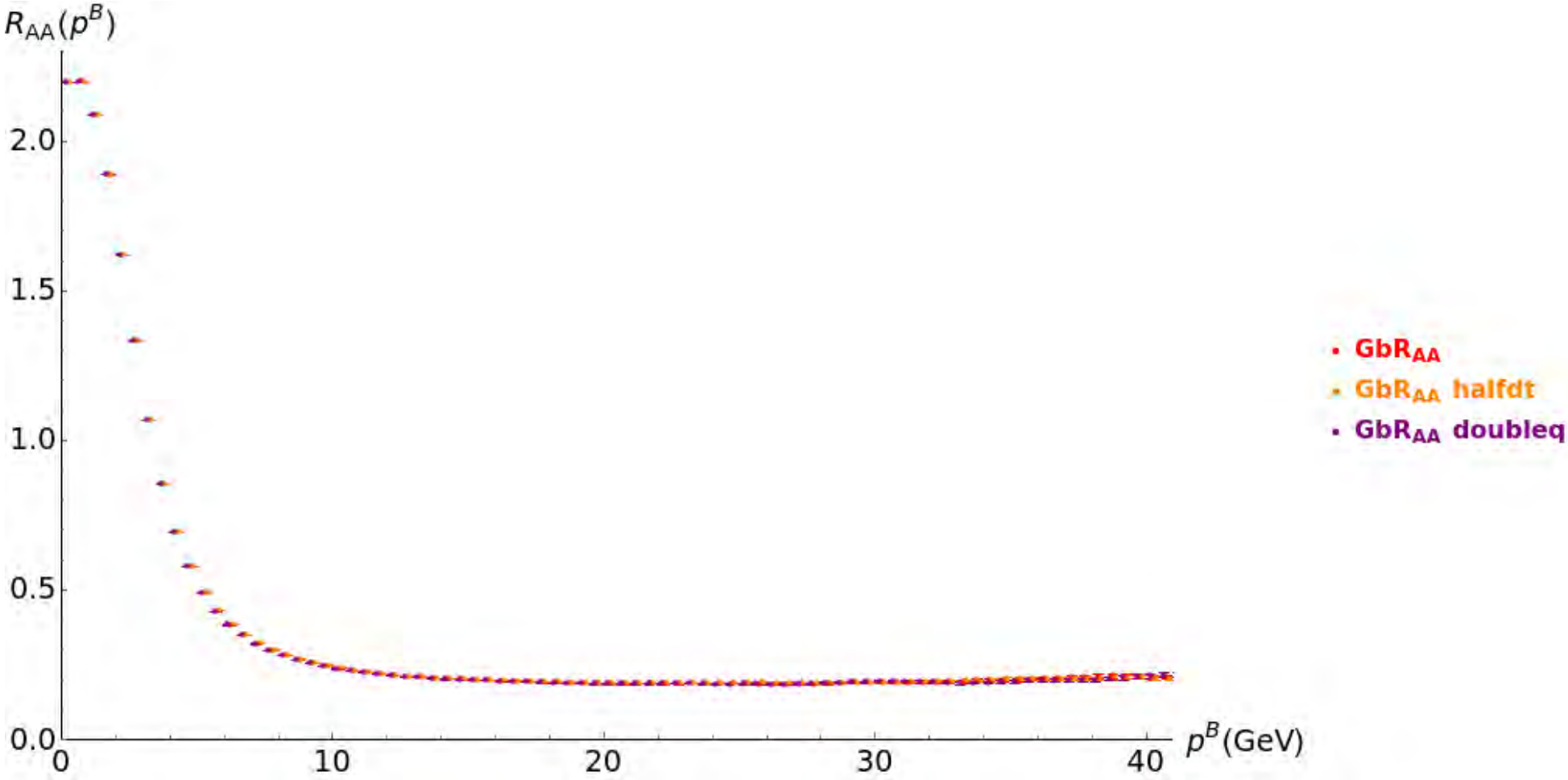

Figure 13: R^B_{AA} vs p^B, for Gubser parameters with double quarks and half dt

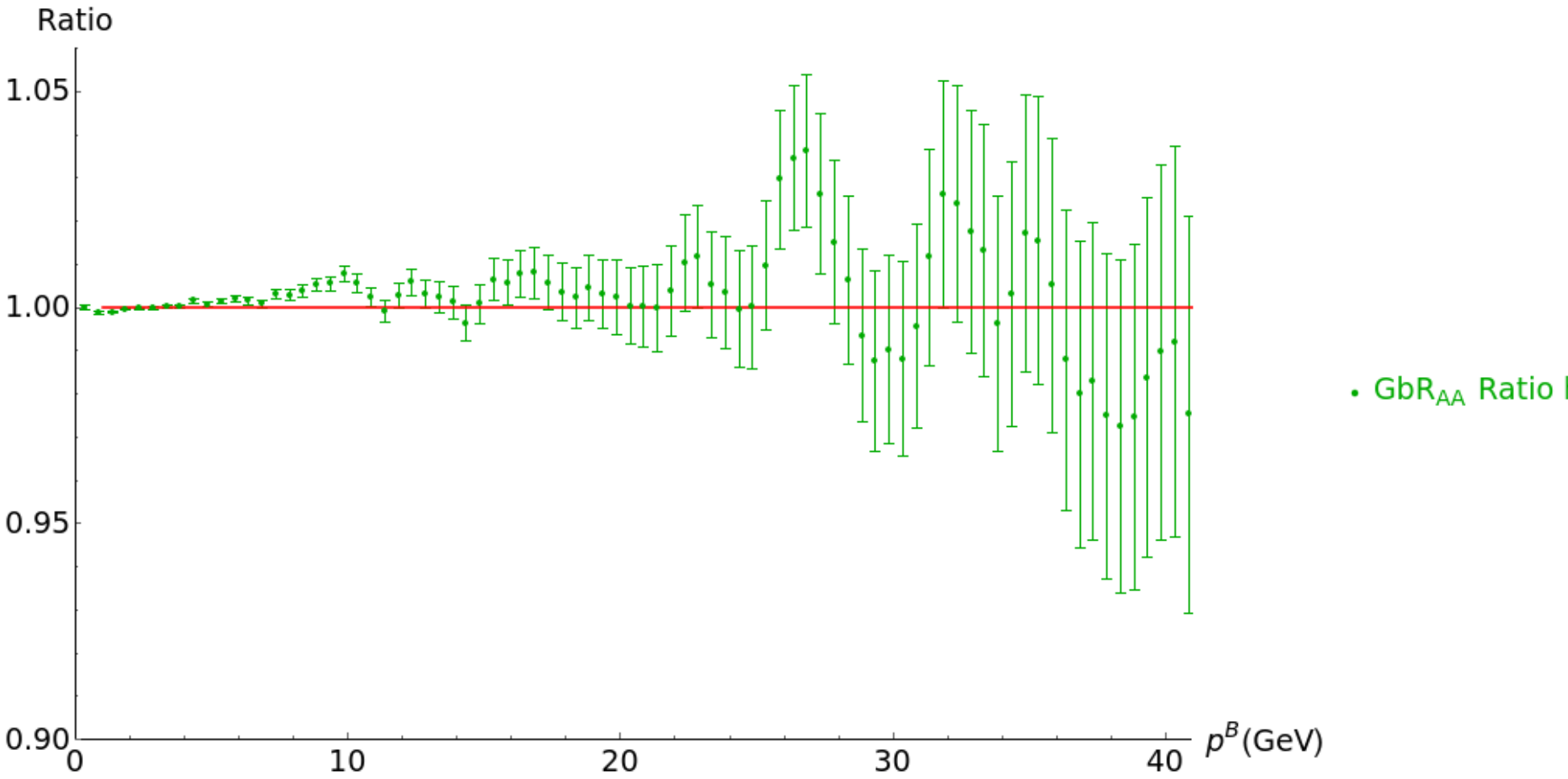

Figure 14: Ratio of half dt to original RAA vs p^B, for Gubser parameters

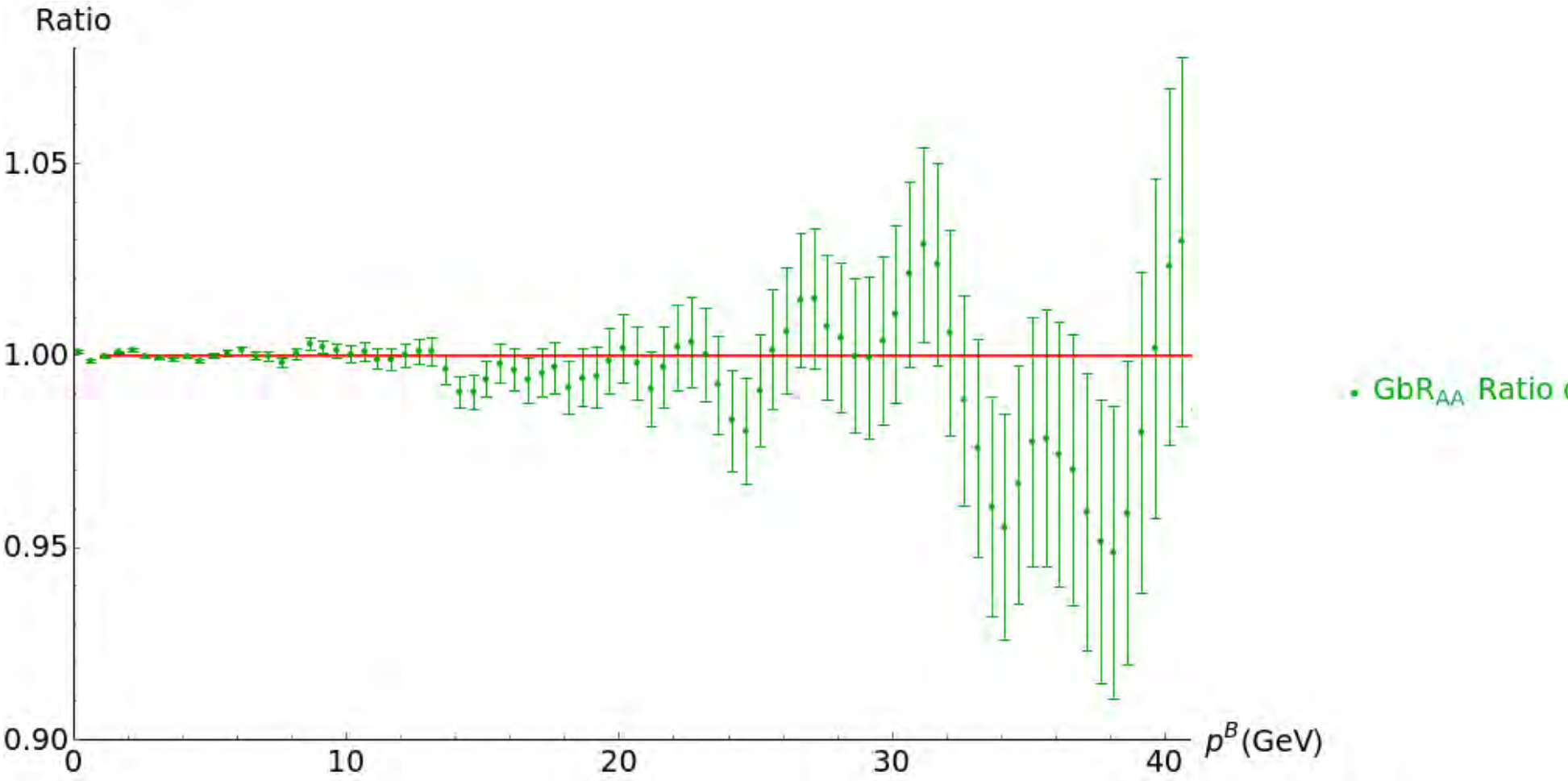

Figure 15: Ratio of double q to original RAA vs p^B, for Gubser parameters

Gubser RAA at 5.5TeV

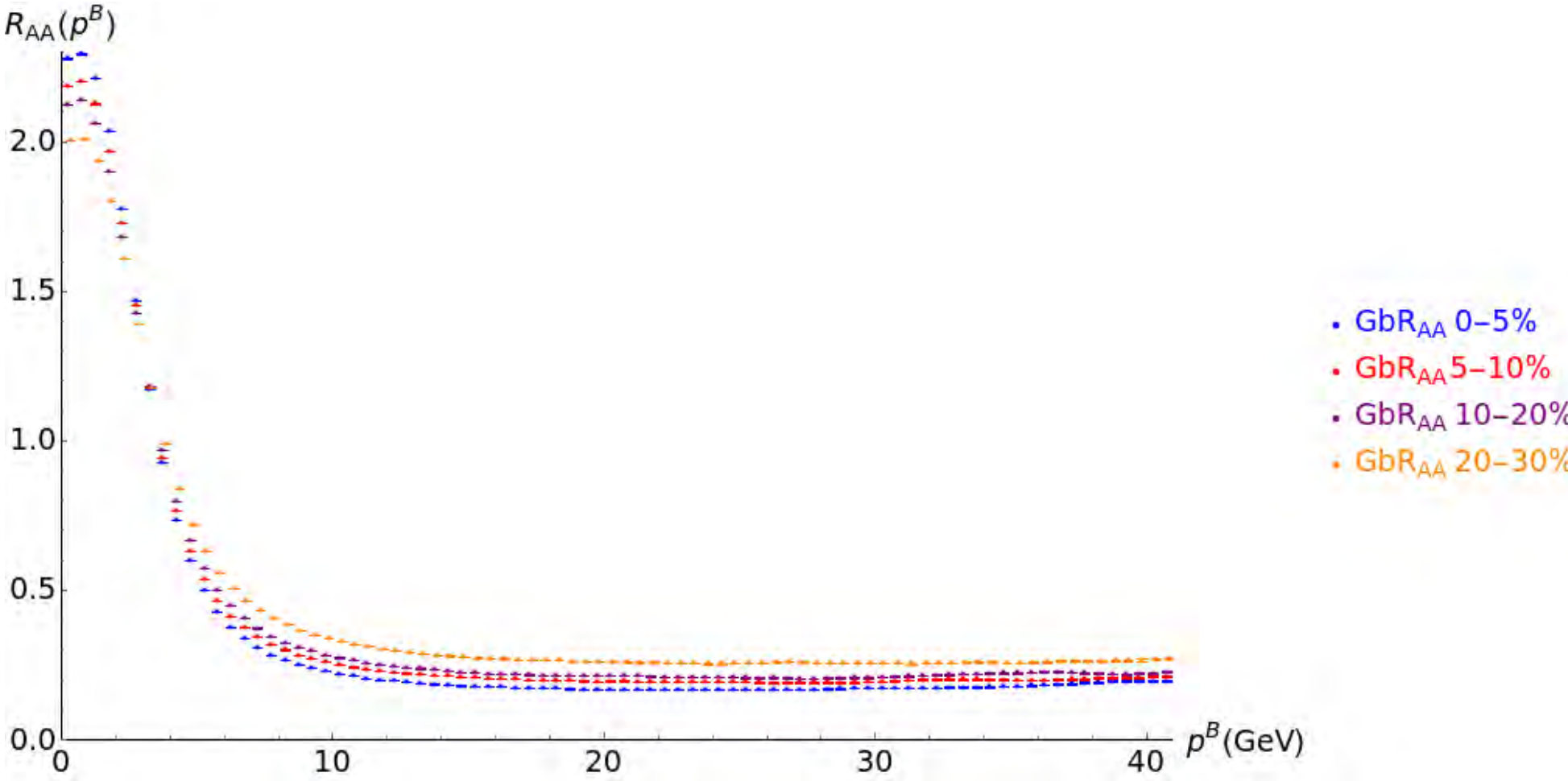

Figure 16: R^B_{AA} vs p^B, for Gubser parameters showing Bmeson suppression at 5.5TeV

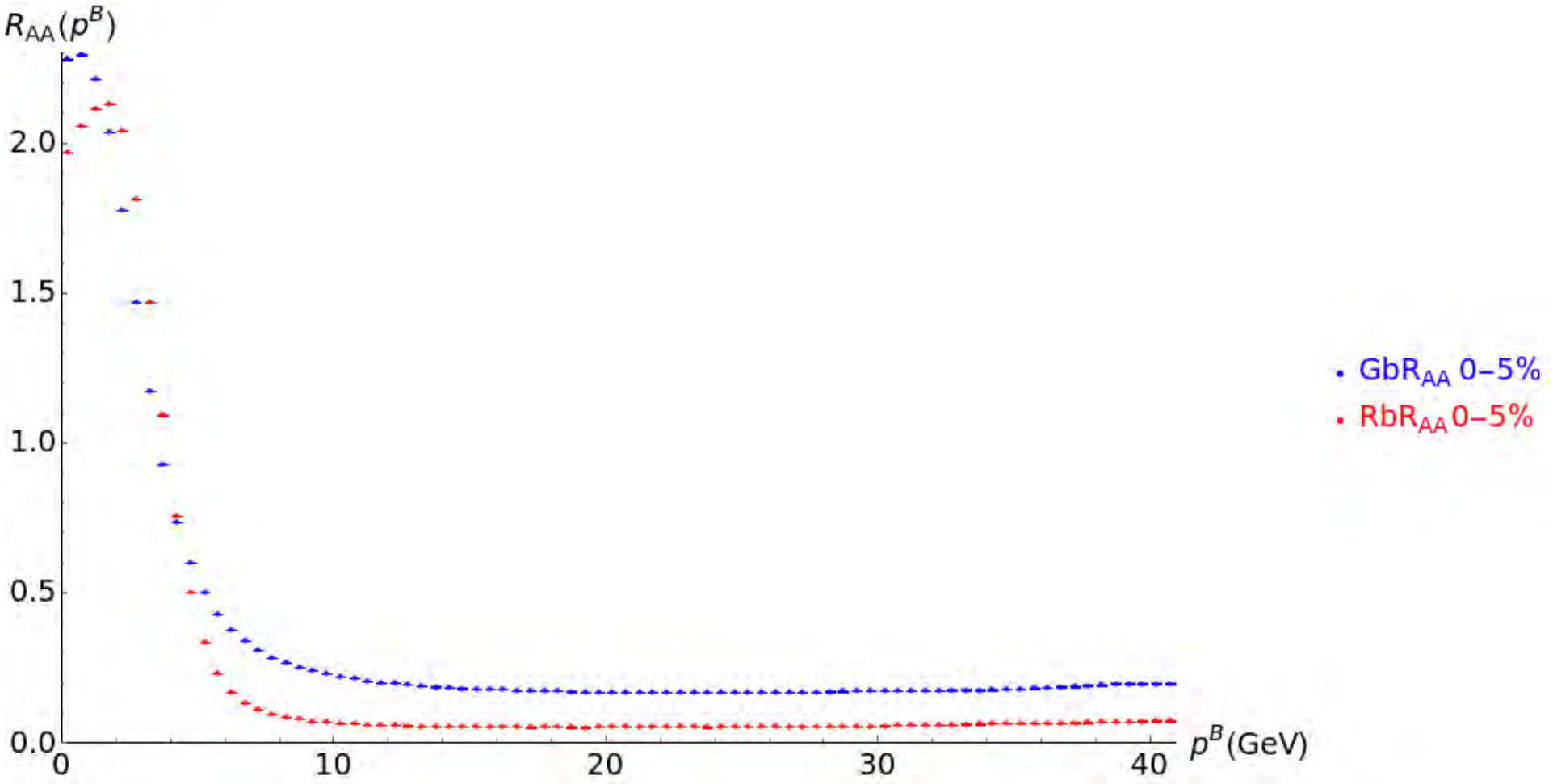

Figure 17: R^B_{AA} vs p^B, showing Bmeson suppression at 5.5TeV (0-5%) for both parameters

Summary and Outlook

- Early universe and Heavy-ion collisions
- Langevin energy loss model
- Nuclear modification factor at various energies
- Improve current results, i.e uncertainties
- Compare our theoretical predictions to experimental data

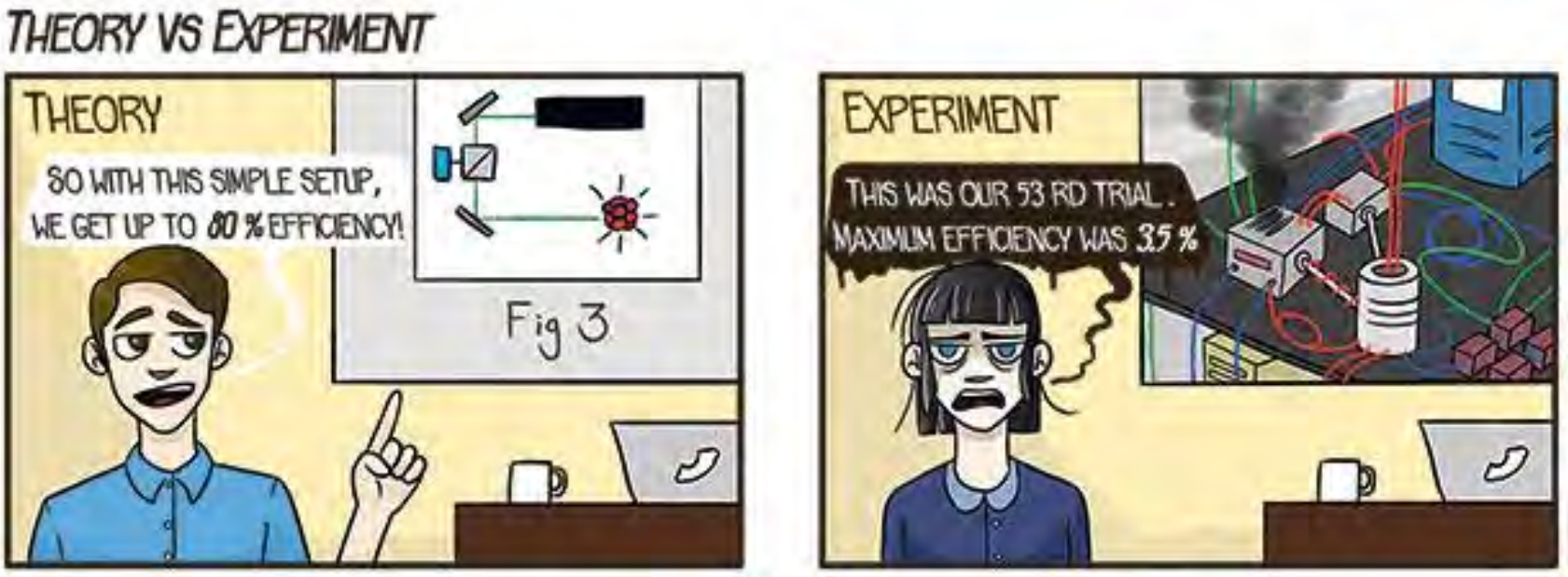

Figure 18: Theory to Experiment [13]

Acknowledgements

Special thanks to my supervisor.

Thank You! Grazie!

Questions? Suggestions?

Sources

1 https://phys.libretexts.org/TextBooks_and_TextMaps/University_Physics/Book%3A_University_Physics_(OpenStax)/Map%3A_University_Physics_III_-_Optics_and_Modern_Physics_(OpenStax)/11%3A_Particle_Physics_and_Cosmology/11.7%3A_Evolution_of_the_Early_Universe

2 https://agenda.infn.it/event/3463/attachments/32894/38725/lnf1.pdf

3 https://torontoist.com/2013/03/toronto-invents-liquefied-helium/

4 https://www.esquire.com/lifestyle/a8043/argentine-ant-control-0810/

5 https://www.dlt.ncssm.edu/tiger/diagrams/phase/PhaseDiagram-H2O.gif

6 http://digitalvortex.info/quark-gluon-plasma-phase-diagram-031fbd9a45/

7 http://www.mundoautomotor.com.ar/web/2009/08/29/seguridad-vial-conduccion-segura/

8 https://www.sciencenews.org/article/early-quark-estimates-not-entirely-realized

9 https://pub.uni-bielefeld.de/download/2905187/2905188/Dissertation%20online.pdf

10 W.A Horowitz

11 https://techieinspire.com/hidden-easter-eggs-android-gingerbread-jelly-bean/

12 https://giphy.com/explore/jello

13 https://timesofmalta.com/articles/view/Theory-vs-experiment.612157

Particle Geometry using Glauber Model

$$\rho(r) = \rho_0 \frac{1 + wr^2/R^2}{1 + exp((r - R)/a)} \tag{3}$$

- Provides a quantitative way to simulate geometrical configuration of the nuclei when they collide
- Allows simulation of the initial conditions in a heavy ion collision
- Computation of geometrical quantities i.e number of colliding/participating nucleons
- We can compute collision densities

Collision density 2.75TeV

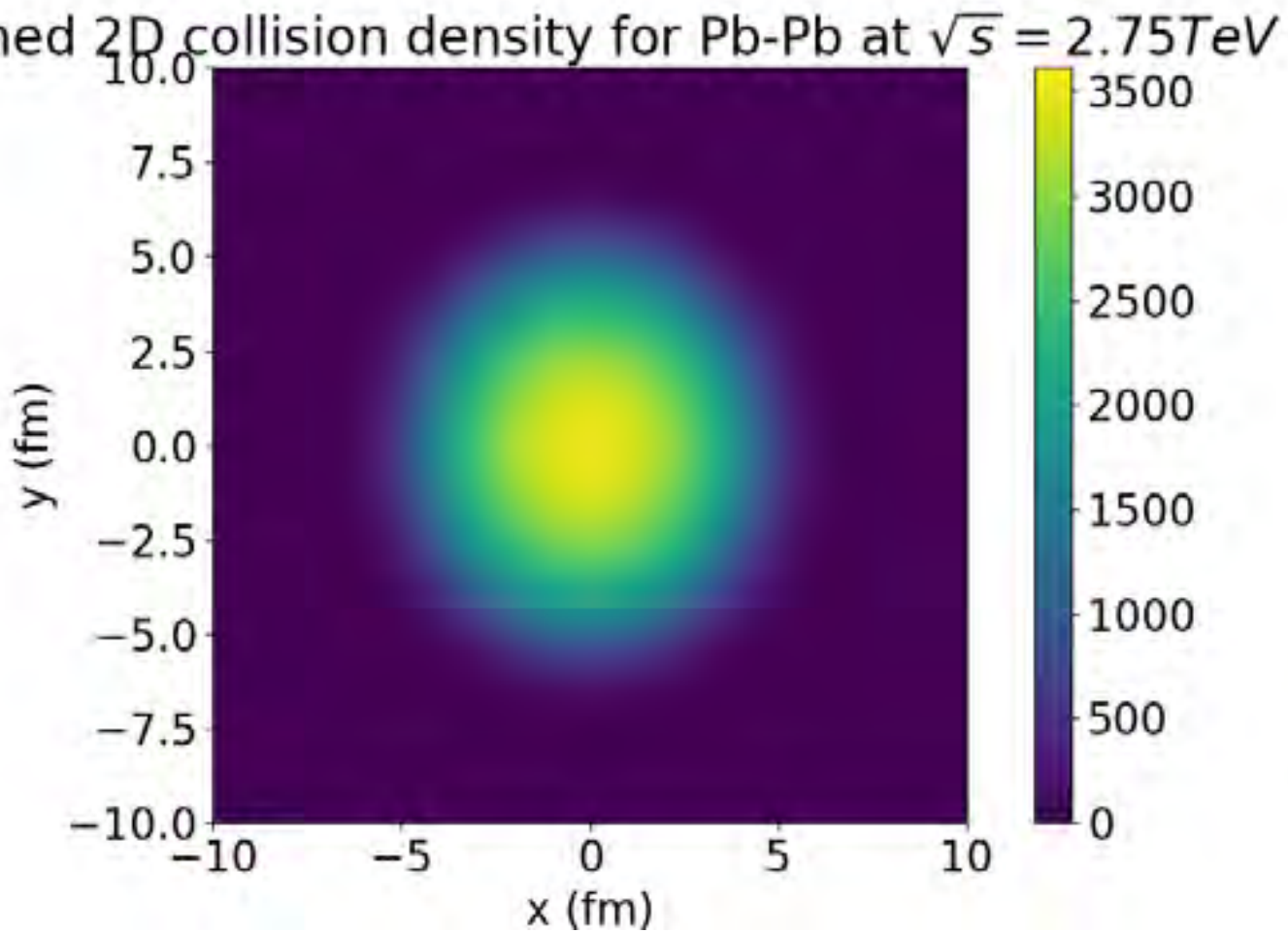

Figure 19: Full 2D collision density binned at b=3.33fm (0-10% centrality class)

More on Langevin Energy Loss

$$\frac{dp_i}{dt} = -\mu p_i + F_i^L + F_i^T \quad (4)$$

$$< F_i^L(t_1) F_j^L(t_2) > = \kappa_L \hat{p}_i \hat{p}_j g(t_2 - t_1), \quad \hat{p} = p_i/|\vec{p}| \quad (5)$$

$$< F_i^T(t_1) F_j^T(t_2) > = \kappa_T(\delta_{ij} - \hat{p}_i \hat{p}_j) g(t_2 - t_1) \quad (6)$$

$$\kappa_T = \pi\sqrt{\lambda} T^3 \gamma^{1/2}, \quad \kappa_L = \gamma^2 \kappa_T \quad (7)$$

$$\gamma \lesssim \gamma_{lect}^{fluc} = \frac{M_Q^2}{4T^2} \quad (8)$$

- Quark initial direction of propagation(assumed uniform) were randomly sampled
- Propagation was through backgrounds generated by the VISHNU2+1D hydrodynamics code
- Pseudo-random number generation was performed using the Ran routine from Numerical Recipes

Gubser and Reasonable

- **Reasonable (QCD) parameters:**
  - 't Hooft coupling is taken to be $\lambda = 4\pi\alpha_s N_c = 4\pi \times 0.3 \times 3$ and $T_{QCD-plasma} = T_{SYM-plasma}$
- **Gubser (N=4 SYM) parameters:**
  - 't Hooft coupling is taken to be $\lambda = 5.5$ and $T_{SYM-plasma} = T_{QCD-plasma}/3^{1/4}$
  - Can "experimentally measure" the strength of H.Q potential in lattice QCD (#/R) and compare to that calculated in AdS/CFT ($\sqrt{\lambda}/R$)
  - Can dial up/down $\sqrt{\lambda}$ to get a description like lattice QCD and that gives the λ=5.5
- In the Gubser prescription, the 't Hooft coupling is smaller by ≈ 2 and T is lower. So the drag for Gubser is smaller then we get less energy loss and less suppression

Heavy quarks position and momentum

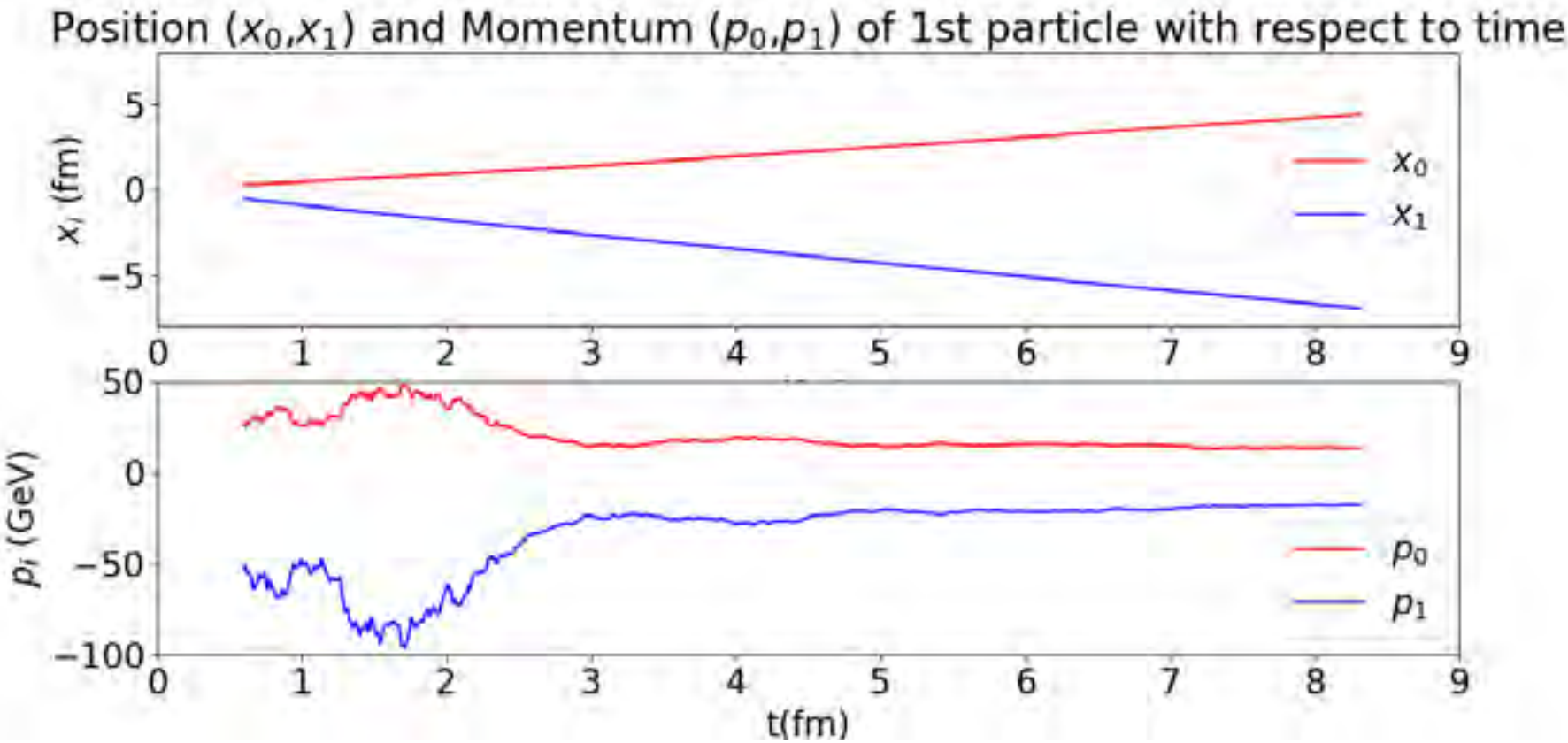

Figure 20: Position and Momentum of a single quark produced at the origin with initial momentum (25,-50)

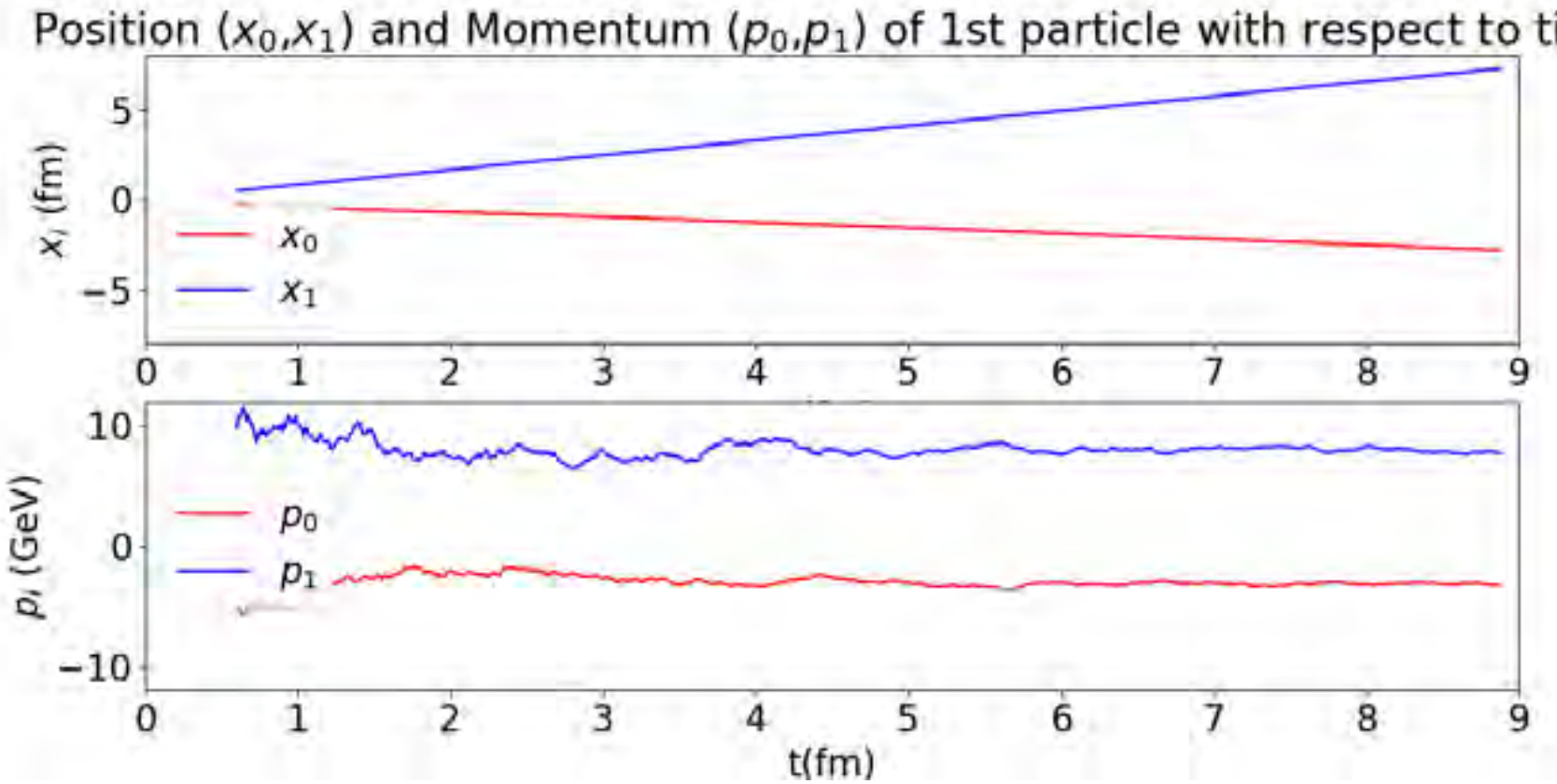

Figure 21: Position and Momentum of a single quark produced at the origin with initial momentum (-5,10)

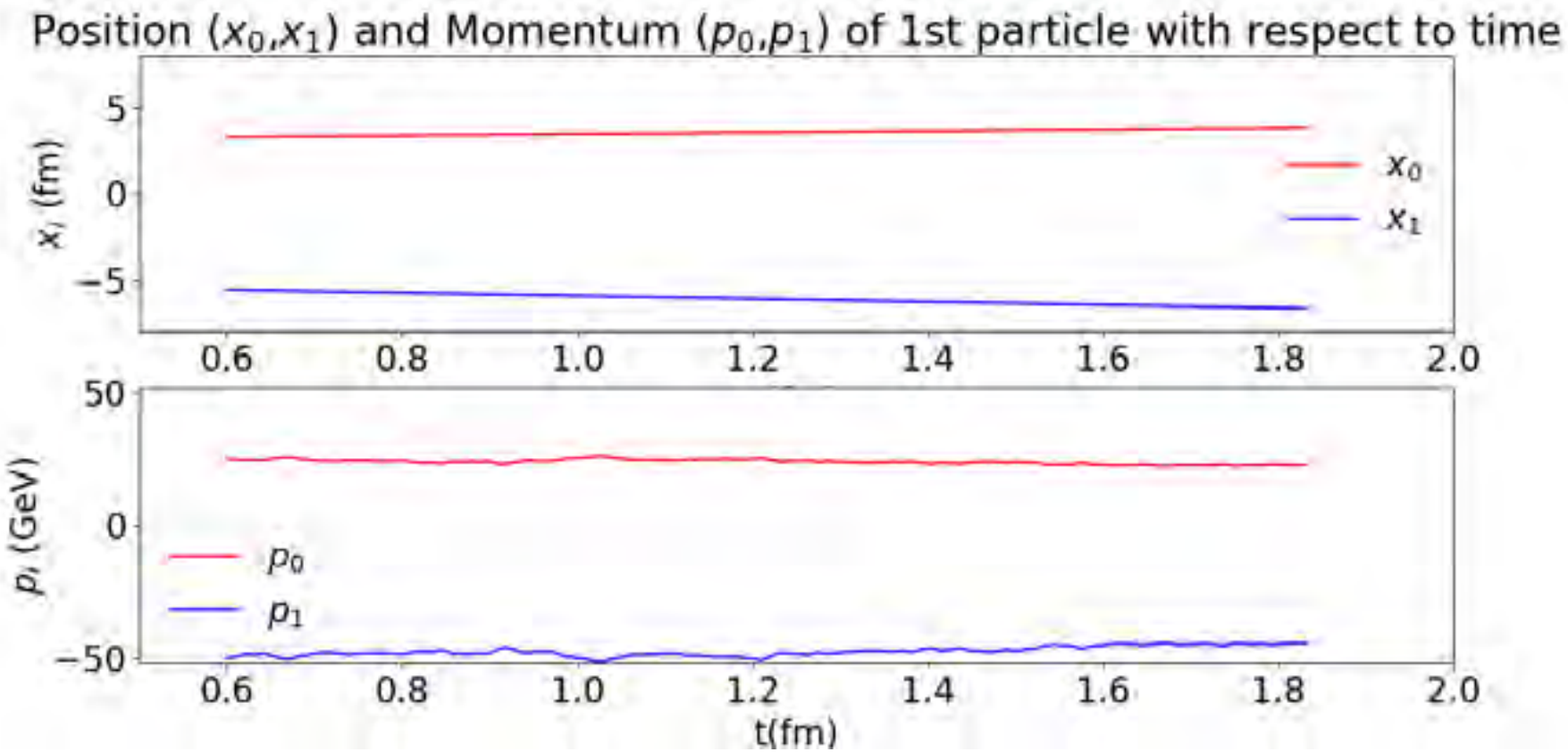

Figure 22: Position and Momentum of a single quark produced at (3,-5) with initial momentum (25,-50)

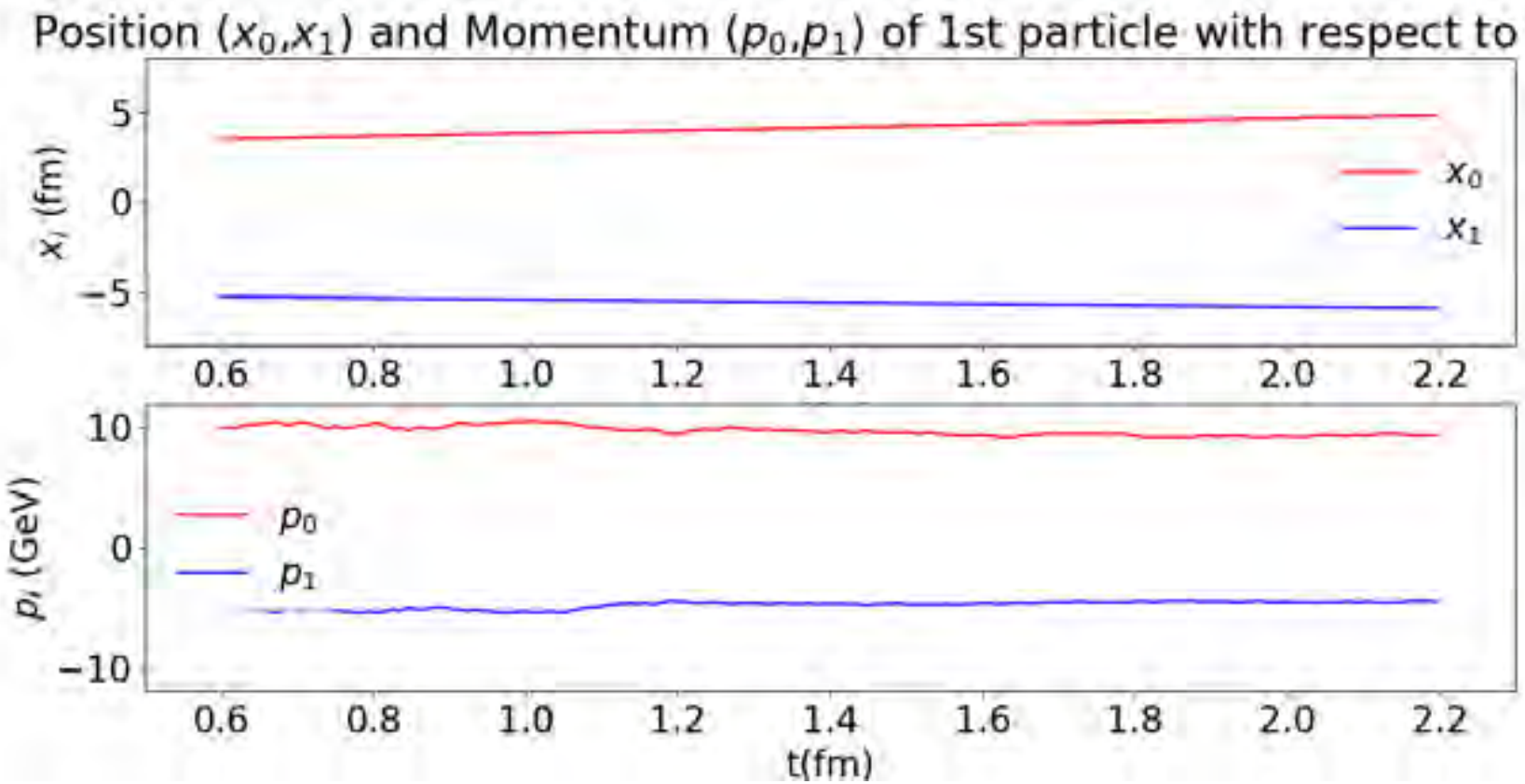

Figure 23: Position and Momentum of a single quark produced at (3,-5) with initial momentum (-5,10)

Statistical Hadronization of Quark-Gluon Plasma in a kinetic approach to Ultrarelativistic Heavy Ion Collision

Giuseppe Galesi

University of Catania
INFN - Laboratori Nazionali del Sud
galesi@lns.infn.it
Collaborators: V. Greco S. Plumari

4th March 2020

Outline

- Kinetic theory and hydrodynamics
- Transport Theory at fixed η/s
  - Description
  - Motivation
- Hadronization tool implementation
  - THERMINATOR 2
  - Freeze-out hypersurface tool
- Summary and conclusion

- Since its discovery many efforts have been done in order to determine QGP's properties such as $\frac{\eta}{s}$
- Very large v_2 coefficient observed at RHIC and LHC experiments on heavy ion collisions
- Both hydrodynamics and kinetic theory have shown that the v_2 coefficient strongly depends on $\frac{\eta}{s}$
- Comparison with experimental data suggests that QGP is an almost perfect fluid with very small $\frac{\eta}{s}$ near the conjectured limit $\sim \frac{1}{4\pi}$

STAR, J. Adams et al., Nucl. Phys. A757, 102 (2005); PHENIX, K. Adcox et al., Nucl. Phys. A757, 184 (2005).

Kinetic theory and hydrodynamics

- Kinetic theory starts from a microscopic description and needs cross sections and mean fields
- Perfect Hydrodynamics is a macroscopic approach based on stress-energy tensor and currents conservation
- To take into account dissipation one has to develop Viscous Hydrodynamics usually according to the Israel-Stewart theory

H. Song and U.W. Heinz, Phys. Rev. C 78, 024902 (2008).
S. Plumari, V. Baran, M. Di Toro, G. Ferini and V. Greco, Phys. Lett. B689 (2010) 18.

Kinetic theory and hydrodynamics

- In Hydrodynamics viscosity is an extrinsic parameter
- In Kinetic theory it is intrinsically included due to the presence of finite cross section
- Standard Kinetic theory is not discussed directly in terms of viscosity
- Standard Kinetic theory is not adequate to constrain $\frac{\eta}{s}$ from the experimental data

Transport theory at fixed $\frac{\eta}{s}$

- Direct link with viscous hydrodynamic language
- Kinetic theory allows to investigate non-equilibrium and dissipation in a wider range both in $\frac{\eta}{s}$ and p_T
- 3+1 dimensional Monte-Carlo cascade for on-shell parton based on the stochastic interpretation of the collision rate
- We start from a given $\frac{\eta}{s}$ to locally infer the microscopic cross section

G. Ferini, M. Colonna, M. Di Toro, and V. Greco, Phys. Lett. B670, 325 (2009).

Transport theory at fixed $\frac{\eta}{s}$

The main equation we want to solve is the Relativistic Boltzmann Equation

$$\left\{p^{\mu}\partial_{\mu}+\left[p_{\nu}F^{\mu\nu}+m^{*}\partial^{\mu}m^{*}\partial_{\mu}^{p}\right]\right\}f\left(x,p\right)=C\left(f\left(x,p\right)\right), \tag{1}$$

with

$$C\left(f\left(x,p\right)\right)=\frac{1}{2E_{p}}\int\frac{\mathrm{d}^{3}q}{\left(2\pi\right)^{3}2E_{p}}\int\frac{\mathrm{d}^{3}p'}{\left(2\pi\right)^{3}2E'_{p}}\int\frac{\mathrm{d}^{3}q'}{\left(2\pi\right)^{3}2E'_{q}}$$
$$\left[f\left(q'\right)f\left(p'\right)\left|M\left(p'q'\rightarrow pq\right)\right|^{2}-f\left(q\right)f\left(p\right)\left|M\left(pq\rightarrow p'q'\right)\right|^{2}\right]$$
$$\left(2\pi\right)^{4}\delta^{4}\left(p+q-p'-q'\right). \tag{2}$$

Transport theory at fixed $\frac{\eta}{s}$

2 ingredients:

1. Space-time grid in (t, x, y, Y_s) coordinates where

$$Y_s = \frac{1}{2} \ln \frac{t+z}{t-z} \tag{3}$$

   is the longitudinal rapidity.

2. Statistical particle method:

$$f_i = \frac{\triangle N_i}{N_{\text{test}} \triangle^3 x_i \triangle^3 p}. \tag{4}$$

Transport theory at fixed $\frac{\eta}{s}$

Initial distribution

- Spatial distribution $\rightarrow$ Glauber model
- Momentum distribution:
  - Thermal distribution for $p_T \lesssim 2$GeV
  - NLO-pQCD fot higher p_T

Transport theory at fixed $\frac{\eta}{s}$

Propagation

1. Evaluate field in each cell
2. Solve Newton equation with Runge-Kutta integration method

Transport theory at fixed $\frac{\eta}{s}$

Collision

Analytical $\frac{\eta}{s}$ approximation according to the Chapmann-Enskog formalism:

$$\frac{\eta}{s} = \frac{1}{15} \frac{\langle p \rangle}{g\left(\frac{m_D}{T}\right) \sigma_{\text{tot}} n}, \tag{5}$$

with

$$g(a) = \frac{1}{50} \int \mathrm{d}y y^6 \left[\left(y^2 + \frac{1}{3} \right) K_3(2y) - y K_2(2y) \right] h\left(\frac{a^2}{y^2}\right) \tag{6}$$

and

$$h(a) = 4a(1+a)\left[(2a+1)\ln(1+1/a) - 2\right]. \tag{7}$$

Plumari et al., arXiV:1208.0481v2

Transport theory at fixed $\frac{\eta}{s}$

Collision

The fundamental formula we use to get the cross section:

$$\sigma_{\text{tot}} = \frac{1}{15}\frac{\langle p \rangle}{g\left(\frac{m_D}{T}\right) n}\frac{1}{\eta/s}. \tag{8}$$

From that we obtain the probability for a $2 \to 2$ collision:

$$P = v_{\text{rel}}\sigma_{\text{tot}}\frac{\triangle t}{\triangle^3 x}. \tag{9}$$

Transport theory at fixed $\frac{\eta}{s}$

Passage to the continuum

The passage from this discretized theory to the exact one corresponds to the limits

$$\triangle t \to 0 \tag{10}$$

$$\triangle^3 x \to 0 \tag{11}$$

but then for having a good sampling of f we would need

$$N_{\text{test}} \to \infty \tag{12}$$

so great computational power is required and we make a compromise.

Transport theory at fixed $\frac{\eta}{s}$

Motivation

- In hydro there is no one to one correspondance between $\delta T^{\mu\nu}$ and δf. Usually one needs to make an ansatz such as

$$\delta f\left(p\right) = \frac{\pi^{\mu\nu}}{\epsilon + P} \frac{p_\mu p_\nu}{T^2} f_{\text{eq}}. \tag{13}$$

  This deviation is not small at $p_{\text{T}} \sim 3\,\text{GeV}$. No good description of mini-jets.
  In our approach we don't make any ansatz for δf.
- Pre-equilibrium distribution function treatment.
- Microscopic hadronization mechanism beyond SHM.

Hadronization tool implementation

THERMINATOR 2

- We want to test our approach with the Statistical Hadronization Model
- We have to consider all the resonance decays
- So we use the program THERMINATOR 2 by M. Chojnacki and Al. [arXiv:1102.0273]
- Inclusion of the full list of hadronic resonances (Hagedorn hypotesis)

All primordial particles are created at the freeze-out hypersurface according to the Cooper-Frye formula

$$E\frac{dN}{d^3p}(p) = (2s+1)\int \mathrm{d}\Sigma_\mu(x)\, p^\mu f(x,p), \tag{14}$$

with

$$f(x,p) = \left\{\exp\left[\frac{p_\mu u^\mu - (B\mu_B + I_3\mu_{I_3} + S\mu_S + C\mu_C)}{T}\right] \pm 1\right\}^{-1}, \tag{15}$$

and

$$\mathrm{d}\Sigma_\mu = \varepsilon_{\mu\alpha\beta\gamma}\frac{\partial x^\alpha}{\partial\alpha}\frac{\partial x^\beta}{\partial\beta}\frac{\partial x^\gamma}{\partial\gamma}\mathrm{d}\alpha\mathrm{d}\beta\mathrm{d}\gamma. \tag{16}$$

Hadronization tool implementation

THERMINATOR 2

The program uses a particular coordinate system consisting in a space-time distance d and three angles θ, ϕ, ζ:

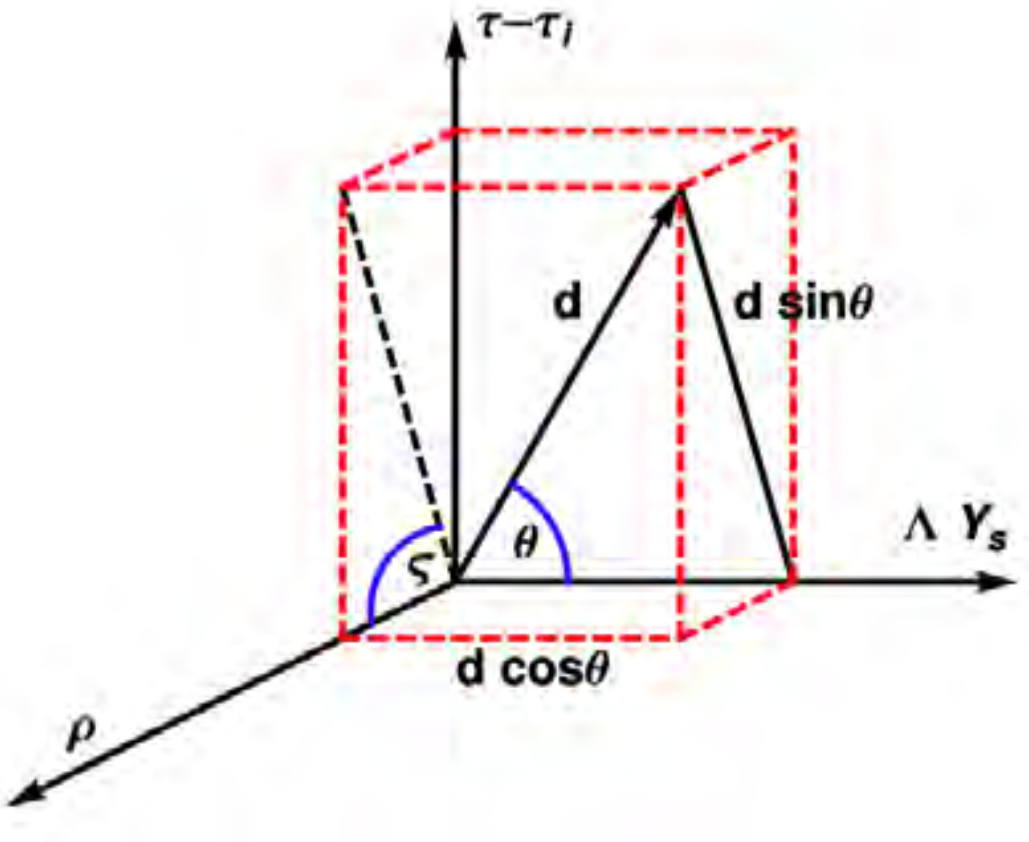

Coordinate transformation

$$t = (\tau_i + d \sin\theta \sin\zeta) \cosh \frac{d \cos\theta}{\Lambda} \tag{17}$$

$$x = d \sin\theta \cos\zeta \cos\phi \tag{18}$$

$$y = d \sin\theta \sin\zeta \sin\phi \tag{19}$$

$$z = (\tau_i + d \sin\theta \sin\zeta) \sinh \frac{d \cos\theta}{\Lambda}. \tag{20}$$

The freeze-out hypersurface is parametrized with a function $d(\theta, \phi, \zeta)$.

Hadronization tool implementation

Freeze-out hypersurface tool

During cascade code execution we freeze cells with a temperature lower than some critical value (155 MeV for example):

- store its coordinates and thermal parameters
- dynamically freeze all the particles inside it

Hadronization tool implementation

Freeze-out hypersurface tool

- We then have to convert the coordinates of the freeze-out points previously stored
- We want the points on a regular grid in θ, ϕ, ζ cordinates so interpolation is needed
- A modified Sheppard interpolation method is being tested for the task
- To reduce statistical error, average over many run of the cascade code is needed

Hadronization tool implementation

Freeze-out hypersurface tool

- Comparison with a set of data for a specific colliding system would in principle allow to fix our model parameters which are dn/dy_i, T_i, T_f, p_{cut}, $\frac{\eta}{s}$.
- Then comparison with other data-sets would have to provide a test for our model

Summary and conclusion

- Hydrodynamics works well but is based on $T^{\mu\nu}$
- A kinetic approach at fixed $\frac{\eta}{s}$ provides f and is directly linked to hydrodynamics
- A test for the validity of this model is under study: SHM
- If SHM will give good results a microscopic hadronization model such as cohalescence could be studied using full f information [arXiv:nucl-th/0301093]

Thanks for your attention!